Intracellular Signaling Mechanisms of Resistance to EGFR-Targeting Agents

by

Kelly Moore Quesnelle

Bachelor of Science, University of Michigan, 2003

Submitted to the Graduate Faculty of

The University of Pittsburgh School of Medicine

in partial fulfillment of the requirements for the degree of

Doctor of Philosophy

University of Pittsburgh

2012

UNIVERSITY OF PITTSBURGH

SCHOOL OF MEDICINE

This dissertation was presented

by

Kelly M. Quesnelle

It was defended on

March 2, 2012

and approved by

Jill M. Siegfried, PhD, Department of Pharmacology & Chemical Biology

Thomas E. Smithgall, PhD, Department of Pharmacology & Chemical Biology

Daniel E. Johnson, PhD, Department of Pharmacology & Chemical Biology

Robert L. Ferris, MD, PhD, Department of Immunology

Dissertation Advisor:

Jennifer R. Grandis, MD, Department of Pharmacology & Chemical Biology

Intracellular Signaling Mechanisms of Resistance to EGFR-Targeting Agents

Kelly M. Quesnelle

University of Pittsburgh, 2012

INTRACELLULAR SIGNALING MECHANISMS OF

RESISTANCE TO EGFR-TARGETING AGENTS

The epidermal growth factor receptor (EGFR) is widely expressed in head and neck squamous cell carcinomas (HNSCC) and activates many growth and survival pathways within tumor cells. EGFR-targeting agents are only modestly effective in treating HNSCC, however, and a consistent mechanism of resistance has not been identified, in part, due to the paucity of preclinical models. This dissertation focuses on generating EGFR-inhibitor resistant preclinical models in order to identify biomarkers that may be predictive of response to these agents.

We have assessed the response of a panel of HNSCC cell lines to the EGFR inhibitors erlotinib and cetuximab to determine their relevance as models of resistance to these agents. We defined a narrow range of response to erlotinib in HNSCC cells *in vitro.* We attempted to generate models of cetuximab resistance in cell line-derived xenografts and heterotopic tumorgrafts directly from primary HNSCC patient tumors. Our studies in HNSCC suggest that heterotopic xenografts are more representative of patient response to cetuximab than cell-line derived xenografts, although we did establish a model of cetuximab resistance from bladder cancer cell line-derived xenografts.

A candidate-based approach was used to examine the role of HER2, HER3, and c-Met on mediating EGFR inhibitor resistance. We identified increased phosphorylation of a carboxyl-terminal fragment of HER2 (611-CTF) in cetuximab-resistant cells. Afatinib, an irreversible kinase inhibitor targeting EGFR and HER2, successfully restored cetuximab sensitivity *in vitro*. When afatinib was combined with cetuximab *in vivo,* we observed an additive growth inhibitory

effect in cetuximab-resistant xenografts. We also show that while c-Met activity is not sufficient to alter cellular response to erlotinib, concomitant inhibition of c-Met and EGFR is required for the deactivation of MAPK in the presence of stimulatory ligands. These data support the proposed role for co-targeting c-Met with EGFR in the treatment of HNSCC.

The studies presented here are significant because, in addition to suggesting that 611-CTF may be a novel biomarker for cetuximab resistance, they provide a thorough assessment of modeling EGFR inhibitor resistance in HNSCC and suggest heterotopic tumorgrafts as a plausible new model for examining cetuximab resistance in future studies.

TABLE OF CONTENTS

LIST OF TABLES

LIST OF FIGURES

PREFACE

ACKNOWLEDGEMENTS

I would like to acknowledge several people and groups who have contributed a great deal to this work. I wish to thank the UPCI Lentiviral Core Facility and Dr. R.W. Sobol for generation of the HER2 siRNA lentiviral particles. I also wish to thank the UPCI Flow Cytometry Core Facility and E. Michael Meyer for his help with live cell sorting experiments. Support for these UPCI Core Facilities was provided by a Cancer Center Support Grant from the National Institutes of Health (P30 CA047904). I would like to thank Dr. Paul Harari (University of Wisconsin), Dr. Tom Carey (University of Michigan), Dr. Theresa Whiteside (University of Pittsburgh), and Dr. Georgia Chen (Emory University) who generously provided several cell lines that I have used throughout this work. I would like to thank Dr. Reza Zarnegar for providing me with a c-Met construct, as well as Drs. Simion Chiosea and Sanja Dacic for their work to generate and analyze the c-Met FISH data presented here. I would like to thank Dr. Sarah Wheeler for her contributions to the tumorgraft model generation, and Dr. Sufi Thomas for sharing her expertise in animal modeling with me. Drs. Laura Stabile, Ann Marie Egloff, and Vivian Lui have been an invaluable resource for help with experimental design and reagents, and I wish to thank them for their time and insights.

Importantly, I would like to thank the members of my Dissertation Committee for their insight and direction throughout the course of my studies: Dr. Jill Siegfried (chairperson), Dr. Daniel Johnson, Dr. Robert Ferris, and Dr. Thomas Smithgall. Finally, I would like to thank my advisor, Dr. Jennifer Grandis, for the innumerable contributions she has made to this work. Dr. Grandis has supported this work intellectually and financially. She has spent scores of hours revising my writings and teaching me how to construct comprehensive and methodical scientific arguments in the process. I am very grateful for her expertise and contributions.

My training was funded, in part, by the following awards:

1. National Institutes of Health: (NIDCR) 1F31 DE020947-01.
2. National Institutes of Health: (NIGMS) T32 GM08424.

Parts of this work appear as published manuscripts on which I am an author:

1. **Quesnelle KM** and Grandis JR. Dual kinase inhibition of EGFR and HER2 overcomes resistance to cetuximab in a novel *in vivo* model of acquired cetuximab resistance. *Clin Cancer Res*. 2011 Sep 15;17(18):5935-44.
2. **Quesnelle KM**, Grandis JR, Munger KL, Posner MR. (In Press 2009) Molecular Pathology: Head and Neck Cancer in Gelmann E, Sawyers C, Rauscher F (Eds), *Molecular Oncology: Causes of Cancer and Targets for Treatment*. New York, NY: Cambridge University Press.
3. **Quesnelle KM**, Boehm AL, Grandis JR. STAT-mediated EGFR signaling in cancer. *J Cell Biochem*. 2007 Oct 1;102(2):311-9. Review.

LIST OF ABBREVIATIONS

ADCC	Antibody-dependent Cell Mediated Cytotoxicity
AKT	Protein Kinase B
AP-1	Activator Protein 1
ATP	Adenosine triphosphate
CBL	Casitas B-Lineage Lymphoma
CTF	Carboxyl-terminal Fragment
CI	Combination Index
CREB	cAMP Response Element-binding
DMEM	Dulbecco's Modified Eagle Medium
DMSO	Dimethyl Sufoxide
EGF	Epidermal Growth Factor
EGFR	Epidermal Growth Factor Receptor
FBS	Fetal Bovine Serum
FCγR	Immunoglobulin G Fc Receptor II

FDA	Food and Drug Administration
GPCR	G Protein Coupled Receptor
GRB2	Growth Factor Receptor Bound Protein 2
HER	Human Epidermal Growth Factor Receptor
HGF	Hepatocyte Growth Factor
HNSCC	Squamous Cell Carcinoma of the Head and Neck
HPV	Human Papillomavirus
IHC	Immunohistochemistry
IP	Intraperitoneal Injection
JAK	Janus Kinase
mAb	Monoclonal Antibody
MAPK	Mitogen Activated Protein Kinase
MEM	Modified Eagle Medium
mTOR	Mammalian Target of Rapamycin
MTT	3-(4,5-dimethylthiazol-2-yl)-2,5-diphenyltetrazolium bromide
NF-kB	Nuclear Factor Kappa-light-chain-enhancer of Activated B Cells
NIDCR	National Institute for Dental and Craniofacial Research

NIGMS	National Institute for General Medical Science
NSCLC	Non-Small Cell Lung Cancer
p53	Also TP53, Tumor Protein 53
PBS	Phosphate Buffered Saline
PDK1	3-Phosphoinositide-dependent Protein Kinase-1
PIP_2	Phosphatidylinositol 4,5-bisphosphate
PIP_3	Phosphatidylinositol (3,4,5)-triphosphate
qPCR	Quantitative Polymerase Chain Reaction
SCC	Squamous Cell Carcinoma
SCID	Severe Combined Immunodeficiency
SDS-PAGE	Sodium Dodecyl Sulfate Polyacrylamide Gel Electrophoresis
SFK	Src Family Kinases
SOS	Son of Sevenless
STAT	Signal Transducer and Activator of Transcription
TGFα	Transforming Growth Factor, α
TKI	Tyrosine Kinase Inhibitor

UPCI	University of Pittsburgh Cancer Institute
VEGF	Vascular Endothelial Growth Factor

1.0 INTRODUCTION

1.1 THE EPIDERMAL GROWTH FACTOR RECEPTOR

1.1.1 EGFR is a Growth Factor Receptor and Tyrosine Kinase

Epidermal growth factor (EGF) was originally identified as a factor causing tooth eruption and eyelid opening in neonatal mice[1, 2]. The epidermal growth factor receptor (EGFR) was later identified as the membranous receptor for this growth factor[3]. EGFR is a 1210 amino acid protein containing four extracellular domains, a transmembrane domain, and an intracellular kinase domain followed by a carboxyl-terminal tail containing several tyrosine residues[4] (Figure 1-1).

EGFR is a tyrosine kinase that is extensively phosphorylated on its carboxyl-terminal tail often following stimulation with ligands such as EGF[5]. EGFR currently has seven known ligands, including EGF, Transforming Growth Factor Alpha (TGFα), amphiregulin, betacellulin, epiregulin, epigen, and heparin-binding EGF[1, 6-11] (Figure 1-1). Each of these ligands contains an EGF-like domain that interacts with extracellular domains I and III of EGFR[12]. Ligand binding to EGFR causes stabilization of EGFR in an open conformation, permitting receptor dimerization via inter-molecular interactions in domain II of the extracellular region[13] (Figure 1-1).

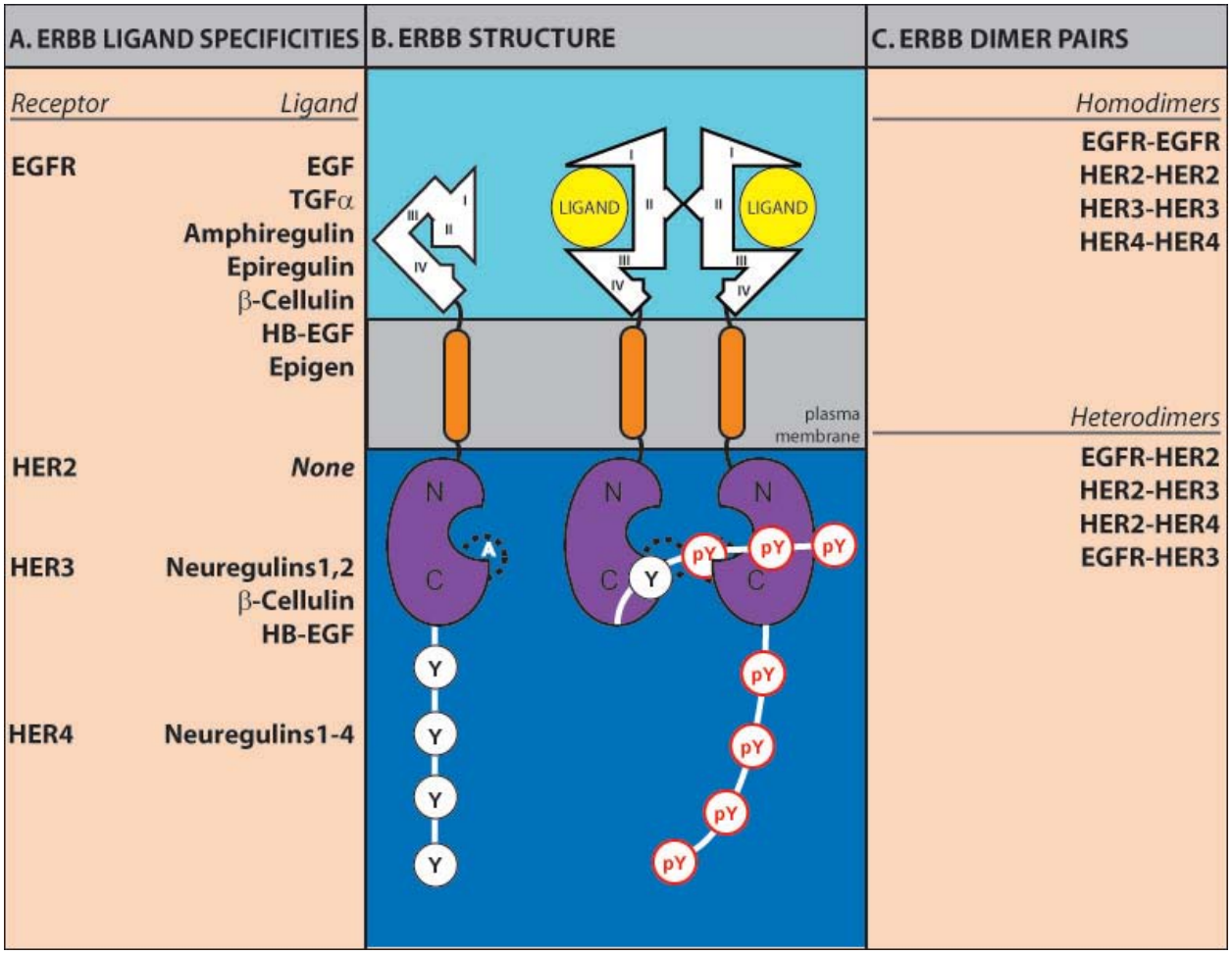

Figure 1-1. The ErbB Family of Tyrosine Kinase Receptors.

A. Each ErbB family member has specific ligands that stabilize the receptors in their open conformation with the exception of HER2, which is ligand-independent. **B.** The monomeric, tethered structure of EGFR, HER3, and HER4 is shown, as well as the dimeric (untethered) structure of these receptors. Because HER2 is ligand-independent, it resembles the untethered structure even when monomeric. The four subunits of the cytoplasmic domain are represented as I-IV. Domains I & III are leucine-rich domains and II & IV are cysteine-rich domains. Interactions between two domain IIs during dimerization bring the intracellular kinase domains into close proximity and enable transphosphorylation of tyrosine residues. The tyrosine kinase domains contain a C-lobe (C), an N-lobe (N), and an activation loop (A), all of which are required for full kinase activity. **C.** While all four ErbB family members are

theoretically capable of homodimerization, only specific endogenous heterodimer pairs have been discovered. This figure is original artwork by Kelly Quesnelle as published in Molecular Pathology: Head and Neck Cancer in Gelmann E, Sawyers C, Rauscher F (Eds), Molecular Oncology: Causes of Cancer and Targets for Treatment. New York, NY: Cambridge University Press.

EGFR phosphorylation is achieved through receptor dimerization or aggregation[14] which can be mediated by receptor overexpression[15, 16] or, more commonly, ligand-dependent mechanisms. Phosphorylation of EGFR activates the receptor because it enhances EGFR kinase activity by increasing the binding affinity of its substrates and the rate of substrate phosphorylation[17]. Ligand-independent activation of EGFR can also occur by mutations that render it constitutively active[18], overexpression of urokinase plasminogen activator receptor via integrin α5B[19], or the silencing of phosphatases which shifts basal levels of EGFR phosphorylation to the activated state[20]. Crosstalk with G-protein-coupled receptors (GPCRs) is another potential mechanism of ligand-independent EGFR activation[21].

1.1.2 **Member of the ErbB Family of Tyrosine Kinase Receptors**

EGFR is a member of the ErbB family of human epidermal growth factor receptor (HER) tyrosine kinases consisting of EGFR (ErbB1), HER2 (ErbB2, Neu), HER3 (ErbB3), and HER4 (ErbB4). Each receptor has a cysteine-rich extracellular region, a transmembrane domain, and an intracellular kinase domain that is highly conserved within the family, although HER3 lacks inherent kinase activity[22]. Likewise, HER2 has long been considered ligand-independent[23, 24], stabilized naturally in the in the open, dimer-permissive conformation. Both homodimers and heterodimers are known to occur within the ErbB Family of receptors (Figure 1-1), and the

ligand-independent nature of HER2 combined with HER3's lack of intrinsic kinase activity bolster the need for familial heterodimerization to impart downstream signaling[12, 24]. Importantly, new studies have described in detail the asymmetric nature of ErbB dimerization, opening the door for future shifts in the paradigm that ErbB family members apart from HER2 function in a ligand:receptor ratio of 2:2[25, 26].

The ErbB Family members are most often found on epithelial cells and stromal cells, naturally occurring basolaterally on epithelial cells to facilitate communication with the mesoderm which contains a wealth of growth factors[27]. Growth factors, including the ligands for EGFR and the other ErbB family members, are often expressed in the mesoderm as membrane-bound precursors that are cleaved by metalloproteinases and other extracellular proteases[28, 29]. These soluble growth factors generated from mesenchymal cells can then act in a paracrine manner to signal growth cascades in normal epithelial cells containing ErbB family members.

Once activated, ErbB receptors recruit adapter molecules such as clathrin that promote receptor endocytosis. Receptors are still active signaling molecules in the endocytic vesicle[30], from which receptors are either recycled[31] or sorted to the lysosome for degradation[32] based on ligand occupancy and prolonged kinase activity. In EGFR, binding of Casitas b-lineage lymphoma (CBL), either directly or through GRB2 at phosphotyrosine residues within the intracellular domain of EGFR results in ubiquitin-mediated trafficking to either the lysosome for recycling or the late endosome for degradation, respectively[33]. Interestingly, receptor endocytosis and downregulation are more prevalent with EGFR than the other members of the ErbB family[34], suggesting the importance of EGFR within the family as a the key temporal regulator of signaling. There is also increasing evidence that ErbB family members may

translocate to the nucleus and serve as transcription factors[35], although the endogenous role of this process in cellular growth remains elusive.

1.1.3 **Role of EGFR in Cancer**

EGFR has been implicated in human cancer for over twenty years[4, 36]. The main mechanisms of increased EGFR activation in oncogenesis are receptor overexpression and a shift from paracrine to autocrine signaling. Autocrine signaling occurs when a cell produces both a ligand and its receptor, as is the case in cancerous cells that often express both EGFR and its ligand, TGFα, leading to uncontrolled cell growth[37]. Expression levels of TGFα and EGFR are increased in tumor cells as well as in the adjacent "normal" mucosa[38, 39], indicating that the upregulation of these genes is an early event in carcinogenesis. Further, expression levels of both TGFα and EGFR within tumors are associated with adverse patient outcome[40], which suggests that not only is the switch to autocrine signaling an early event in carcinogenesis but also a persistent phenomenon in tumor progression.

EGFR and/or the other ErbB family members are overexpressed or otherwise implicated in many solid tumor carcinomas including esophageal, gastric, colorectal, pancreatic, hepatocellular, breast, endometrial, ovarian, prostate, lung, head and neck, and glioma[41-54]. Co-expression of EGFR with multiple members of the ErbB family is indicative of worse outcome than EGFR alone[55]. HER2 and HER3 have known oncogenic functions in several cancer types, but the role of HER4 in cancer is more controversial. Unlike other family members, HER4 is not correlated with advanced malignant phenotypes such as angiogenesis, tumor progression, or metastasis[56].

1.1.3.1 EGFR in Squamous Cell Carcinoma of the Head and Neck

Head and neck cancer accounts for approximately 4% of all malignancies in the United States[57] and it is the sixth most common cancer worldwide, indicating the large public health problem presented by head and neck cancers[58]. The five year survival rate for squamous cell carcinoma of the head and neck is approximately 50% and is highly dependent on the stage at diagnosis[59]. In addition to smoking and drinking, human papillomavirus (HPV) has been implicated in a significant subset of oropharyngeal cancers, particularly in cancers that arise in patients under the age of forty-five[60]. p53 is also mutated in a large percentage of head and neck cancers[61], generally independently of HPV infection[62]. Because HPV is known to degrade p53 protein[63], these data suggest the importance of p53 as the main molecular alteration in HNSCC.

EGFR is also known to play a role in the molecular pathogenesis of HNSCC. Wild-type EGFR protein, as detected by immunohistochemistry (IHC), is found to be expressed at moderate to high levels in up to ninety percent of HNSCC tumors by IHC[64]. Transcriptional activation contributes to increased EGFR expression levels and may represent the primary mechanism of EGFR overexpression in HNSCC[65]. Elevation of EGFR at the protein level has been detected in up to ninety percent of head and neck cancer patients, and expression levels correlate with poor patient survival[66]. HER2 is expressed at moderate to low levels in HNSCC[67], and HER3 expression is increased in HNSCC as compared to normal oral epithelium[68]. HER4 is not expressed in HNSCC[69].

There are several mechanisms of regulation that may alter EGFR transcript or protein levels in HNSCC, including rates of transcription, synthesis, and degradation. Gene transcription

of EGFR is abrogated by environmental factors that inhibit autocrine signaling of the receptor through TGFα[65]. Amplifications of EGFR at the genetic level have also been reported in a fraction of HNSCC[70, 71] and seem to occur mainly in HPV-negative tumors[72]. Patients with increased gene copy numbers and/or expression levels of EGFR have a significantly higher instance of progression and poorer survival[71, 73, 74]. Furthermore, expression of TGFα in primary HNSCC tumors is associated with decreased survival indicating a role for autocrine EGFR activation in HNSCC tumorigenesis[40, 75, 76].

A well-characterized mutation of EGFR, EGFRvIII, accounts for a large amount of ligand-independent EGFR activation in HNSCC[77]. The EGFRvIII variant is a frameshift deletion in the extracellular domain of the receptor that results in constitutive activation of the receptor[78] (Figure 1-2). Since EGFRvIII is constitutively active and lacks a ligand binding domain, it may be resistant to antibodies or drugs that inhibit cellular growth in other places apart from the kinase domain of EGFR[77, 79, 80]. It is worth noting that EGFRvIII expression is lost *in vitro* in head and neck cancer cell lines so endogenous data on this variant is sparse[81]. These cumulative findings indicate an important role for EGFR in HNSCC tumorigenesis and progression.

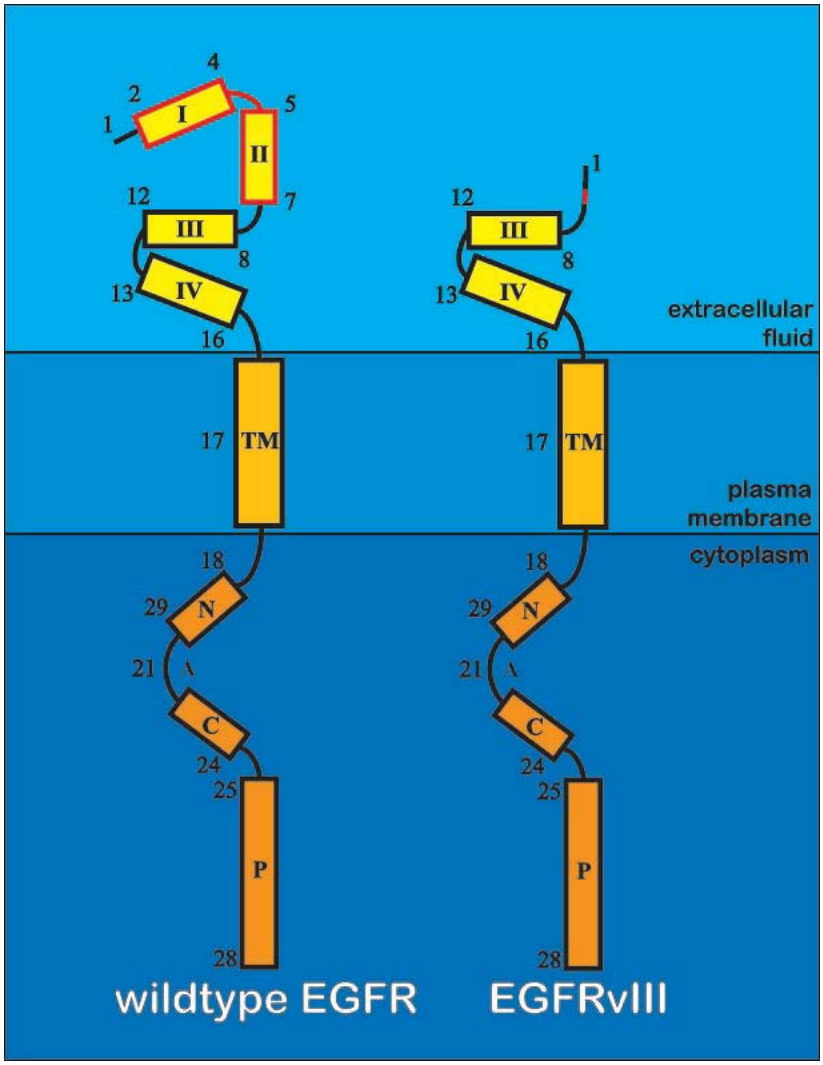

Figure 1-2. The EGFRvIII Mutation.

The EGFRvIII mutation is characterized by a frameshift mutation resulting in deletion of exons 2-7 as shown. Domains are represented as labeled rectangles with numbered exon boundaries. Abbreviations: TM=transmembrane domain; N=N-lobe; A=Activation loop; C=C-lobe; P=Autophosphorylation domain. This figure is original artwork by Kelly Quesnelle as published in Molecular Pathology: Head and Neck Cancer in Gelmann E, Sawyers C, Rauscher F (Eds), Molecular Oncology: Causes of Cancer and Targets for Treatment. New York, NY: Cambridge University Press.

1.1.4 **EGFR Signaling & Cellular Function**

EGFR signaling is involved in diverse cellular processes including growth, differentiation, and survival[82]. The main downstream signaling cascades for EGFR include: Src Family Kinases (SFK), Mitogen Activated Protein Kinases (MAPK), Signal Transducers and Activators of Transcription (STAT), and Protein Kinase B, also known as AKT (Figure 1-3).

Activated EGFR can bind and phosphorylate Src and other Src Family Kinases, which serve as oncogenic protein tyrosine kinases within the cell when activated by EGFR or other mechanisms[83]. Ligand binding to EGFR has been shown to activate STAT1, STAT3, and STAT5 via Src[84]. Additionally, EGFR has been shown to be phosphorylated by c-Src on Y845[85] and STAT5b may be activated downstream of this pathway, providing a means by which c-Src indirectly activates STAT5b through EGFR[86]. Src is also known to activate Ras for subsequent activation of the MAPK pathway[87, 88].

STAT proteins serve as transcription factors whose target genes identified to date contribute to a broad scope of functions including proliferation, differentiation, and survival[89]. Of all the STAT proteins, STAT3 target genes have been most thoroughly investigated. STAT3 target genes involved in cell cycle regulation include those encoding CyclinD1, CyclinD3, c-Myc, $p21^{wafl}$, and p27. Vascular Endothelial Growth Factor (VEGF) is the product of a STAT3 target gene involved in angiogenesis, and MMP-2 and MMP-9 are products of STAT3 target genes that contribute to migration and invasion. STAT3 target genes involved in the inhibition

of apoptosis include Survivin, Mcl-1, and Bcl-X_L[90]. EGFR is known to activate STAT proteins directly[91] or indirectly through Src (as described above) or Janus Kinases (JAK).

The role for JAKs in ligand-induced EGFR activation of STAT3 is cell-type dependent. JAKs provide maximal activation of STAT proteins in an EGF-dependent signaling scenario. Inhibiting JAKs in breast cancer cell lines, however, only partially blocks EGF-dependent STAT protein activation, further supporting the role of Src in STAT-mediated EGFR signaling. In the absence of EGF stimulation, Src and JAK cooperate to mediate STAT3 signaling in breast cancer cell lines. However, in the presence of EGF stimulation, STAT3 is activated via EGFR and Src kinase activity is cooperative but not required[92].

Proline-rich Tyrosine Kinase 2 (PYK2) has been implicated as a co-mediator of STAT protein activation with c-Src in response to EGF stimulation. Treatment of breast cancer cells with EGF induced STAT3-mediated cell proliferation by recruiting c-Src, PYK2 and STAT3 to EGFR where STAT3 is phosphorylated at Y705[93]. Forced expression of EGFR did not, however, increase phosphorylation of STAT3 at Y705, suggesting that EGFR is required for phosphorylation at this specific residue, but is not a sufficient catalyst for this event. This could also be due to negative regulation in the MAPK pathway, where MAPK1 activation caused by EGFR activation inhibited STAT3 phosphorylation at Y705[94].

Ligand-activated EGFR commonly signals downstream to the Ras/Raf/MAPK pathway mediating cell proliferation and survival. In this pathway, Growth Factor Receptor-Bound Protein 2 (GRB2) activates Son of Sevenless (SOS), which dissociates GDP from Ras to permit GTP binding as Ras activation[95]. Ras subsequently activates Raf and PI3K, in turn, indirectly activates many proteins required for cellular growth including Nuclear Factor Kappa-light-chain-

enhancer of Activated B Cells (NF-kB), cAMP Response Element-binding (CREB), Ets-1, activator protein 1 (AP-1) and c-Myc[96]. Because there is a great deal of overlap between MAPK- and STAT-mediated signaling pathways, there is also tremendous amount of feedback between these two pathways.

In breast cancer cell lines, GRB2 and STAT3 bind to the same tyrosine phosphorylation sites on EGFR (Y1086 and Y1068), which enables further negative regulation to occur when GRB2 binds to EGFR with a higher affinity than STAT3. GRB2 has a similar regulatory effect on STAT1, but not STAT5a[97]. This is not the only scenario in which competitive binding to EGFR is shown to negatively regulate STAT protein activation. Physical interaction of STAT1 and STAT3 with EGFR occurs across multiple domains in the carboxyl terminus of EGFR. SOCS-1 and SOCS-3 also interact with the cytoplasmic domain of EGFR, likely inducing ubiquitination and degradation of ligand-bound EGFR and resulting in a decrease of STAT1 and STAT3 activation[98].

TGFα stimulates proliferation of esophageal carcinoma cell lines via autocrine signaling through EGFR, and is shown to stimulate constitutive activation of STAT3[99]. Increased STAT3 activation increases proliferation in head and neck cancer cells and is caused, at least in part, by TGFα-mediated activation of EGFR[100]. Treatment of HNSCC cell lines with TGFα has also been shown to increase activation of several Src family kinases[101].

Another large downstream signaling pathway for EGFR is the AKT pathway. AKT is localized to the membrane when it binds phosphatidylinositol 3,4,5-triphosphate (PIP_3). This membrane localization results in the subsequent phosphorylation, or activation, of AKT by phosphoinositide dependent kinase 1 (PDK1) or mammalian target of rapamycin complex 2

(mTORC2)[102]. PIP_3 is the phosphorylated form of phosphatidylinositol 4,5-bisphosphate (PIP_2). This phosphorylation is carried out by phosphoinositide-3-kinase (PI3K), which can be activated directly or indirectly by EGFR[103]. Once activated, AKT is involved in cell growth, invasion, metastasis, and resistance to apoptosis[104].

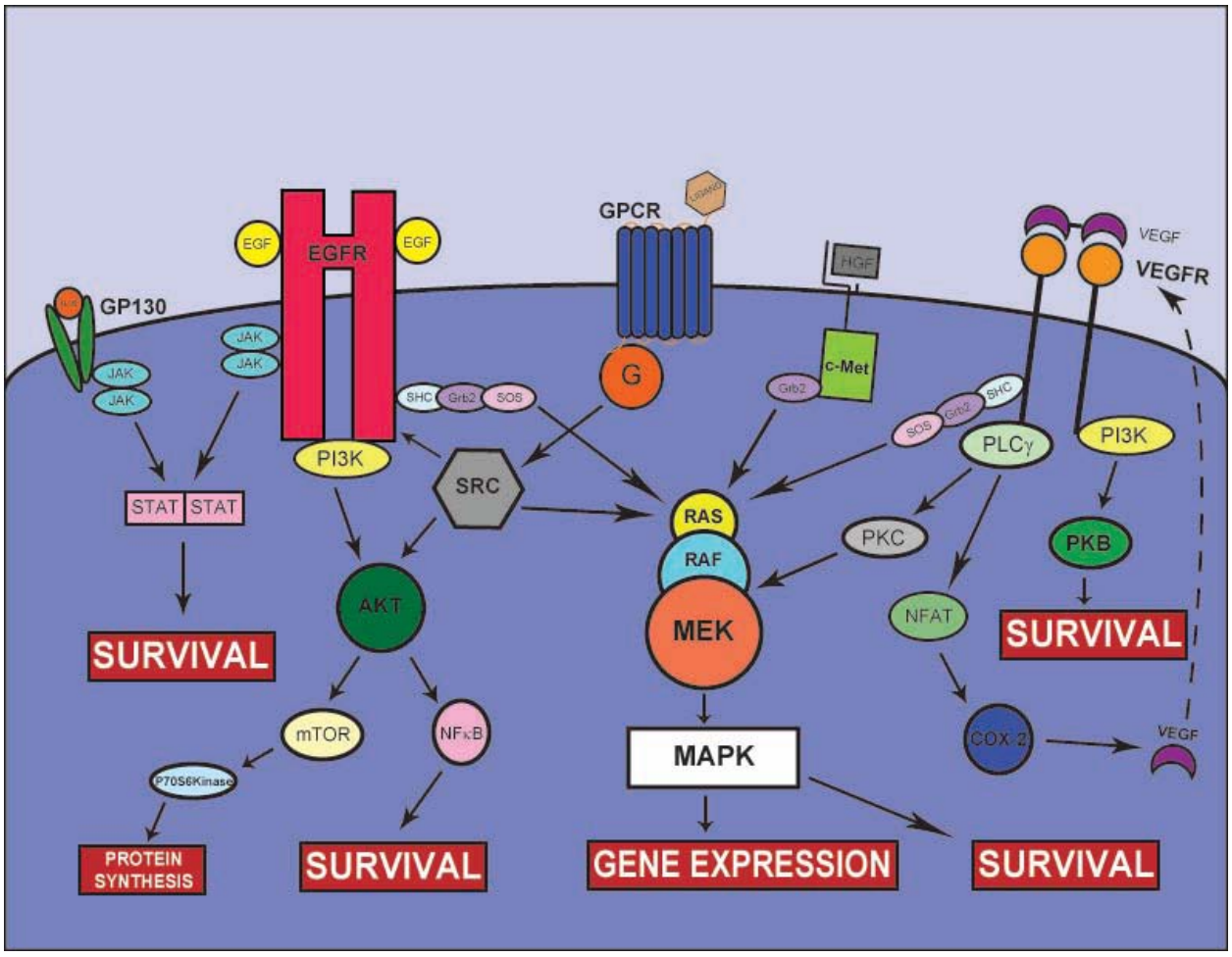

Figure 1-3. EGFR Signaling

The EGFR signaling pathway is very diverse and can be alternatively activated by several other molecules including integrins, GPCRs, c-Met, VEGF, and Src. IL-6 bound to GP130 can activate the STAT pathway. GPCRs can activate MAPK directly or activate EGFR via Src phosphorylation. Both Hepatocyte Growth Factor (HGF) and VEGF can activate the MAPK pathway independently of EGFR, the latter in an autocrine fashion. This figure is

original artwork by Kelly Quesnelle as published in Molecular Pathology: Head and Neck Cancer in Gelmann E, Sawyers C, Rauscher F (Eds), Molecular Oncology: Causes of Cancer and Targets for Treatment. New York, NY: Cambridge University Press.

1.2 PHARMACOLOGIC INHIBITON OF EGFR

There are currently two primary approaches to targeting EGFR, monoclonal antibodies against EGFR (mAb) and small molecule tyrosine kinase inhibitors (TKI) specific for EGFR. Alternative approaches to targeting EGFR include an antisense oligonucleotide of EGFR[105] and biologics and compounds that target multiple family members of the ErbB family[106]. The work in this dissertation focuses primarily on mAbs and TKIs that target EGFR since these are the most widely used EGFR-targeting agents.

1.2.1 **Tyrosine Kinase Inhibitors**

Small molecule TKIs bind directly into the adenosine triphosphate (ATP)-binding pocket of the tyrosine kinase domain thus preventing phosphate transfer and signaling[107]. There are currently two TKIs with exquisite sensitivity to EGFR that have been approved for use in the United States by the Food and Drug Administration (FDA). The first, gefitinib, was approved for use in non-small cell lung cancer (NSCLC)[108] but is currently under review for market withdrawal due to lack of clinical response and because of the approval of erlotinib, another TKI that targets EGFR[109]. Erlotinib currently has FDA-approval for use in pancreatic cancer and

NSCLC and is in late clinical development for use in head and neck cancer. It is unknown whether erlotinib and gefitinib are equally effective in the treatment of cancer, but they have similar response rates in clinical trials[110, 111]. The main advantage to erlotinib over gefitinib is FDA approval of a stronger dosing regimen for erlotinib as compared to gefitinib[112]. Despite widespread expression of EGFR in many cancer types, reported response rates to erlotinib in cancers that do not harbor EGFR mutations are modest (around 4%) when erlotinib is used as monotherapy [113] or in conjunction with other chemotherapies (around 21%)[114, 115].

EGFR mutations exist in lung cancer that enhance tumor sensitivity to gefitinib and erlotinib to roughly 75%[108, 116, 117]. The L858R mutation increases the affinity of EGFR for ATP, increasing its kinase activity by 50% compared to wild type[118]. A loss of four amino acids in exon 19, the LREA deletion, also permits enhanced kinase activity although the precise mechanisms of this activity has not been reported[119]. These two mutations account for over 90% of the EGFR inhibitor sensitizing mutations in lung cancer[112]. These mutations are not found in other cancers such as HNSCC[120].

1.2.2 **Monoclonal Antibodies**

There are currently two monoclonal antibodies approved for use in the United States by the FDA. Cetuximab, a chimeric human-mouse mAb, directly blocks the function of EGFR by binding to the ectodomain and preventing ligand binding and subsequent receptor activation[121, 122]. Cetuximab is also capable of activating an anti-tumor immune response termed antibody-dependent cell mediated cytotoxicity (ADCC)[123, 124]. Cetuximab increases responsiveness of head and neck cancer patients to radiation therapy from 64% with radiation alone to 74% with radiation plus cetuximab[125]. Likewise, cetuximab increases responsiveness of head and neck

tumors to other chemotherapies. A response rate of 20% is observed with other chemotherapies alone and this increased to 36% when cetuximab added to the treatment regimen[126]. When used as a monotherapy, however, the response rate to cetuximab alone is a modest 10-13%[127]. Cetuximab is currently FDA approved for use in head and neck cancer and colorectal cancer[125, 128].

Panitumumab is a fully humanized EGFR monoclonal antibody against EGFR that differs in its isotype (IgG_2) from cetuximab (IgG_1), which leads to different mechanisms of immune-mediated cell death. Namely, panitumumab does not activate ADCC in the same way that cetuximab does due their differing isotypes[129]. Panitumumab is currently approved for use in colorectal cancer and has response rates around 10%[130].

Mutations that are known to confer sensitivity to EGFR-targeting TKIs do not seem to play a role in altering sensitivity to EGFR mAbs in clinical trials[131, 132]. Preclinical data is more variable, however. Animal studies show enhanced sensitivity to cetuximab in the context of the L858R mutation[133, 134], but no benefit is seen when cetuximab is administered in the setting of exon 19 deletion[134].

Taken together, monotherapy data from mAbs and TKIs targeting EGFR suggest that EGFR targeting alone may not be as effective as predicted by the widespread expression and activation of EGFR. Further, there does not appear to be a consistent biomarker or mutation that can predict response to these agents in many solid tumor types[125, 135] as mutations in the tyrosine kinase domain of EGFR that confer sensitivity to EGFR-targeting agents in lung cancer are not present in all cancer types[136].

1.3 RESISTANCE TO EGFR INHIBITORS

1.3.1 **Primary Resistance to EGFR Inhibitors**

Primary resistance, or *de novo* resistance, occurs when a tumor never responds to certain chemotherapy. Primary resistance is known to occur with both erlotinib and cetuximab, and also in the context of EGFR-activating mutations despite their increased response rate to EGFR TKIs. While nearly 75% of EGFR mutant tumors respond to EGFR TKIs, 25% of mutant NSCLCs demonstrate primary resistance[137]. Most tumors, apart from a subset of NSCLC, lack EGFR sensitizing mutations and are not responsive to EGFR TKIs at all[138].

There are very few trials where cetuximab has been used as a monotherapy based on the general lack of response to its use in this manner. Monotherapy response rates to cetuximab are stagnant around 10% in both head and neck and colorectal cancer, indicating that some 90% of patients do not respond to cetuximab when used as a monotherapy[127, 139]. Combination treatments are the most successful when cetuximab is combined with radiation, but even in these cases 25% of patients do not respond to cetuximab[125].

1.3.2 **Acquired Resistance to EGFR Inhibitors**

Acquired resistance to EGFR TKIs is a phenomenon that occurs in virtually all patients treated with EGFR TKIs, despite the presence of EGFR sensitizing mutations in NSCLC[140]. The following definition of acquired resistance to an EGFR inhibitor was presented by Jackman, Pao, Engleman, Kris, Janne, Lynch, Johnson, and Miller for use in NSCLC[141]:

"We propose the following criteria be used to define more precisely acquired resistance to EGFR TKIs. All patients should have the following criteria: previous treatment with a single-agent EGFR TKI (e.g., gefitinib or erlotinib); either or both of the following: a tumor that harbors an EGFR mutation known to be associated with drug sensitivity or objective clinical benefit from treatment with an EGFR TKI; systemic progression of disease…while on continuous treatment with gefitinib or erlotinib within the last 30 days; and no intervening systemic therapy between cessation of gefitinib or erlotinib and initiation of new therapy."

Acquired resistance to cetuximab is a common occurrence, although not one that is (literally) defined as well as acquired resistance to EGFR TKIs. The phenomenon of disease progression during treatment with cetuximab is documented, however. One recent study described disease progression in 298/599 patients (49.7%) receiving cetuximab plus chemotherapy for front-line treatment of metastatic colorectal cancer[142]. The study authors observed, on average, an increase in time to progression of 1.2 months when cetuximab is added to the standard, front-line treatment regimen for metastatic colorectal cancers that lack mutations known to alter response to EGFR targeting agents. Again, these data along with other studies demonstrate the widespread phenomenon of acquired resistance to cetuximab.

1.3.3 **Somatic Mutations & Gene Amplifications Associated with Resistance to EGFR Inhibitors**

The most common genetic alteration resulting in resistance to EGFR inhibitors is the T790M mutation in lung cancer. This "gatekeeper" mutation replaces the drug-permissive threonine in the catalytic cleft of EGFR with a bulkier methionine residue to prevent binding of EGFR TKIs to EGFR. The T790M mutation occurs as a secondary mutation in approximately

50% of NSCLC tumors that harbor EGFR activating mutations[140, 143]. Rarely, the T790M mutation occurs in patients with lung cancer who have not been treated previously with an EGFR TKI[144]. Recent studies show that 2/369 (0.54%) patients with NSCLC who have not had prior treatment with EGFR TKI appear to harbor T790M mutations[145], and there is evidence to suggest that this mutation confers enhanced kinase activity in addition to TKI resistance[146]. Importantly, there is no evidence that this mutation occurs in any cancer type other than NSCLC[120].

Mutations are also known to occur in the GTPase domain of K-Ras, both in NSCLC and in colon cancer. These activating K-Ras mutations obviate the need for EGFR signaling to drive cell growth in tumors and, as such, confer resistance to both EGFR TKI and mAbs. In NSCLC, K-Ras mutation occurs in 15-25% of tumors with wild type EGFR and are associated with primary resistance to EGFR TKIs[147]. In lung cancer, K-Ras mutations occur at a rate of 43% and are associated with primary resistance to mAbs[148, 149]. K-Ras mutations are rare in HNSCC and other cancers and have not been associated with resistance to EGFR inhibitors in these cancer types[150].

Finally, genomic amplification of c-Met has been identified as a mechanism of resistance to EGFR TKI in both EGFR wild type and EGFR-L8585R lung cancer. In NSCLC tumors, c-Met is amplified at a rate of 22% in EGFR-TKI resistant tumors harboring the EGFR-L858R mutation[151]. c-Met amplification can also occur at rates up to 5% in NSCLC tumors with wild type EGFR and wild type K-Ras[152].

1.3.4 **Signaling Mechanisms of Resistance to EGFR Inhibitors**

Pinpointing mechanisms of resistance to EGFR-targeted therapy has proven difficult. EGFR signaling is promiscuous (Figure 1-3) and no consistent genetic alteration appears to confer resistance or sensitivity to EGFR targeting agents. EGFR mediates some of the most potent and redundant signaling pathways in cancer cells, including the MAPK, AKT, and JAK/STAT pathways. These pathways can be activated by cytokines or other growth factors[153] (Figure 1-3). Additionally, GPCRs can provide a means of resistance to EGFR-targeted antibodies by activating the autophosphorylation domains of EGFR directly[21].

Combination therapies that target two or more molecules involved in oncogenesis may prove to be the most efficacious modality when trying to limit off-target side effects. *In vitro* studies have suggested that alternative signaling may drive resistance to EGFR tyrosine kinase inhibitors in some cancers due to the redundancy of growth factor receptors on intracellular signaling cascades[154-156]. c-Met, the hepatocyte growth factor receptor, contributes to TKI resistance in lung cancer by activating MAPK in an EGFR-independent fashion[157] and is over expressed in many cancer types including HNSCC[158]. Increased activation of c-Met mediated by HGF has been shown to cause primary resistance to EGFR TKIs in EGFR mutant lung cancer[159, 160]. The role of Src and c-Met and the therapeutic potential of targeting these pathways concurrently with EGFR is currently being investigated in head and neck cancers. Src is a downstream effector molecule of EGFR in both the AKT and MAPK pathways that can be activated by other kinases, such as c-Met, independent of EGFR. Dimerization with HER2 or HER3 has also been identified as a mechanism of resistance to inhibitors targeting EGFR[154]. EGFR targeting in conjunction with inhibitors of VEGF and/or GPCRs are also ongoing. As the

molecular scaffolding underlying EGFR signaling becomes better understood, these combination therapies will continue to evolve.

1.4 RATIONALE, HYPOTHESIS, AND SPECIFIC AIMS

1.4.1 **Rationale & Hypothesis**

Despite ubiquitous expression of EGFR in HNSCC, FDA-approved agents targeting EGFR are only effective in a subset of patients, suggesting that alternative signaling mechanisms may be activated in the setting of EGFR blockade. There are currently no known HNSCC mutations that can serve as the basis for prospectively identifying patients who are likely to benefit from EGFR targeting. While results of one trial suggested that lower expression levels of EGFR correlated with response to cetuximab when administered in combination with cisplatin chemotherapy, other studies have failed to corroborate this association[125, 135]. HPV-positive HNSCCs have a better prognosis, regardless of therapy, but no association between HPV and response to EGFR-targeting agents has been reported.

Elucidation of mechanisms of resistance to EGFR inhibitors has been limited by: 1) the difficulty in obtaining post-treatment tissue from patients treated with EGFR inhibitors; and 2) the paucity of preclinical models of EGFR inhibitor resistance. Two preclinical models of resistance to EGFR-targeting agents are reported. One model is frequently generated in the literature and consists of cell clones selected for gefitinib resistance[161, 162] and the other is cell clones selected for cetuximab resistance from Dr. Paul Harari at the University of Wisconsin[162, 163]. Both of these models were generated by prolonged exposure to EGFR

inhibition *in vitro* and the cetuximab resistant model has not been consistent *in vivo*[162, 164]. Therefore, to determine mechanisms of EGFR inhibitor resistance, additional preclinical models are needed.

HNSCC represents an ideal model in which to study such mechanisms since two major classes of EGFR-targeting agents are either FDA-approved (cetuximab, monoclonal antibody) or under clinical investigation (erlotinib, tyrosine kinase inhibitor, TKI). **I hypothesize that signaling through alternative pathways including c-Met, HER2, and/or HER3, is associated with resistance to EGFR-targeting agents.** I propose to generate preclinical models of resistance to EGFR inhibitors to identify biomarkers or pathways associated with EGFR inhibitor resistance that can be targeted to enhance response to EGFR blockade. I plan to accomplish these goals by addressing the following specific aims:

1.4.2 **Specific Aim 1: To Examine the Role of c-Met, HER2 and HER3 in EGFR-Targeting Antibody Resistance**

Published literature suggests increased phosphorylation of HER2 and HER3 in cetuximab-resistant models[163]. I will generate *in vivo* models of acquired resistance to cetuximab. Cetuximab-resistant cells will be stably transfected with HER2 and/or HER3 shRNA to determine the contribution of HER2 and/or HER3 signaling to the cetuximab resistance phenotype. Interrogation of signaling molecules downstream of HER2 and/or HER3, along with combination targeting of EGFR, HER2, and/or HER3 both *in vitro* and *in vivo*, will elucidate downstream signaling pathways that can be inhibited to overcome cetuximab resistance. Forced

expression of HER2 and/or HER3 will determine if either or both of these ErbB receptors are sufficient for cetuximab-resistance in HNSCC. Differences in c-Met protein expression and/or phosphorylation will also be assessed in these models.

1.4.3 **Specific Aim2: To Examine the Role of c-Met, HER2, and HER3 in EGFR Kinase Inhibitor Resistance**

My preliminary results indicate increased phosphorylation of c-Met in TKI-resistant cells and a subsequent enhanced sensitivity to c-Met kinase inhibitors in these cells. The role of c-Met in mediating response to EGFR TKI will be determined using c-Met siRNA *in vitro* and by targeting c-Met in TKI-resistant xenografts *in vivo*. Forced expression of c-Met will be examined to determine if c-Met is sufficient for TKI resistance in HNSCC. Differences in HER2 and HER3 protein expression and/or phosphorylation will also be assessed in these models.

2.0 PRECLINICAL MODELING OF EGFR INHIBITOR RESISTANCE

2.1 INTRODUCTION

Valid preclinical models of EGFR inhibitor resistance are a prerequisite for understanding the molecular mechanisms that may contribute to such resistance. In these studies we sought to probe a panel of HNSCC cell lines for their response to the EGFR targeting agents erlotinib and cetuximab with the goal of generating preclinical models of resistance to these agents.

2.1.1 **Modeling Erlotinib Resistance**

Several groups have generated models of acquired resistance to erlotinib using HNSCC cells[158, 162]. These models have been created by exposing an erlotinib-sensitive cancer cell line to increasing concentrations of erlotinib *in vitro* over an extended period of time. This serves as a means by which to study acquired resistance to erlotinib, which is thought to occur eventually in nearly all patients who are treated with erlotinib (Paragraph 1.3.2).

Studies suggest that the majority of EGFR expressing tumors, however, demonstrate primary resistance to EGFR TKIs (Paragraph 1.3.1). Modeling primary resistance to erlotinib in preclinical models has been challenging due to the relatively arbitrary nature of establishing dose thresholds for erlotinib response using *in vitro* cell systems. Many breast and lung cancer cell

lines demonstrate IC_{50}s values that are below 10μM for erlotinib whereas acquired models of erlotinib resistance typically have IC_{50}s values exceeding 10μM[165, 166]. The intratumoral concentration of erlotinib has not been reported, however, so defining any threshold of resistance *in vitro* is subjective and may not be representative of patient response.

2.1.2 **Modeling Cetuximab Resistance**

Approximately 25% of patients have primary resistance to cetuximab when used with radiation (Paragraph 1.3.1) and there are published preclinical models of this type in gastric cancer[167] and lung cancer[168] but currently no preclinical models of primary resistance in HNSCC have been published to date. This may be due to challenges of detecting growth inhibition with cetuximab treatment *in vitro.* Cetuximab produces strong anti-tumor effects on human cancer cells *in vivo*[169, 170], but it has sub-optimal anti-proliferative effects *in vitro*[171, 172] and is best modeled *in vitro* using invasion assays[173].

Alternatively, estimates suggest that acquired resistance to cetuximab occurs in roughly 50% of wild-type K-Ras patients with colon cancer receiving cetuximab (Paragraph 1.3.2). Such resistance is traditionally modeled by growing cells *in vitro* under chronic exposure to increasing concentrations of drug to select for cells that can grow in the presence of cetuximab. This approach has been used to generate models of resistance to cetuximab in lung cancer[163] and HNSCC, although the reproducibility of these models has been challenging[164].

Efforts to generate models of cetuximab resistance from wild type tissues *in vivo* have been unsuccessful to date. One group was able to generate xenografts derived from a colon cancer cell line that re-grew in the presence of cetuximab, but these tumors were generated from

a cell line known to harbor an activating K-Ras mutation[174, 175]. Another group generated an *in vivo* model of cetuximab resistance but was unable to culture cells from their cetuximab resistant xenografts[171]. A consistent preclinical model of cetuximab resistance would enable us to better elucidate the mechanisms driving this resistance and could serve as a tool with which to probe combination therapies that may enhance the efficacy of cetuximab.

2.2 MATERIALS AND METHODS

2.2.1 **Cells and Reagents**

SCC1 was derived from a primary HNSCC tumor and both SCC1 and the cetuximab-resistant clone SCC1c8 were maintained in Dulbecco's Modified Eagle Medium (DMEM) with 10% fetal bovine serum (FBS) and 0.4ug/mL hydrocortisone [163]. HN-5, OSC-19, PCI-52, UM-22A, CAL33, 1483, and CAL27 are primary HNSCC cell lines and UM-22B, 686LN, and PCI-15B are derived from metastatic cervical lymph nodes from patients with HNSCC[176]. OSC-19 cells were maintained in Modified Eagle Medium (MEM) with 10% FBS and 1% non-essential amino acids. HN-5 and 686LN cells were maintained in DMEM/F-12 + 10% FBS. PCI-52, PCI-15B, UM-22A, UM-22B, CAL33, 1483, CAL27, T24, and A431 cells were maintained in DMEM + 10% FBS. T24 is derived from a transitional bladder carcinoma[177] and A431 is an epidermoid carcinoma of the vulva[178]. UM-22A and UM-22B cells were a generous gift from Dr. Tom Carey (University of Michigan) and PCI-52 and PCI-15B cells were a generous gift from Dr. Theresa Whiteside (University of Pittsburgh). HeLa cells are a cervical cancer cell line maintained in DMEM + 10% FBS[179]. All cell lines were validated by

genotyping within 6 months of their use using the AmpFISTR Identifiler System (Applied Biosystems). Cetuximab-resistant clones were maintained in media with 100nM cetuximab. Cetuximab (Erbitux, ImClone Systems and Bristol-Myers Squibb) was purchased from the University of Pittsburgh Pharmacy. Afatinib was obtained from Boehringer Ingelheim as a powder and resuspended in DMSO for *in vitro* studies or 0.5% methylcellulose with 0.4% tween 80 in saline for animal studies. Trastuzumab (Herceptin, Genentech) was purchased from the University of Pittsburgh Pharmacy and diluted as recommended in the package insert. Erlotinib was purchased from Chemietek and resuspended in DMSO for cell studies and methyl cellulose for animal studies.

2.2.2 **Cell Line Xenograft Modeling**

Subcutaneous xenografts were generated from six different epithelial cancer cell lines (T24, CAL33, A431, OSC-19, SCC1, and SCC1c8) (n=6 for all cell lines except T24 where n=12) in athymic nude mice using one million cells with Matrigel (BD Biosciences). After tumor formation (7-10 days), mice received 0.8mg of cetuximab by intraperitoneal (i.p.) injection twice weekly. Tumors were measured twice weekly. If tumors progressed after 14 days of treatment, dosing was increased to 1.0mg of cetuximab twice weekly and then 0.8mg of cetuximab three times per week after 28 days. If no tumors were present, the animal was sacrificed after 90 days of treatment. If tumors were present, the animal was sacrificed at 90 days or when the tumor diameter exceeded 20mm. Tumors were removed, digested, and suspended as single cells, which were propagated in culture and re-inoculated as two subcutaneous xenografts. These tumors were treated with 0.8mg of cetuximab three times per week immediately following tumor formation.

For the HNSCC cetuximab model generation, subcutaneous xenografts were created from PCI-52, UM-22A, UM-22B, CAL27, HN-5, 1483, OSC-19, SCC1, SCC1c8, and CAL33 cell lines. Two million cells were inoculated subcutaneously onto each flank of athymic nude mice (n=6 xenografts per cell line). Cetuximab treatment was initiated at 0.2mg twice weekly by i.p. injection immediately following tumor formation (generally 7-14 days post-inoculation) for PCI-52, UM-22A, CAL27, HN-5, 1483, OSC-19, SCC1, and SCC1c8 cells. Cetuximab treatment was initiated by i.p. injection at 0.02mg twice weekly in UM-22B cells once median tumor volume exceeded $50mm^3$ (generally 7-14 days post-inoculation). After the first week at these doses, cetuximab dose was increased to 0.04mg five times per week. After two weeks at this dose, cetuximab dose was increased to 0.2mg twice weekly for the remainder of the study. Cetuximab treatment was initiated at 0.02mg twice weekly by i.p. injection in CAL33 cells once the median tumor volume exceeded $300mm^3$ (generally 7-14 days post-inoculation). Cetuximab dosing was increased to 0.04mg twice weekly after one the first week of treatment and 0.08mg twice weekly after the second week of treatment. Following two weeks of treatment at 0.08mg twice weekly, cetuximab dose was increased to 0.2mg twice weekly for the remainder of the study. A summary of the dosing scheme is provided (Table 2-1).

2.2.3 **HNSCC Tumorgraft Modeling**

For HNSCC tumorgraft model generation, tumors were generated as follows. Following HNSCC tumor resection, patient samples were quality controlled by the University of Pittsburgh Medical Center's Department of Pathology for 70% tumor composition, de-identified, and delivered in antibiotic/antimycotic solution. Tissues were collected under the auspices of a tissue bank protocol approved by the University of Pittsburgh Institutional Review Board. Tumor

samples were cut into 25mg pieces and fresh frozen or used for implantation. Non-obese diabetic/severe combined immunodeficiency (NOD/SCID) mice that are interleukin 2R gamma null (Jackson Laboratories; Bar Harbor, ME) were anesthetized using isofluorane and a small incision made in the flank. 25mg of patient tumor was placed in the pocket of the incision site and the wound closed with surgical adhesive. Analgesic was administered and the animals were monitored until fully ambulatory. Mice were kept in isolation for 7-10 days and checked daily for wound healing. Mice were checked weekly for tumor formation.

Once tumor size reached approximately $50mm^3$, generally 4-6 weeks after surgery, mice were treated with 0.02mg of cetuximab by i.p. injection twice weekly. These tumors can be referred to as passage 1. When tumor size increased beyond the maximum allowable size under IACUC guidelines, the animals were sacrificed and 25mg of the tumor was used to create new tumorgrafts in 2-4 animals as described above, this time termed passage 2. This process was repeated and the data shown here are from passage 3. Passage 2 tumors received cetuximab at 0.04mg of cetuximab twice weekly. Passage 3 tumors received cetuximab initially at 0.08mg twice weekly, then this dose was increased to 0.2mg twice weekly.

2.2.4 **Single Agent Treatment Animal Studies**

For the differential sensitivity study using T24 and T24PR3 cells treated with cetuximab, one million parental and resistant cells were blindly injected on opposite flanks of the same mouse (n=7 mice) with Matrigel. Treatment began following tumor formation. Animals were treated with 2.0mg of cetuximab three times weekly by i.p. injection.

For the differential sensitivity study using CAL33 and CAL33B cells treated with cetuximab, two million CAL33 or CAL33B cells were blindly injected on opposite flanks of the same mouse (n=5 mice). Treatment began once median tumor volume exceeded $50mm^3$ (generally 7-14 days post-inoculation). Animals were treated with 0.2mg of cetuximab twice weekly by i.p. injection.

For the comparative studies using erlotinib and cetuximab to treat xenografts derived from 686LN and HeLa cells, one million cells were injected subcutaneously with Matrigel (BD Biosciences). 686LN and HeLa cells were inoculated on opposite flanks of athymic nude mice (n=9 mice per treatment). Following tumor formation (7-10 days post-inoculation), animals were treated with erlotinib or cetuximab. Erlotinib was administered at 50mg/kg five times per week by oral gavage. Cetuximab was administered as 1.0mg twice weekly by i.p. injection.

2.2.5 **Metabolic Activity Assays**

Cells were plated to 50% confluency a 24-well plate. Media was changed to contain new media and the appropriate drug or control at 24 hours. 3-(4,5-Dimethylthiazol-2-Yl)-2,5-Diphenyltetrazolium Bromide (MTT) was added for 30 minutes 72 hours following drug treatment. Cells were rinsed with phosphate buffered saline (PBS) and lysed with dimethyl sulfoxide (DMSO). DMSO extracts were measured at 570nm in an uQuant spectrophotometer to determine formazan production versus standard controls. Each drug treatment or control was run in triplicate wells and the data shown here is the result of three independent experiments.

2.2.6 **Flow Cytometry**

Flow cytometry was conducted at the UPCI Flow Cytometry Core Facility using a Beckman Coulter MoFlo High Speed Sorter. α-EGFR (ab-Cam) was labeled with Alexa Fluor488 (Invitrogen) and cells were counter-stained with Propidium Iodine. Propidium-Iodine labeled cells were excluded from analysis, then cells were bracketed to capture a low percentage tail population of EGFR-null cells on 686LN. These same brackets were applied to the HeLa cell line and gated events were calculated from 50,000 live events for each cell line.

2.2.7 **Immunoblotting**

Immunoblots were performed on cell lysates collected at 70-80% confluency in normal growth media. Lysates were resolved on sodium dodecyl sulfate polyacrylamide gel electrophoresis (SDS-PAGE) gels and transferred to nitrocellulose membranes prior to antibody staining (EGFR, BD Transduction Lab; pAKT and AKT, Cell Signaling). Densitometry was performed using Image J.

2.2.8 **Invasion Assays**

Five thousand cells were plated in the inner well of a Matrigel Invasion Chamber (BD Biosciences) in serum free-media. Wells were placed into media containing 10% FBS and drugs were added to both chambers where indicated. After 24 hours, cells invading through the Matrigel coated membrane were stained and counted.

2.2.9 **Statistical Analyses**

Erlotinib relative IC_{50} with associated 95% confidence intervals were calculated using GraphPad Prism v5.0. All nonlinear regression curves for erlotinib response had an R^2 value greater than 0.70. P-values were generated for invasion assays using a homoscedastic two-tailed Student's t-Test. Nonparametric Spearman correlations were used to determine the relationship of EGFR protein levels to erlotinib IC_{50}. Statistical analysis for single agent treatment animal studies was conducted using non-paired, two-tailed student's t-tests.

2.3 RESULTS

2.3.1 **Generation of a Cetuximab-Resistant Preclinical Model**

In order to study mechanisms of cetuximab resistance, we created a preclinical model based on the previously published *in vivo* generated model of trastuzumab-resistance[180]. Subcutaneous tumor xenografts were established using five cetuximab-sensitive epithelial cancer cell lines (T24, CAL33, A431, OSC-19, SCC1) as well as one previously described cetuximab-resistant epithelial cancer cell line, SCC1c8[163]. These cell lines were chosen because we originally thought they were a panel of HNSCC cell lines (UM-22B, 1483, CAL33, OSC-19, and SCC1, SCC1c8) with the vulva carcinoma cell line, A431. A431 was the original cell line used for the discovery of cetuximab and a cetuximab sensitive control in this experiment[181]. Upon retrospective cellular genotyping, however, we determined that the UM-22B and 1483 cell lines were actually the T24 transitional bladder cancer cell line. Nevertheless, T24, CAL33, A431, OSC-19, and SCC1 are all epidermal cell lines lacking mutations that are known to confer

resistance to cetuximab, making them appropriate cell lines with which to develop resistance models.

For these experiments, xenograft-bearing athymic nude mice were treated with increasing concentrations of cetuximab over the course of three months. Animals were initially treated with moderate doses of cetuximab that are equivalent to four times that of a human dose (0.8mg twice weekly). This was increased to doses equivalent to six times the standard human dose of cetuximab (0.8mg three times per week) over the course of three months. A majority of the epithelial carcinoma-derived xenografts regressed with cetuximab treatment, including the head and neck cancer cell line SCC1 and its *in vitro* derived cetuximab resistant clone, SCC1c8 (Figure 2-1A).

While most xenografts treated with cetuximab were cetuximab-sensitive, four cetuximab-resistant tumors (T24PR1-4) emerged out of the twelve original xenografts from T24 bladder carcinoma cells (Figure 2-1A). Cetuximab-resistant tumors T24PR1-4 were surgically removed from sacrificed animals and digested into single cell suspensions that were used to generate cell lines of the same name *in vitro* and additional xenografts *in vivo*. Xenografts from the cetuximab-resistant cells persisted despite treatment with doses of cetuximab equivalent to six times the human dose of cetuximab (0.8mg three times per week) immediately upon tumor formation (generally 7-10 days post-inoculation, Figure 2-1B). The persistent growth of tumors derived from *in vivo* generated cetuximab-resistant cells as compared to *in vitro* generated cetuximab-resistant cells in high doses of cetuximab demonstrates the validity of *in vivo* generation for models of drug resistance, especially for therapeutic agents such as monoclonal antibodies that are known to have anti-tumor effects that cannot be reproduced under cell culture conditions.

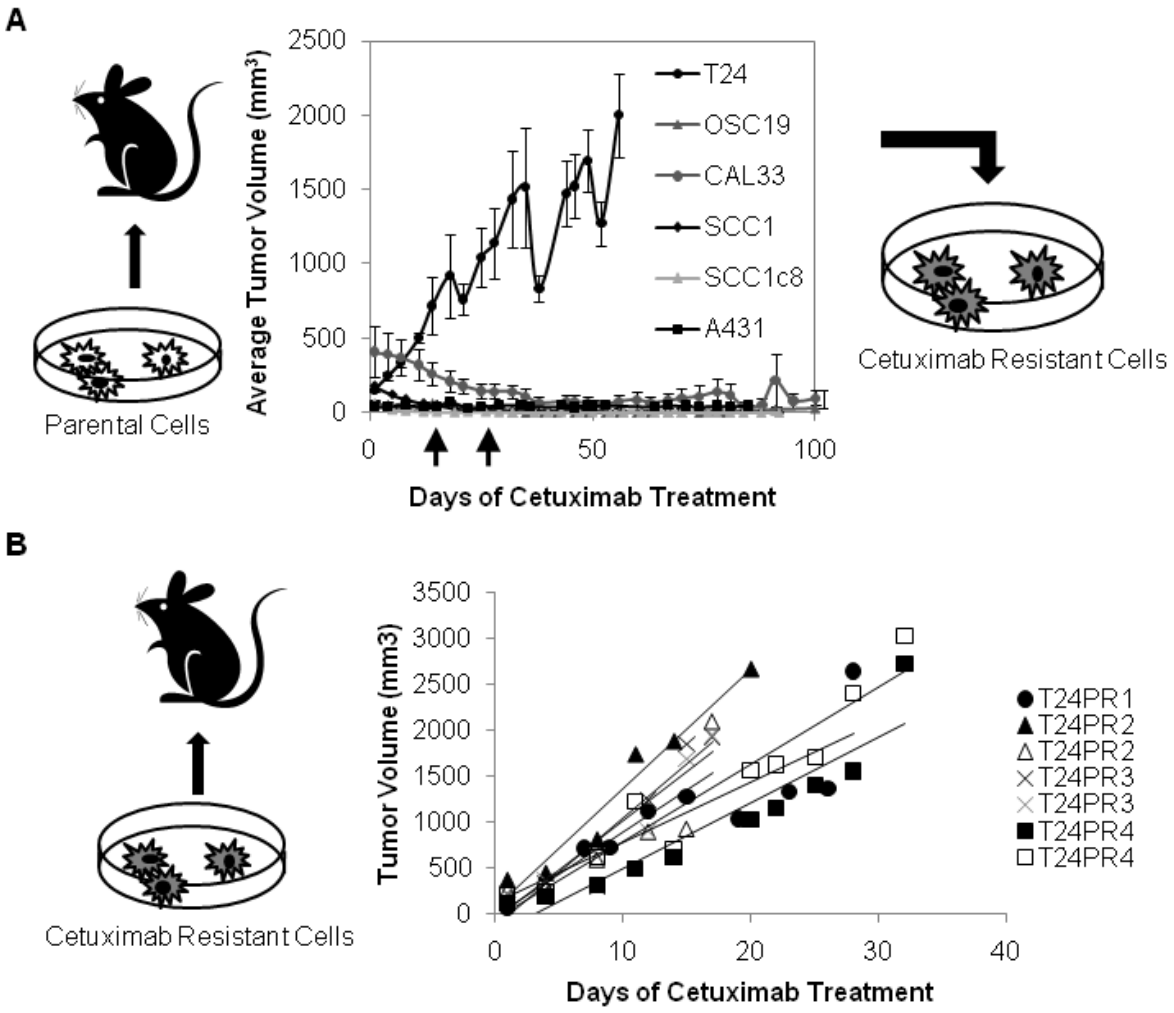

Figure 2-1. Generation of a cetuximab-resistant bladder cancer model *in vivo.*

A. T24, CAL33, A431, OSC-19, SCC1, and SCC1c8 cells were used to generate xenografts in athymic nude mice (n=6 for CAL33, A431, OSC-19, SCC1 and SCC1c8; n=12 for T24) that were exposed to increasing concentrations of cetuximab by i.p. injection (0.8mg 2x/week increased to 1.0mg 2x/week then increased to 0.8mg 3x/week; doses increased in non-responsive xenografts only as indicated by arrows). Resistant tumor cells were then harvested and propagated in culture and **B.** re-inoculated to form xenografts that were treated with 0.8mg 3x/week immediately following tumor formation.

To distinguish acquired resistance to cetuximab from intrinsic resistance, we compared cetuximab sensitivity between the cetuximab-sensitive parental cells and the cetuximab-resistant clones. To test this *in vivo*, athymic nude mice (n=7 mice) were inoculated with sensitive cells on one flank and resistant cells on another flank. Following tumor formation, animals were randomized based on tumor volumes and treated with high concentrations of cetuximab (2.0mg three times per week). Cetuximab-sensitive tumors demonstrated a 64.8% reduction in tumor volume on day 10 of cetuximab treatment compared to a 3.9-fold increase in cetuximab-resistant tumor volumes on day 10 of cetuximab treatment (p=0.002, Figure 2-2A). Tumors were harvested after ten days of cetuximab treatment, frozen, fixed, cryosectioned and TUNEL-stained to detect apoptotic cells. 61.7% of cells from cetuximab-sensitive tumors (T24) were apoptotic compared to only 26.3% of the cells from tumors derived from cetuximab resistant cells (T24PR3, Figure 2-2A, p=0.03). These results demonstrate that by gradually increasing the dose of cetuximab *in vivo* over the course of 28 days, cetuximab resistant tumors can be generated.

To demonstrate the differential cetuximab sensitivity of this model *in vitro*, we performed invasion assays since cetuximab does not inhibit proliferation *in vitro*[172]. Cetuximab has been previously reported by us and others to successfully decrease cell invasion through a Matrigel coated transwell-migration chamber[182, 183]. In this model, cetuximab decreased the invasion of parental T24 cells by 55.5% after 24 hours. In contrast, cetuximab only inhibited the invasion of T24PR3 and T24PR4 cells by 1.7% (p=0.0009) and 8.7% (p=0.0001), respectively (Figure 2-2B).

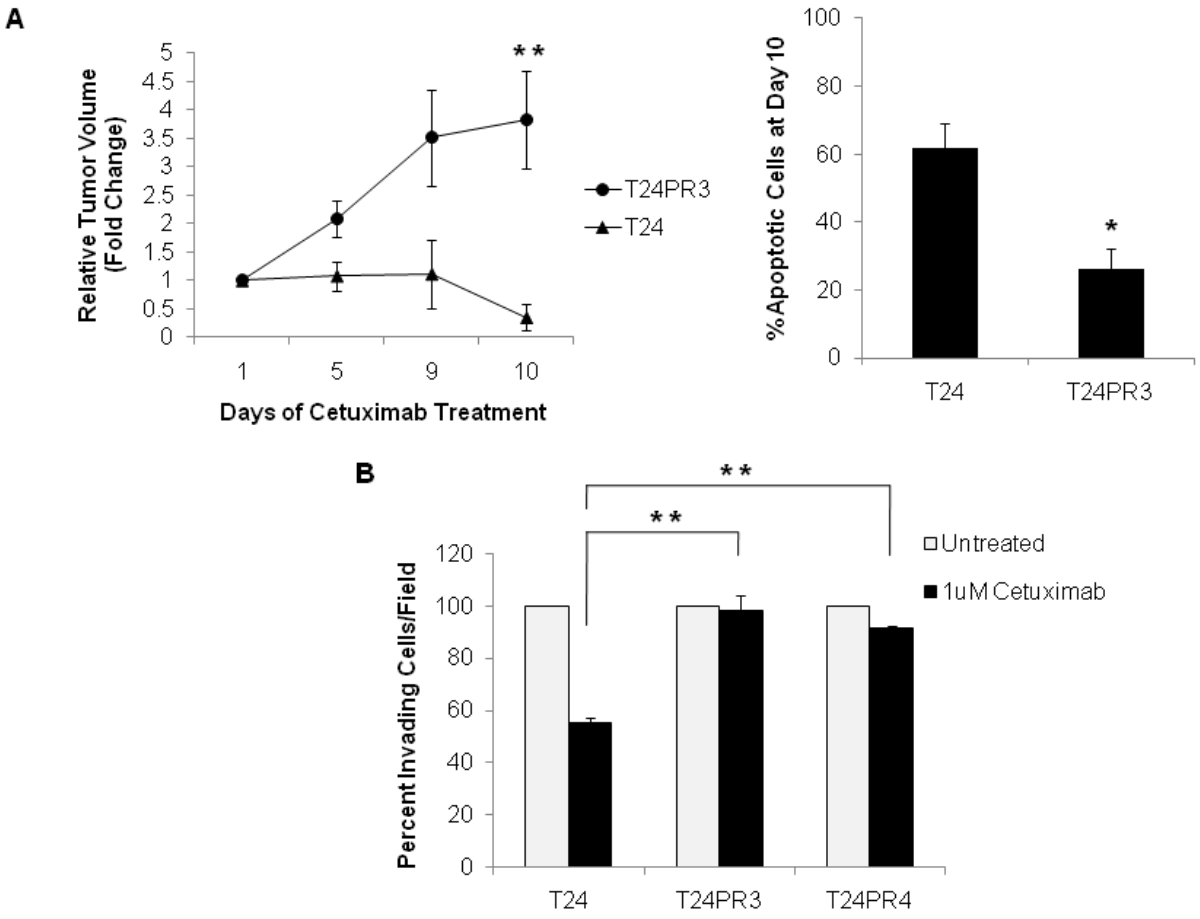

Figure 2-2. Validation of a cetuximab-resistant model *in vitro* & *in vivo.*

A. Xenografts were generated by subcutaneous inoculation of one million tumor cells in athymic nude mice (n= 7) from cetuximab-sensitive T24 or cetuximab-resistant T24PR3 cells and treated with cetuximab (2.0mg 3x/week by i.p. injection) immediately following tumor formation, generally 7-10 days (**p<0.005). TUNEL staining was performed on frozen, fixed tumors to detect apoptotic cells. Data shown is the average of cells counted in quadruplicate 20X fields of view for two tumors per cell type (*p<0.05). **B.** Invasion studies were carried out with serum-free media containing either 1μM cetuximab or drug-free media. Invasion chambers were placed in the same media containing 10% FBS. After 24 hours, invading cells were stained and counted (**p<0.005). Data are the result of two independent experiments run in duplicate.

It is worth noting that the T24 model has been previously reported to contain an Ha-Ras activating mutation[184]. Given the extensive evidence that K-Ras mutations confer resistance to cetuximab in colon cancer[148], the contribution of the H-Ras mutation to the cetuximab resistance mechanisms described in the present study remain unknown. To date, there is one published report based on *in vitro* work demonstrating that Ha-Ras is capable of conferring resistance to cetuximab by constitutively activating ERK and AKT[185]. While we believe this pathway is unlikely to contribute to the cetuximab resistance phenotype *in vivo* since the parental and the resistant cells are isogenic (both contain the mutation), we wanted to examine any differences in AKT phosphorylation between the sensitive and resistant cells. No significant changes were observed in expression of basal or phosphorylated MAPK (not shown) or AKT (Figure 2-3) between the cetuximab sensitive and cetuximab resistant clones. While T24PR4 expressed slightly decreased levels of pAKT compared to T24 ($p=0.513$), T24PR3 expressed slightly increased pAKT compared to T24 ($p=0.776$). Neither difference was statistically significant (Figure 2-3).

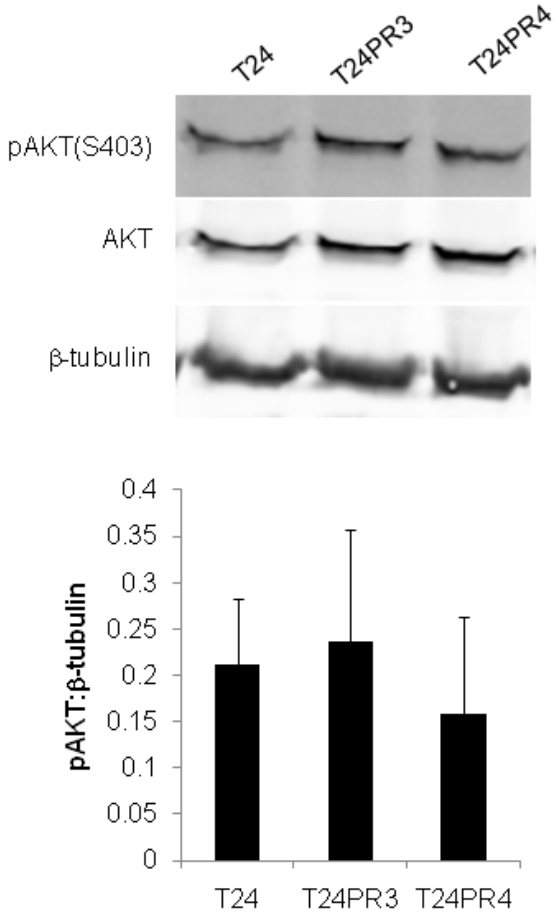

Figure 2-3. AKT is not overexpressed or hyperphosphorylated in cetuximab resistant cells.

Cell lysates were collected under basal conditions when cells reached 70% confluence. Whole cell lysates were analyzed by Western Blot and probed for p-AKT(Ser 403), AKT, and β-tubulin. Densitometry is the result of three independent experiments where intensity of the p-AKT bands was compared to β-tubulin.

2.3.2 **HNSCC Cell Lines are Highly Sensitive to Cetuximab**

Based on our success in generating a model of cetuximab resistance using bladder cancer cells, we attempted to generate models of cetuximab resistance using a similar approach in HNSCC cell lines. Because our initial studies were conducted using a starting dose of cetuximab that is equivalent to four times the human dose of cetuximab (0.8mg twice weekly in Figure 2-1A) and these studies only yielded resistant tumors from one cell line, we decided to decrease the starting dose of cetuximab to that of the therapeutic dose used in humans (0.2mg twice weekly). To that end, we attempted to generate xenografts each from eight HNSCC cell lines: PCI-52, UM-22A, HN-5, 1483, CAL27, OSC-19, SCC1, SCC1c8 (n=6 xenografts per cell line). Each of these cell lines has been reported previously in the literature to form tumors in mice[176]. The SCC1c8 cell line is the reported model of cetuximab resistance generated *in vitro* from the HNSCC cell line SCC1[163], but this cell line was not resistant to cetuximab in our previous study (Figure 2-1). Nearly all inoculations produced tumors, with the exception of the PCI-52 cell line from which only one xenograft was established (Figure 2-4).

Treatment was initiated when tumors were palpable (generally 7-14 days post-inoculation) with lower doses of cetuximab (0.2mg twice per week) than were used previously (Figure 2-1) with the rationale that treating smaller tumors with lower doses of cetuximab would facilitate the selection of resistant tumor cells more effectively than in our previous study. When treatment began, the median tumor volume was $<40mm^3$ across all tumor types (Figure 2-4). A summary of treatment schedules for the HNSCC cell line derived xenografts can be found in Table 2-1. The vast majority of tumors responded to treatment with this low dose of cetuximab. We maintained cetuximab treatment for a total of 2-3 months for each cell line xenograft model to determine the incidence of spontaneous tumor recurrence as was observed for *in vivo*

generated models of trastuzumab resistance[180]. However, no HNSCC cell line xenograft recurrence was observed.

Three tumors did demonstrate persistent growth in the presence of cetuximab treatment, one xenograft from the PCI-52 cell line (PCI-52A) and two xenografts from the OSC-19 cell line (OSC-19E & OSC-19F, Figure 2-4). We were unable to isolate any epidermal cells in culture from the PCI-52A xenograft; only fibroblasts were grown from this tumor in culture and differential digestion methods were unsuccessful to remove contaminating fibroblasts. Further, cells isolated *in vitro* from PCI-52A did not generate new xenografts when inoculated into another athymic nude mouse. Likewise, cells from the OSC-19E tumor did not prorogate in culture or as a xenograft when inoculated into another athymic nude mouse. Cells from OSC-19F failed initially to grow in culture, but they did form another small xenograft that never exceeded $15mm^3$. Efforts to propagate this secondary tumor were unsuccessful in culture or as another xenograft.

Cell Line	Treatment Initiation Requirements	Cetuximab Dose (mg) x Frequency (days per week)	Total Amount of Cetuximab Per Week (mg)	Days on Dose
PCI-52	Upon palpitation, generally 7-14 days. Median tumor volume <40mm^3.	0.2x2	0.4	35
UM-22A		0.2x2	0.4	65
CAL27		0.2x2	0.4	65
HN-5		0.2x2	0.4	80
1483		0.2x2	0.4	80
OSC-19		0.2x2	0.4	80
SCC1		0.2x2	0.4	49
SCC1c8		0.2x2	0.4	49
UM-22B	Median tumor volume >50mm^3.	0.02x2	0.04	7
		0.04x5	0.2	14
		0.2x2	0.4	14
CAL33	Median tumor volume >300mm^3.	0.02x2	0.04	7
		0.04x2	0.08	7
		0.08x2	0.16	14
		0.2x2	0.4	28

Table 2-1. Summary of cetuximab dosing in HNSCC xenograft model generation.

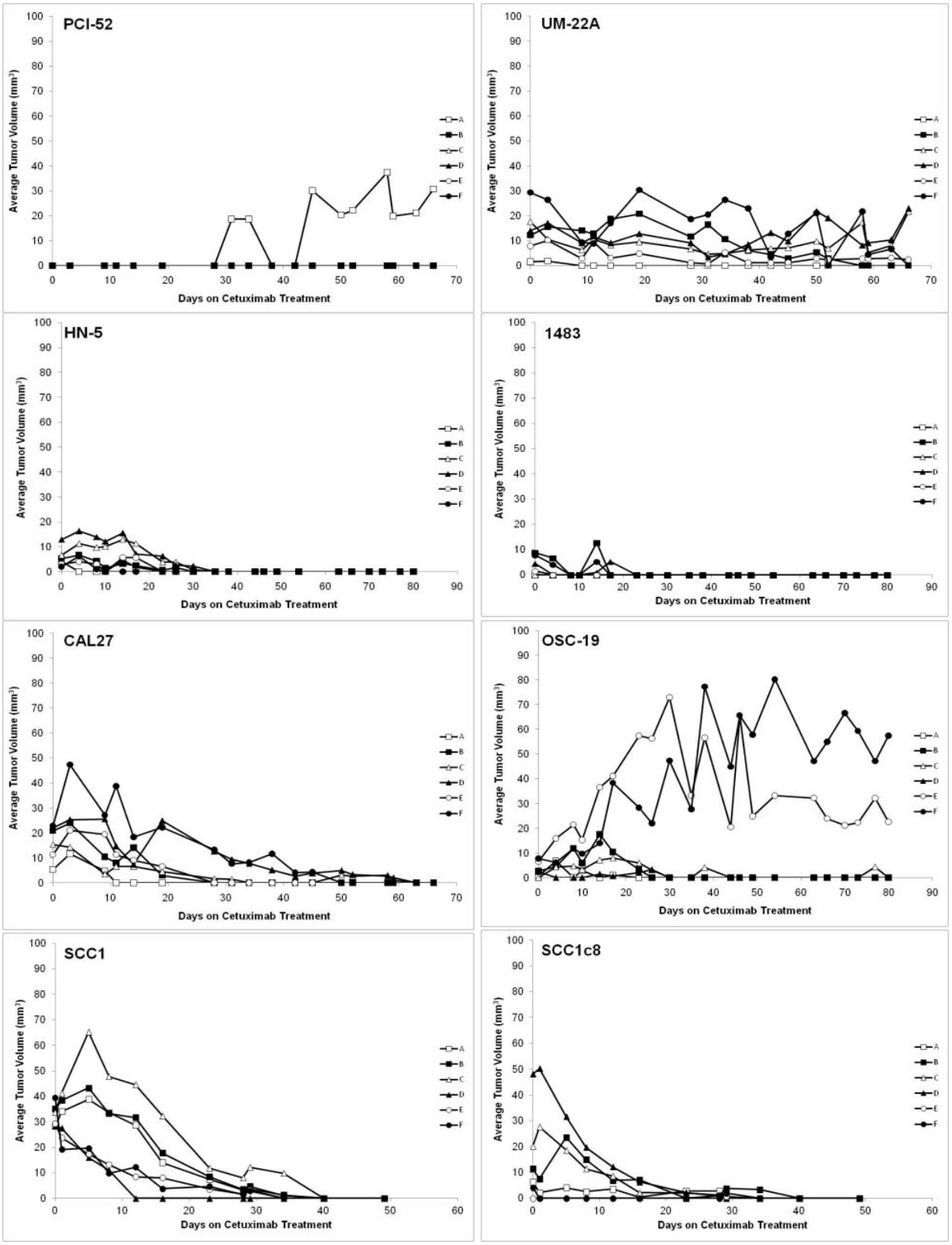

Figure 2-4. HNSCC cell lines are sensitive to cetuximab at therapeutic doses *in vivo*.

Xenografts were created in nude mice from 8 HNSCC cell lines (PCI-52, UM-22A, CAL27, HN-5, 1483, OSC-19, SCC1, SCC1c8) using two million cells per inoculation. Animals were treated with 0.2mg of cetuximab 2x/week by i.p. injection using, for 7-11 weeks as indicated. Treatment was initiated upon tumor palpitation, generally 7-14 days following inoculation. Median tumor volume at the start of treatment is less than $40mm^3$ for all cell lines.

Because these attempts at model generation were unsuccessful, we altered our methodology to include larger starting tumor volumes and lower doses of cetuximab. We attempted to generate cetuximab resistant xenografts using the UM-22B cell line with these modified conditions. We generated six xenografts using UM-22B cells, and we did not begin treatment of the animals until the median tumor volume exceeded $50mm^3$ (Figure 2-5A). We also used a sub-therapeutic dose of cetuximab for initial treatment. A summary of the treatment regimen used in this experiment can be found in Table 2-1. The animals were treated initially with approximately one-tenth the therapeutic dose of cetuximab, administered as 0.02mg twice weekly by i.p. injection. The xenografts did not respond to cetuximab at this dose during the first week of treatment. We then increased the dose of cetuximab to 0.04mg five times per week. There was a mixed response to this sub-therapeutic dose, but after two weeks at this dose no tumors had regressed completely (Figure 2-5A). Finally, we increased treatments to the therapeutic dose of cetuximab, 0.2mg twice per week. All tumors had dramatic responses to this dose of cetuximab (Figure 2-5A) but tumor regression was delayed by up to 14 days in UM-22B-derived xenografts (Figure 2-5A) compared with the other HNSCC cell line xenografts (Figure 2-4), suggesting that larger tumor volumes and sub-therapeutic doses of cetuximab may facilitate the selection of cetuximab-resistant cells.

In order to enhance the selection of cetuximab-resistant cells, we further increased tumor starting volumes and the amount of time during which animals were treated with sub-therapeutic doses of cetuximab. We did not begin treatment on the CAL33 xenografts until the median tumor volume exceeded 300mm^3. One xenograft (CAL33F) was nearly 600mm^3 when treatment began (Figure 2-5B). Further, we allowed four weeks of sub-therapeutic cetuximab administration to mice harboring CAL33-derived xenografts.

During the first seven days on treatment, animals with xenografts from CAL33 cells received 0.02mg of cetuximab twice weekly. No tumors responded to treatment at this dose. During days 7-14 of treatment, animals received 0.04mg of cetuximab twice weekly. No tumors responded to this dose of cetuximab. Animals were then given 0.8mg of cetuximab twice weekly during days 14-28 of treatment. During this two-week period, we observed dramatic reductions in tumor volume for all xenografts (Figure 2-5B). Following this month of treatment at sub-therapeutic doses, we treated animals with a therapeutic dose of cetuximab, 0.2mg twice weekly for an additional month. During this time, all tumors regressed but one tumor subsequently had spontaneous re-growth (CAL33B, Figure 2-5B). A summary of the treatment regimen used in this experiment can be found in Table 2-1.

To determine if this spontaneous re-growth was indicative of acquired cetuximab resistance, the CAL33B tumor was disaggregated and grown under cetuximab selection pressure *in vitro.* This cell strain is called CAL33AR1. Equal numbers of CAL33AR1 and CAL33 parental cells were used to generate xenografts in athymic nude mice (n=5 per cell line). Once tumor volumes exceeded 50mm^3, animals were treated with 0.2mg of cetuximab twice weekly for two weeks. After 15 days, no significant differences in tumor volumes were observed (Figure 2-5C), suggesting that this model of cetuximab resistance is not reproducible.

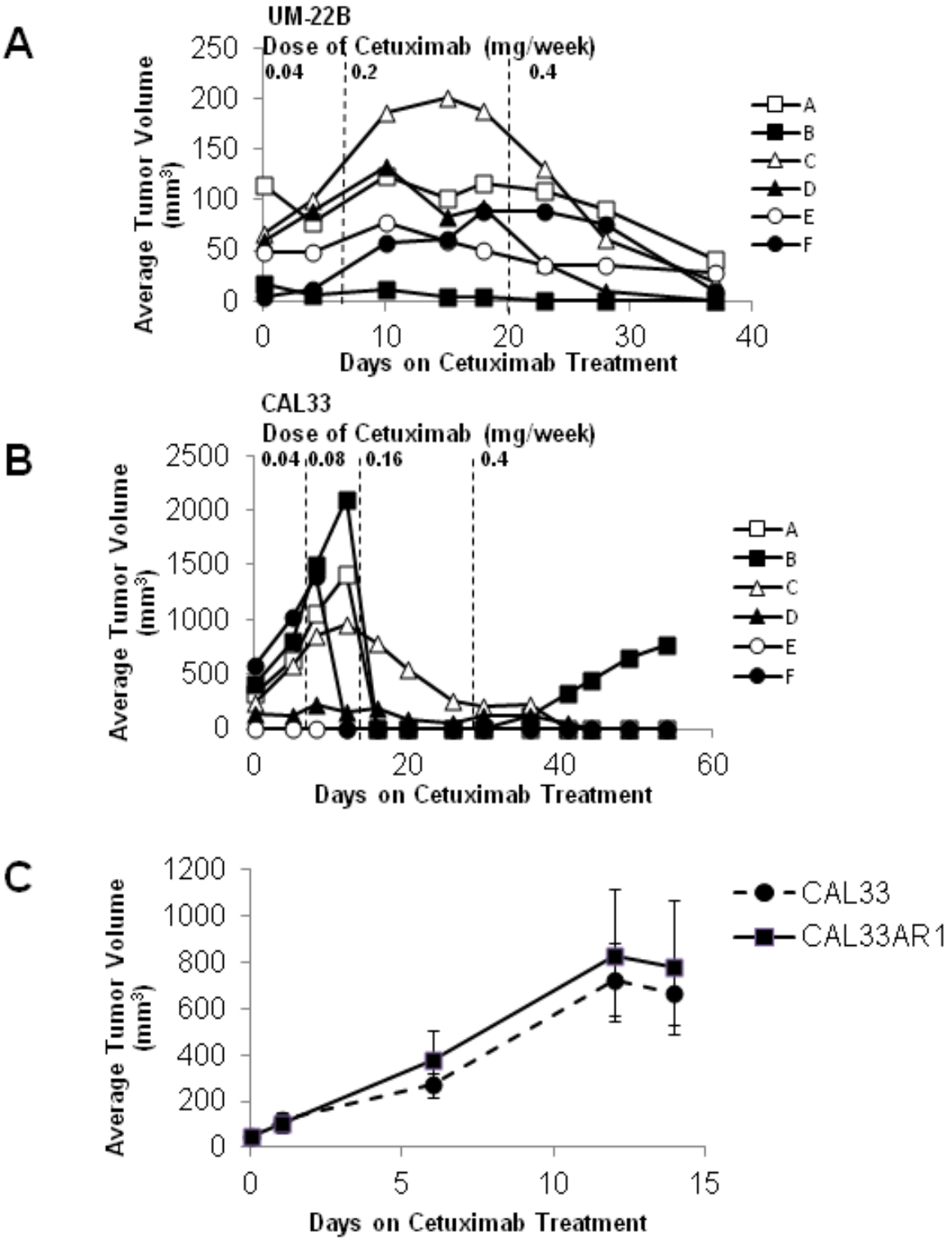
A
UM-22B
Dose of Cetuximab (mg/week)
0.04
0.2
0.4
Average Tumor Volume (mm3)
Days on Cetuximab Treatment
A
B
C
D
E
F
B
CAL33
Dose of Cetuximab (mg/week)
0.04
0.08
0.16
0.4
Average Tumor Volume (mm3)
Days on Cetuximab Treatment
C
Average Tumor Volume (mm3)
Days on Cetuximab Treatment
CAL33
CAL33AR1

Figure 2-5. HNSCC cell lines are sensitive to cetuximab at sub-therapeutic doses *in vivo.*

A. Xenografts were created in nude mice from UM-22B cells using two million cells per inoculation. Treatment was initiated when tumors reached a median tumor volume of approximately 50mm^3, generally 7-14 days post inoculation. Animals received cetuximab as 0.02mg 2x/week by i.p. injection. After one week of treatment (dashed line) the dose was increased to 0.4mg 5x/week for two weeks and then raised to 0.2mg 2x/week (dashed line). **B.** Xenografts were created in nude mice from CAL33 cells using two million cells per inoculation. Treatment was initiated when tumors reached a median tumor volume of approximately 300mm^3, generally 7-14 days post inoculation. Animals initially received cetuximab as 0.02mg 2x/week by i.p. injection. After one week of treatment (dashed line), the dose was increased to 0.04mg 2x/week. After another week (dashed line), the dose was increased to 0.08mg 2x/week. After two more weeks (dashed line) the animals began one month of treatment at the therapeutic dose, 0.2mg 2x/week. **C.** Xenografts were created in nude mice from the resistant CAL33 tumor cell line (Cal33AR1) and the parental CAL33 cell line (n=5 tumors per cell line). Two million cells were used per inoculation, and animals were treated once median tumor volume reached 50mm^3. Animals were treated for two weeks with the therapeutic dose of cetuximab, 0.2mg 2x/week. No significant differences were observed in tumor volumes ($p=0.732$).

2.3.3 **HNSCC Heterotopic Tumorgrafts May Serve as Models of Cetuximab Resistance**

Data suggests that therapeutic results in preclinical cell line xenograft models of cancer may not accurately predict for human response to the same agents[186]. A more translational model system that is recognized as more representative of human response to anti-cancer agents is "ex"plant xenografts, or tumor grafts[187, 188]. This model is sometimes also referred to as heterotopic xenografts. Tumorgrafts are tumors that are surgically transplanted directly from human patients into severe combined immunodeficiency (SCID) mice. Mice bearing the SCID mutation have impaired T and B cell lymphocytes, as compared to the immunocompromised athymic nude mice that lack only T cells. The combined immunodeficiency of SCID mice provides enhanced abrogation of the immune system compared to nude mice.

Because our attempts to generate cetuximab resistance models with HNSCC cell lines in nude mice were not reproducible, we next attempted to generate cetuximab resistance models with HNSCC tumorgrafts. The work in this section was performed with Dr. Sarah Wheeler, a collaborator in our laboratory. Dr. Wheeler performed all the animal surgeries and was responsible for some treatments and measurements. Kelly Quesnelle crafted the experimental design, performed the majority of treatments and measurements and performed all data analysis. Tumorgrafts from three HNSCC patient tumors were created by implanting approximately 25mm of each human tumor into the flanks of anesthetized SCID mice. Once tumor volume reached $50mm^3$, animals were treated with sub-therapeutic doses of cetuximab (0.02mg twice weekly). All tumors progressed at these doses to the maximum allowable tumor volume under IACUC guidelines. Once maximum tumor volume was reached, tumorgrafts were passaged into new SCID mice and the dose of cetuximab was increased with each subsequent passage of the tumors. During the third passage of these tumorgrafts, we started treatment at a sub-therapeutic

dose of cetuximab (0.08mg twice weekly) and increased to the therapeutic dose of cetuximab (0.2mg twice weekly) in non-responsive tumorgrafts. A summary of this treatment can be found in Table 2-2.

We created tumorgrafts from three HNSCC patient tumors, identified as 11-6031, 11-5845, 11-5822 and at least 30% of tumorgrafts from each patient tumor demonstrated growth in the presence of therapeutic doses of cetuximab (0.2mg twice weekly, Table 2-2). From the 11-6031 tumor, 2/2 tumorgrafts (100%) demonstrated growth during treatment with 0.2mg of cetuximab twice weekly. The final volume of these tumorgrafts after 18 days of treatment was 240% greater, on average, than their starting volumes. From the 11-5845 tumor, 11/15 tumorgrafts (73%) demonstrated growth during treatment with 0.2mg of cetuximab twice weekly. The final volume of these 11 tumorgrafts after an average of 14 days on treatment was a 270% increase, on average, relative to the starting tumor volumes. From the 11-5822 tumor, 5/16 tumorgrafts (31%) demonstrated growth during treatment with the therapeutic dose of cetuximab, 0.2mg twice weekly. The final volume of these 5 tumorgrafts after an average of 16 days on treatment was a 89% increase, on average, relative to the starting tumor volumes. These rates of resistance (31-100%) are much more representative of HNSCC patient response rates to cetuximab, suggesting the relevance of tumorgrafts for modeling cetuximab resistance.

Table 2-2. Response rates of HNSCC explants xenografts to cetuximab

Heterotopic xenografts generated from three unique HNSCC patient tumors demonstrated selection to cetuximab at subtherapeutic doses (0.08mg 2x/week) of cetuximab. Xenografts that did not regress more than 50% under these conditions were increased to a therapeutic dose of cetuximab (0.2mg 2x/week). Starting and ending tumor volumes for 36 heterotopic xenografts are shown here. Data shown is in collaboration with Dr. Sarah Wheeler.

HN Identifier	Xenograft Identifier	Initial Tumor Volume (mm^3)	Final Tumor Volume (mm^3)	Days of Cetuximab Treatment	Biweekly dose of cetuximab (mg)	Change in Tumor Volume (%)
11-6031	442.R1.1L	334.35	1058.25	18	0.08-0.2	217%
	442.R1.1R	240.28	873.38	18	0.08-0.2	263%
11-5845	210.R1.1.1L	108.46	418.12	19	0.08-0.2	286%
	210.R1.1.1R	76.70	467.74	19	0.08-0.2	510%
	210.R1.4.1R	209.19	212.95	19	0.08-0.2	2%
	210.R1.4.1L	did not grow	did not grow	19	0.08-0.2	n.a.
	210.R1.4.2L	71.68	0.00	8	0.08-0.2	-100%
	210.R1.4.2R	74.39	89.10	8	0.08-0.2	20%
	210.R1.2.2L	160.38	708.66	15	0.08-0.2	342%
	210.R1.2.2R	0.00	203.84	15	0.08-0.2	204%
	210.R2.4.1L	51.72	0.00	12	0.08-0.2	-100%
	210.R2.4.1R	75.40	89.10	12	0.08-0.2	18%
	210.R2.2.1L	47.31	0.00	8	0.08-0.2	-100%
	210.R2.2.1R	36.68	0.00	8	0.08-0.2	-100%
	210.R2.4.2L	0	104.37	12	0.08-0.2	104%
	210.R2.4.2R	224.45	2982.1	12	0.08-0.2	1229%
	210.R2.2.2L	0	91	12	0.08-0.2	91%
	210.R2.2.2R	94.94	250.58	12	0.08-0.2	164%
11-5822	197.R3.2.2L	did not grow	did not grow	17	0.08-0.2	n.a.
	197.R3.2.2R	146.96	334.34	17	0.08-0.2	128%
	197.R3.1.2L	138.53	102.24	21	0.08-0.2	-26%
	197.R3.1.2R	48.1	81.55	21	0.08-0.2	70%
	197.R2.1.1L	80.36	64.7	14	0.08-0.2	-19%
	197.R2.1.1R	57.92	132.95	14	0.08-0.2	130%
	197.R2.2.1L	136.66	91.4	14	0.08-0.2	-33%
	197.R2.2.1R	170.39	151.76	14	0.08-0.2	-11%
	197.R2.2.2L	519.38	962.78	14	0.08-0.2	85%
	197.R2.2.2R	366.58	484.38	14	0.08-0.2	32%
	197.R3.1.1L	193.97	59.73	22	0.08	-69%
	197.R3.1.1R	288.34	74.91	22	0.08	-74%
	197.R2.1.2L	did not grow	did not grow	12	0.08	n.a.
	197.R2.1.2R	116.4	7.3	12	0.08	-94%
	197.R2.3.1L	559.33	27.05	14	0.08	-95%
	197.R2.3.1R	316.16	83.2	14	0.08	-74%
	197.R2.3.2L	399.98	50.34	14	0.08	-87%
	197.R2.3.2R	71.17	34.11	14	0.08	-52%

2.3.4 **HNSCC Cell Lines Have a Narrow Range of Sensitivity to Erlotinib**

Unlike cetuximab models of resistance in HNSCC, preclinical models of acquired resistance to erlotinib are more widespread[158, 161]. We received the previously published isogenic cell pair consisting of the HNSCC cell line 686LN and its EGFR TKI resistant subclone, 686LNR30, from Dr. Georgia Chen (Emory University)[161]. Cellular genotyping to confirm the isogenicity of these cell lines determined that the resistant subclone was not an HNSCC cell line but rather a type of cervical cancer cell line, HeLa. This mislabeling left us without an isogenic model of acquired resistance to erlotinib. However, because most primary tumors in HNSCC are resistant to erlotinib treatment, we chose to focus our studies on models of primary resistance in HNSCC. We determined response to erlotinib across a panel of HNSCC cell lines, rather than relying on one cell model, with the goal of identifying primary resistance to erlotinib in HNSCC.

We performed cell viability assays on a panel of eight HNSCC cell lines after 72 hours of growth in the presence of erlotinib or vehicle control to determine erlotinib sensitivity. There was a narrow range of erlotinib IC_{50}s from 1.56μM (HN-5) to 6.6μM (UM-22A, Figure 2-6). Because all of these HNSCC cell lines have IC_{50}s to erlotinib below 10μM, we included HeLa cells as an erlotinib-resistant control (IC_{50}=44.60μM). The narrow range of IC_{50}s to erlotinib in HNSCC cell lines, coupled with the scarcity of information regarding intratumoral erlotinib concentrations in head and neck cancer, makes it highly subjective to delineate sensitivity versus resistance based on these *in vitro* data.

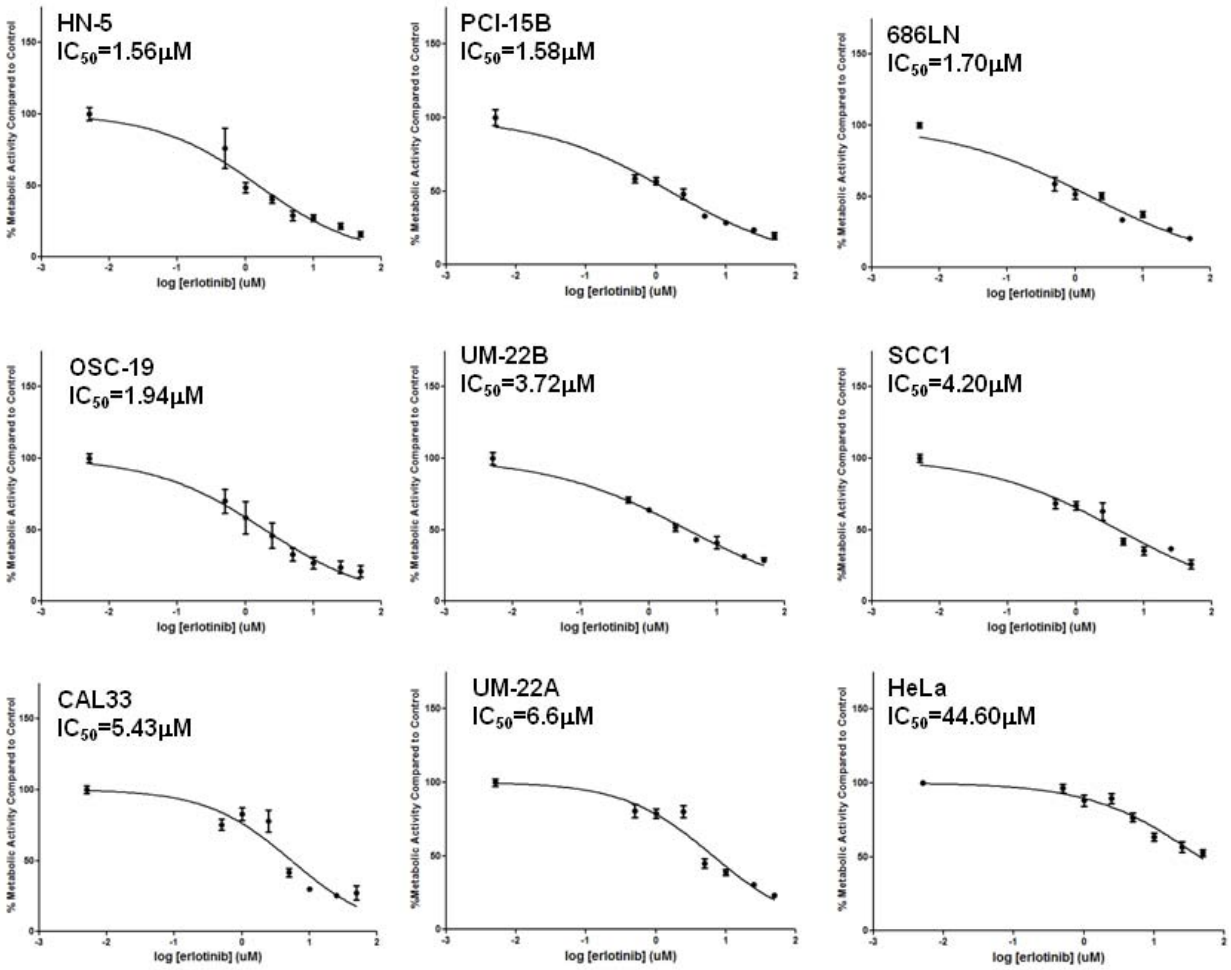

Figure 2-6. HNSCC cells have a narrow range of sensitivity to erlotinib.

A panel of 8 HNSCC cell lines (HN-5, PCI-15B, 686LN, OSC-19, UM-22B, SCC1, CAL33, UM-22A) were treated in triplicate with erlotinib for 72 hours followed by MTT assay. Relative IC_{50}s were calculated from three independent experiments. IC_{50} values range from 1.56μM to 6.6μM in HNSCC cell lines. HeLa cells were used as a control to demonstrate *in vitro* resistance to erlotinib (IC_{50}=44.60μM).

To determine erlotinib sensitivity *in vivo,* we used 686LN as a representative HNSCC cell line since the range of sensitivities to erlotinib is relatively narrow. We have shown previously that 686LN cells are sensitive to cetuximab *in vivo* (Figure 2-4), so we used these as a control to establish HeLa cells as an EGFR-inhibitor resistant model *in vivo* (Figure 2-7A). Nine mice were inoculated with equal numbers of 686LN and HeLa cells on opposite flanks and we observed a significant difference in tumor volumes following 10 days of cetuximab treatment ($p=0.0013$). HeLa cells are not sensitive to cetuximab *in vivo,* while 686LN cells are sensitive to cetuximab *in vivo.* In line with this, we used HeLa cells as an erlotinib-resistant control to test the sensitivity of 686LN cells to erlotinib *in vivo.* Following 10 days of erlotinib treatment, there is also a significant difference in tumor volumes between 686LN and HeLa cells ($p=0.0036$) (Figure 2-7B). These data demonstrate that 686LN cells are sensitive to EGFR inhibition *in vivo,* while HeLa cells are not.

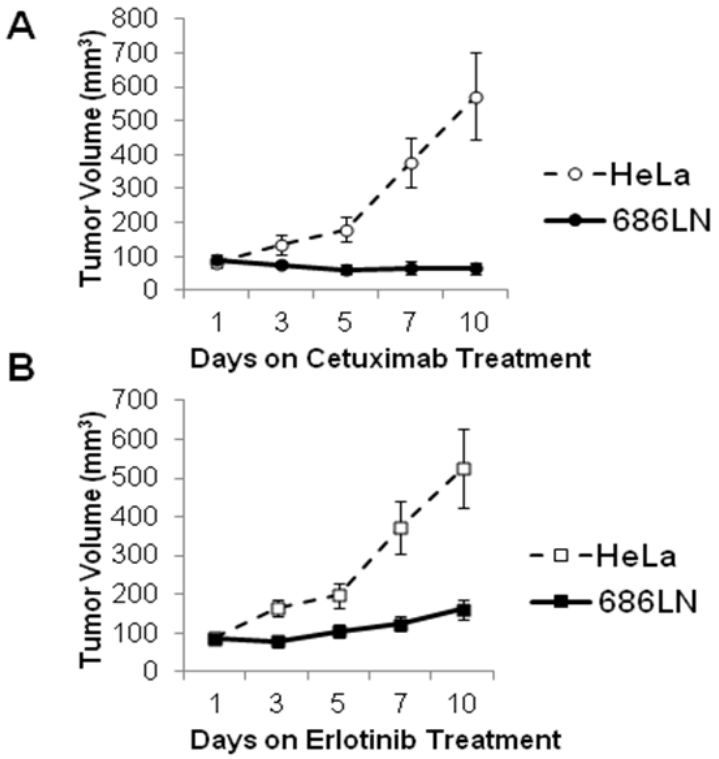

Figure 2-7. 686LN cells are sensitive to erlotinib *in vivo.*

A. 686LN cells and HeLa cells are differentially sensitive to cetuximab *in vivo*. The 686LN cell line was used to create xenografts in nude mice from one million cells per xenograft with Matrigel (n=9). HeLa cells were used as a cetuximab-resistant control at a rate of one million cells per inoculation to create xenografts (n=9). Animals were treated with a higher than therapeutic dose of cetuximab, 1.0mg 2x/week, by intraperitoneal injection and a significant difference in tumor volumes was observed between the two cell lines on day 10 (p=0.0013). **B.** The HNSCC cell line 686LN was used to create xenografts in nude mice from one million cells per xenograft with Matrigel (n=9). HeLa cells were used as an erlotinib-resistant control at a rate of one million cells per inoculation to create erlotinib-resistant control xenografts (n=9). Animals were treated with 50mg/kg erlotinib five times per week by oral gavage and a significant difference in tumor volumes was observed between the two cell lines on day 10 (p=0.0036).

2.3.5 **Sensitivity to EGFR Inhibitors Correlates with EGFR Protein Levels**

High EGFR levels have been reported to correlate with improved responses to erlotinib in head and neck cancer and non-small cell lung cancer patients[70, 189-192]. This suggests that erlotinib-resistant cells may not be dependent on EGFR signaling. To test this in our models, we first determined the cell surface levels of EGFR in 686LN cells, which we have shown to be sensitive to both erlotinib and cetuximab *in vitro* and *in vivo*, and in HeLa cells, which we have shown to be resistant to both erlotinib and cetuximab *in vitro* and *in vivo.* As has been reported in HNSCC patients, we detected a lower number of EGFR-negative cells in 686LN versus HeLa (0.20±0.01% for 686LN cells and 14.85±0.24% for HeLa cells, Figure 2-8A).

We attempted to extrapolate this finding to our panel of eight HNSCC cell lines by assessing EGFR protein expression levels from whole cell lysates (Figure 2-8B). A Spearman correlation analysis of immunoblot densitometry from three representative experiments showed a statistically significant correlation between EGFR protein level and erlotinib response *in vitro* ($r=-0.8333$, $p=.0154$).

Data from recent trials in NSCLC suggests that high EGFR expression correlates with response to cetuximab, in accordance with similar observations for erlotinib[193]. In HNSCC, one study has examined EGFR copy number and found no associations with cetuximab response, although protein levels of EGFR were not assessed in this study[194]. Consistent with other *in vitro* studies of cetuximab resistance[195], we found that EGFR was downregulated in

cetuximab-resistant T24PR3 and T24PR4 cells compared to the isogenic parental T24 cells (Figure 2-8C).

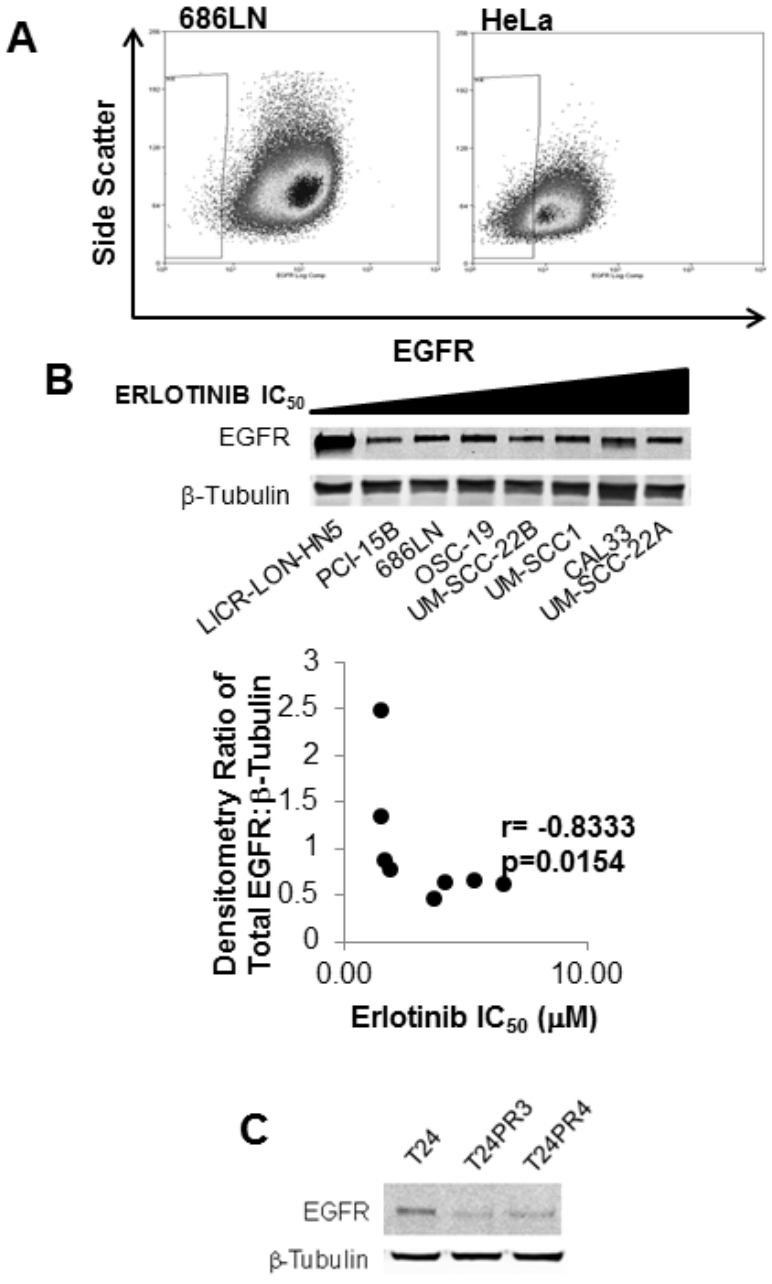

Figure 2-8. EGFR protein levels correlate with sensitivity to EGFR inhibitors.

A. 686LN cells have higher levels of EGFR on the cell surface compared to the EGFR-inhibitor resistant HeLa cell line. Live cell sorting was used on 686LN cells and HeLa cells with gating to exclude cells that uptake propidium iodine and to identify a population of low-EGFR expressing cells (0.20±0.01% for 686LN cells and 14.85±0.24% for HeLa cells). **B.** EGFR expression correlates with erlotinib sensitivity in HNSCC cells. Whole cell lysates were created from cells plated at 70% confluency in standard media and proteins were resolved and immunostained (α-EGFR, BD Transduction Labs). Densitometry was calculated as an average from three independent experiments. **C.** EGFR levels are reduced in cetuximab resistant cell models T24PR3 and T24PR4 compared to cetuximab sensitive T24 parental cells. Whole cell lysates were created from cells plated at 70% confluency in standard media and proteins were resolved and immunostained (α-EGFR, BD Transduction Labs).

2.4 DISCUSSION

Acquired resistance to cetuximab is an important clinical problem in cancer patients treated with this FDA-approved EGFR monoclonal antibody. Elucidation of the mechanisms of acquired resistance has been limited by the paucity of preclinical models. The T24 model of cetuximab resistant bladder cancer presented in the current study was generated *in vivo* and shown to be statistically significant *in vivo* across several doses of cetuximab, including 1.0mg three times per week and 2.0mg three times per week. These more robust dosing schedules were chosen because they are higher than the therapeutic human dose, they are used widely by others in the literature[77, 196], and doses greater than 0.25mg three times per week have been previously identified as the optimal therapeutic doses of cetuximab in pharmacokinetic studies using mice[197]. Further, one group initially reported *in vitro* generated models of trastuzumab resistance and subsequently reported that these models were not reproducible *in vivo*, suggesting

that *in vitro* generated models of antibody-resistance may not extend to *in vivo* settings and underscoring the importance of generating models of resistance to biological therapeutics *in vivo*[198].

The T24 model presented here could be used to study the anti-tumor effects of ADCC *in vivo* in the future in addition to the other mechanisms already described here. The athymic nude mouse model used in these experiments could be used to study ADCC, as others have knocked out the FCγR (Immunoglobulin G Fc Receptor II found on NK cells, responsible for ADCC response) in nude mice and showed reduced anti-tumor effects of human IgG1 backbone antibodies in the FCγR -/- compared to FCγR +/+ mice in the setting of treatment with trastuzumab and rituximab which share the same IgG1 human backbone as cetuximab that is responsible for binding the FCγR and initiating ADCC[199].

Our attempts to generate models of resistance using genotypically validated HNSCC cell lines were unsuccessful across all ten cell lines. Alterations in tumor size and cetuximab dose were all performed in attempts to optimize the conditions under which resistant models may be generated. Unfortunately, none of these alterations managed to yield a cell line that was less sensitive to cetuximab than the original parental cell line from which they were generated.

Literature has shown that tumor size correlates with decreased sensitivity to chemotherapy and EGFR inhibitor response in mice[200, 201]. Gross tumor volume also correlates with worse outcome for head and neck cancer patients receiving cetuximab with radiation[202]. We hypothesized that increasing tumor size may decrease the responsiveness of tumors to cetuximab. Our data did not support this hypothesis, however, since even greater than

10-fold increases in tumor volume did not seem to affect response to cetuximab in the HNSCC cell line xenografts (Figure 2-4 and Figure 2-5).

The T24 model was successfully generated using xenografts created from one million cancer cells inoculated with Matrigel (BD Biosciences) (Figure 2-1). Subsequent animal studies (Figure 2-4 and Figure 2-5) were unsuccessful at generating models of cetuximab resistance and these xenografts were generated using two million cancer cells without the presence of Matrigel. Matrigel is a basement membrane milieu comprised of laminin, collagen IV, heparan sulfate proteoglycan, nidogen and entactin[203, 204]. Matrigel, and, more specifically, laminin can dramatically increase the malignant phenotype of cell lines by increasing invasiveness, tumor volume, adhesion, migration, and collagenase IV activity (which increases invasion)[205-207]. There is also evidence to suggest that Matrigel can increase resistance to cytotoxic drugs *in vitro*[208]. It is not known to what extent the inclusion of Matrigel may have altered the tumor microenvironment and contributed to the generation of the T24 model, or to what extent the absence of Matrigel inhibited the development of HNSCC resistant tumors. Our data does show that exclusion of Matrigel did not alter the sensitivity of 686LN cells to cetuximab, though, suggesting that the contribution of Matrigel to inhibitor resistance is minimal, if any.

We were met with more success generating resistance models using the explant xenograft model from human tumor tissues. Our efforts at generating cell strains from these tumorgrafts have been unsuccessful to date, but the fact that between 30% and 100% of tumorgrafts are resistant to cetuximab is much more representative of human response rates to cetuximab than our cell line xenograft results. There was a range of tumorgraft response rates to cetuximab at the therapeutic dose that was highly variable across the three patient tumors (0%, 27%, and 69% for our three tumors). While these are interesting data that may correlate with variations in

patient response or molecular pathogenesis determinants such as the presence of HPV or EGFRvIII, our sample size in the current study is too limited to perform these types of correlations. In the current study, we have presented a novel way to generate cetuximab resistant models and given preliminary evidence that larger sample sizes are warranted for future studies in which clinical correlations can be addressed.

Defining primary resistance to erlotinib is challenging because the physiological concentration of intratumoral erlotinib is not well studied in HNSCC. The maximum plasma concentration, C_{max}, of erlotinib in cancer patients receiving the standard oral dose of 150mg/day has been reported in non-smokers as 950ng/mL (2.45μmol/L) and in smokers as 1055ng/mL (2.2μmol/L)[209]. A study using ^{11}C-labeled erlotinib to detect tissue distribution of erlotinib in mice with lung cancer xenografts has suggested that erlotinib concentrations in the tumor can be up to four-fold higher than blood concentrations. This effect is correlated with erlotinib sensitivity, i.e. erlotinib-sensitive tumors can have up to four-fold higher intratumoral erlotinib concentrations where erlotinib-resistant tumors have intratumoral erlotinib concentrations similar to those of the blood[210]. One study has reported clinical concentrations of intratumoral erlotinib in aerodigestive tract tumors. This study corroborates the preclinical findings and reports higher intratumoral erlotinib concentrations in patients who responded to erlotinib treatment. Erlotinib-responding tumors had intratumoral erlotinib concentrations of 4.1μM and 4.8μM, where erlotinib-resistant tumors had lower intratumoral erlotinib concentrations, 1.7μM and 0.3μM[211]. This suggests that concentrations higher than the maximum blood plasma concentration are achievable intratumorally in erlotinib-sensitive tumor tissues, but studies examining this in large cohorts of patients have not yet been reported.

We examined EGFR expression levels in our cell lines and found that total levels of EGFR protein correlate with EGFR inhibitor sensitivity (Figure 2-8B). Reduced levels of EGFR at the cell surface is thought to play a role in both erlotinib and cetuximab resistance[212, 213], and here we observed decreased EGFR levels both on the cell surface and in the whole cell lysates of EGFR inhibitor resistant cells. Importantly, our data contrasts with one report of clinical erlotinib use in HNSCC where EGFR protein levels are not indicative of erlotinib response[113]. While this does not negate our hypothesis that EGFR inhibitor resistant tumors are driven by EGFR-independent growth, it does speak to the disconnect between preclinical and clinical observations.

In conclusion, we have examined antitumor responses to cetuximab using a panel of HNSCC cell line xenografts as well as tumorgrafts from human tumor tissues. In accordance with the literature, we find that tumorgrafts are potentially more representative of patient response to cetuximab than HNSCC cell line xenografts. We did, however, successfully generate and validate a novel *in vivo* model of cetuximab resistance using a bladder cancer cell line. This model can be used to study mechanisms of resistance to cetuximab.

In order to create a model with which to study erlotinib sensitivity, we determined the response of a panel of HNSCC cell lines to erlotinib and correlated this sensitivity with EGFR expression levels. These data provide a thorough and descriptive study of preclinical modeling of EGFR inhibitor resistance in HNSCC and can serve as a guideline for future studies using these models. Taken together, these findings demonstrate the need for development of additional preclinical models of cetuximab resistance and provide a platform by which to examine mechanisms of resistance to EGFR targeting agents.

3.0 KINASE INHIBITION OF HER2 AND EGFR CAN OVERCOME RESISTANCE TO AN EGFR-TARGETING ANTIBODY

3.1 INTRODUCTION

In the absence of genomic mutations in KRAS or EGFR, no definitive signaling mechanism is known to confer resistance to the EGFR inhibitor cetuximab. Alternative signaling through HER2, HER3, and c-Met have all been implicated in cetuximab resistance. Combined with our finding that cetuximab-resistant bladder cancer cells have reduced levels of EGFR (Figure 2-8C), signaling through HER2, HER3, and c-Met may provide a viable means for EGFR-independent cell growth in these cells.

3.1.1 HER2 and HER3 Signaling in Cetuximab Resistance

One possible mechanism of cetuximab resistance may involve redundant signaling through other ErbB family members (HER re-programming), including HER2 and HER3. Co-expression of multiple ErbB family members is more predictive of shortened survival than expression of EGFR alone in some cancers[55] and co-activation of EGFR with HER2 has been implicated in resistance to trastuzumab, a HER2-targeting agent, in breast cancer models[180]. EGFR is also shown to be upregulated after long term exposure to trastuzumab[214], further reinforcing the critical nature of these redundant pathways to cellular growth in malignancies. Blockade of HER2 or HER3 has been shown to re-sensitize lung cancer cells to cetuximab *in*

vitro[163], likely because HER2 and HER3 signaling occurs through many of the same downstream effectors as EGFR, including MAPK and PI3K[215]. HER2 gene amplification has also been found in lung cancer patients with acquired or *de novo* cetuximab resistance[98]. Further, it is known that HER3 can compensate for inhibition of EGFR and HER2 in breast cancer models[216]. Taken together, these data suggest that HER2 or HER3 signaling may serve as a mechanism of growth in cetuximab resistant tumor cells.

3.1.2 **C-Met Signaling in Cetuximab Resistance**

Like the other ErbB family members, c-Met signals through many of the same downstream pathways as EGFR including MAPK and PI3K and is even capable of activating EGFR and HER3 for signaling[217]. It is known that c-Met amplification is a key mechanism of acquired resistance to EGFR tyrosine kinase inhibitors in lung cancer (Paragraph 1.3.3), but data implicating c-Met in cetuximab resistance are rare. c-Met activation has been implicated in preclinical models of cetuximab resistance in gastric cancer[167]. Additionally, c-Met protein expression correlates with decreased progression-free survival in colon cancer patients who have been treated with cetuximab[218], suggesting that c-Met may play a role in cetuximab resistance.

3.2 MATERIALS AND METHODS

3.2.1 Cells and Reagents

SCC1 was derived from a primary HNSCC tumor and both SCC1 and the cetuximab-resistant clone SCC1c8 were maintained in DMEM with 10% FBS and 0.4ug/mL hydrocortisone [163]. OSC-19 cells were maintained in MEM with 10% FBS and 1% non-essential amino acids. CAL33, T24, and A431 cells were maintained in DMEM + 10% FBS. All cell lines were validated by genotyping within 6 months of their use using the AmpFISTR Identifiler System (Applied Biosystems). Cetuximab-resistant clones were maintained in media with 100nM cetuximab. Cetuximab (Erbitux, ImClone Systems and Bristol-Myers Squibb) was purchased from the University of Pittsburgh Pharmacy. Afatinib was obtained from Boehringer Ingelheim as a powder and resuspended in DMSO for *in vitro* studies or 0.5% methylcellulose with 0.4% tween 80 in saline for animal studies. Trastuzumab (Herceptin, Genentech) was purchased from the University of Pittsburgh Pharmacy and diluted as recommended in the package insert. Erlotinib was purchased from Chemietek and dissolved in DMSO for *in vitro* studies.

3.2.2 Combination Treatment Animal Study

Two million parental and resistant cells were injected on opposite flanks of the same mouse (n=40) with Matrigel and animals were stratified by tumor volume[219] into four groups then randomly distributed from each group into four treatment groups with ten animals per group. Animals were treated with cetuximab, afatinib, or both. The treatments and measurements were performed by an individual blinded to the treatment. 1.0mg of cetuximab or

vehicle control was given by i.p. injection three times per week by and 0.4mg afatinib or vehicle control was given daily by oral gavage.

3.2.3 **Invasion Assays**

Five thousand cells were plated in the inner well of a Matrigel Invasion Chamber (BD Biosciences) in serum free-media. Wells were placed into media containing 10% FBS and drugs were added to both chambers where indicated. After 24 hours, cells invading through the Matrigel coated membrane were stained and counted.

3.2.4 **Immunoblotting**

Immunoblots were performed on 70% confluent cell lysates after plating in drug-free media. Lysates were resolved on SDS-PAGE gels and transferred to nitrocellulose membranes prior to antibody staining with the following antibodies: HER2 and 611-CTF, (clone F11, sc-7301) Santa Cruz; pHER2 and 611-CTF, Y1248 (2247s) Cell Signaling; pSerine, BD Transduction Labs; Cortactin, Upstate Biotechnology; c-Met, Santa Cruz; p-c-Met (Y1234/5), Cell Signaling; HER3 and p-HER3 (Y1289), Cell Signaling. Densitometry was performed using Image J software.

3.2.5 **shRNA Experiments**

Lentiviral particles were provided by Dr. R.W. Sobol and the University of Pittsburgh Cancer Institute (UPCI) Lentiviral Facility. Virus stocks were generated by co-transfection of the shRNA expression plasmid (pLK0.1; Mission shRNA library from Sigma) into 293-FT cells together with the packaging plasmids pMD2.g (VSVG), pRSV-REV, pMDLg/pRRE. Forty-eight

hours post transfection viral particles were collected in the culture supernatant, filtered (0.45 μM) and stored at -80˚C or used immediately to transduce the target cells.

3.2.6 **Metabolic Activity Assays**

Cells were plated at a density of 30,000 cells per well in 24-well plates to achieve a density approximately 50% confluent. Cells were treated the following day with vehicle control (0.05% DMSO) or various concentrations of erlotinib or afatinib (250nm-50μM). After 72 hours, media was replaced with 3-(4,5-Dimethylthiazol-2-yl)-2,5-diphenyltetrazolium bromide (MTT) for 30 minutes. Cells were then washed with PBS and DMSO was added to dissolve the purple reduction product of MTT, formazan. Formazan containing DMSO was read on the spectrophotometer at 540nm and compared to vehicle controls to determine level of cell viability.

3.2.7 **Statistical Analyses**

Erlotinib and afatinib relative IC_{50} with associated 95% confidence intervals were calculated using GraphPad Prism v5.0. The nonlinear regression curves for erlotinib and afatinib response had R^2 values greater than 0.70. P-values were generated for the combination treatment animal study using a Mann-Whitney test for non-parametric data. P-values were generated for invasion assays using a homoscedastic two-tailed Student's t-Test. Statistical analyses for immunoblots were conducted using homoscedastic student's t-tests.

3.3 RESULTS

3.3.1 **HER3 is Not Differentially Expressed or Phosphorylated in the Cetuximab Resistance Model**

We used a candidate-based approach to explore differences in the cetuximab-sensitive and cetuximab-resistant cells, focusing primarily on the expression and phosphorylation of c-Met and the ErbB family members. HER3 was expressed at low levels in T24, T24PR3, and T24PR4 clones, and we observed no significant difference in expression of total or phosphorylated levels of HER3 across these cell lines (Figure 3-1).

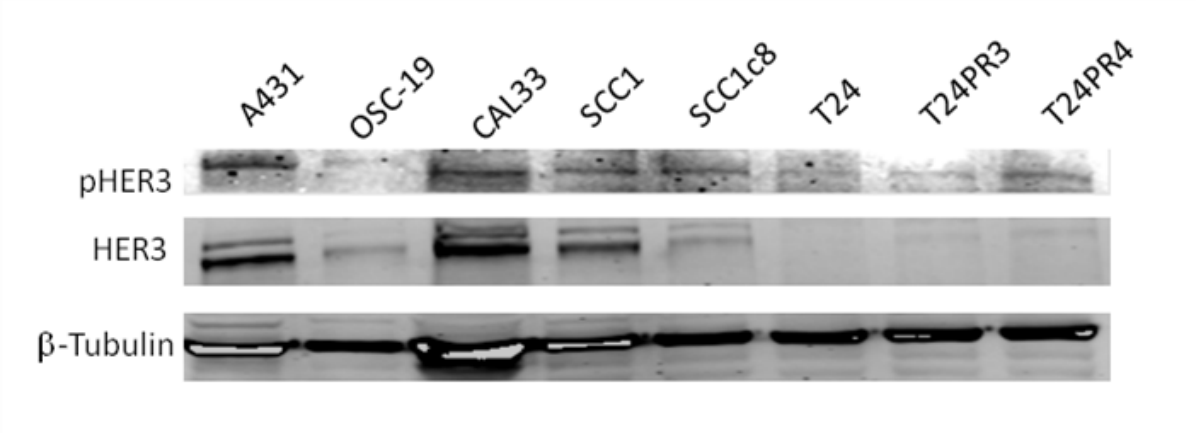

Figure 3-1. HER3 is unchanged in cetuximab resistant cells.

Cell lysates were collected under basal conditions when cells reached 70% confluence. Whole lysates were analyzed by Western Blot and probed for HER3 and pHER3(Y1289, Cell Signaling).

3.3.2 **C-Met Contains a Polymorphism and Is Not Differentially Expressed or Phosphorylated at Y1234/5 in the Cetuximab Resistance Model**

Mutational analysis of the T24 cell line identified a T1010I mutation in the c-Met receptor. While this was originally thought to be an oncogenic mutation[220], newer and more comprehensive data suggests that this is merely a normal polymorphism[221]. Here, we examined the basal expression and phosphorylation of c-Met in our cetuximab sensitive (T24) and cetuximab resistant (T24PR3, T24PR4) cells, and found no significant difference between basal levels of c-Met protein expression or phosphorylation at Tyr1234/5 across cetuximab sensitivity and resistant cells (Figure 3-2).

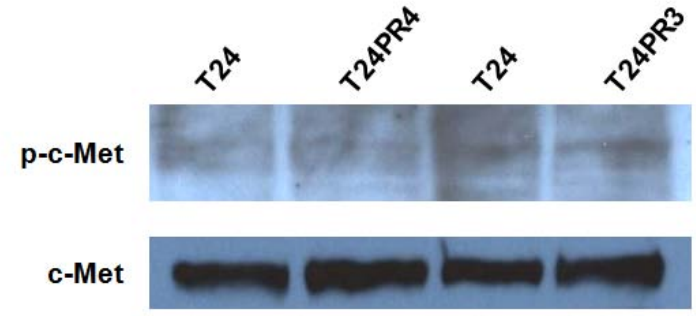

Figure 3-2. c-Met is not differentially expressed or phosphorylated in cetuximab resistance model.

Cell lysates were collected under basal conditions when cells reached 70% confluence. Whole lysates were analyzed by Western Blot and probed for c-Met(Santa Cruz) and pMet(Y1234/5, Cell Signaling).

3.3.3 **Cetuximab-Resistant Cells Express a Hyperphosphorylated Form of 611-CTF, a Carboxyl-Terminal HER2 Fragment**

While there was no significant change in the expression or phosphorylation at Tyr1248 of full length HER2 among cetuximab-sensitive and cetuximab–resistant cells, we did observe a significant increase in phosphorylation of 611-CTF, a carboxyl-terminal fragment of HER2, in only the cetuximab resistant cells (Figure 3-3). Despite the abundance of total 611-CTF protein in T24, T24PR3 and T24PR4 and other cells, 611-CTF appears to be phosphorylated at Tyr1248, the site responsible for MAPK activation, in only the cetuximab resistant clones, T24PR3 and T24PR4. Densitometry confirms T24PR3 and T24PR4 cells to significantly express phosphorylated 611-CTF at levels 5.6 ($p=0.0223$) and 5.9 ($p=0.0309$) fold higher, respectively, than T24 cells (Figure 3-3).

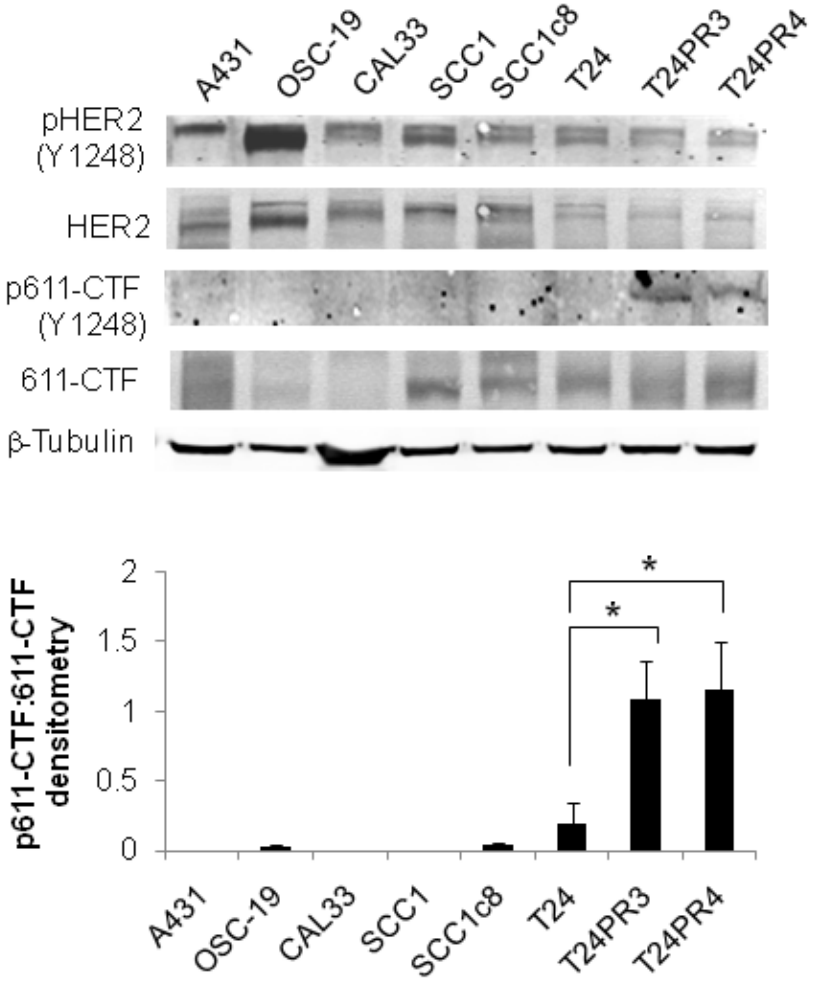

Figure 3-3. Expression of hyperphosphorylated 611-CTF protein in cetuximab-resistant cells.

Cell lysates were collected under basal conditions when cells reached 70% confluence. Whole lysates were analyzed by Western Blot and probed for HER2 and pHER2 (185 kDa), 611-CTF and p611-CTF (110 kDa HER2 fragment). Densitometry is the result of three individual experiments where intensity of the p611-CTF bands were compared to the intensity of 611-CTF bands on the same gel (*$p<0.05$).

We also observed increased phosphorylation of cortactin, a known downstream target of 611-CTF (Figure 3-4, $p=0.039$)[222]. 611-CTF has been described as a 110 kDa alternative

translation product of HER2 containing the c-terminal, intracellular and transmembrane domains along with a truncated extracellular domain[223]. 611-CTF has been shown to promote tumor growth and metastasis in breast cancer cells *in vivo*[224] and it has also been implicated in cell motility and invasiveness[222], further enforcing its metastatic function.

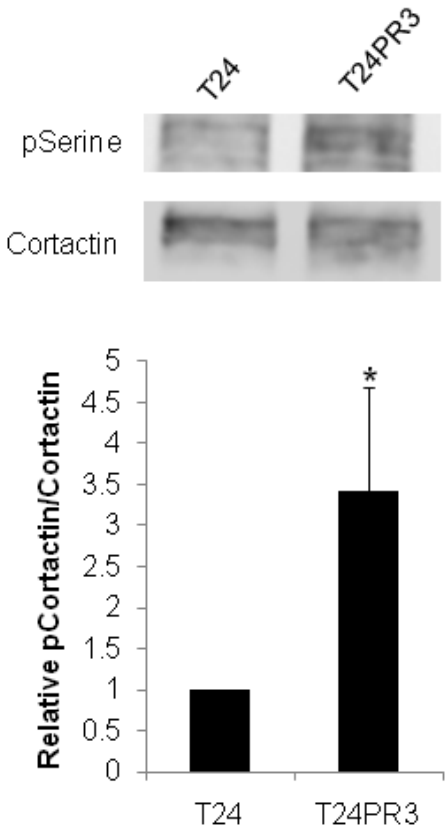

Figure 3-4. Increased phosphorylation of cortactin, a downstream effector of activated 611-CTF, in cetuximab resistant cells.

Cell lysates were collected under basal conditions when cells reached 70% confluence. Whole lysates were analyzed by Western Blot and probed for pSerine and cortactin. Densitometry is the result of six individual experiments where intensity of the pSerine bands for each cell type was compared to their respective cortactin bands from the same gel. Phosphorylation ratios for each cell line were compared to the T24 cell line for reference (*$p<0.05$).

3.3.4 **Inhibiting HER2 Can Restore Sensitivity to Cetuximab *In Vitro***

To determine the functional role of phosphorylated 611-CTF in mitigating resistance to cetuximab, we treated T24PR3 cells with cetuximab and HER2 shRNA or various HER2-targeting agents. First, we used lentiviral shRNA transduction to knock down full-length HER2 and 611-CTF in four separate clones of T24PR3 (Figure 3-5A). HER2 knockdown in clones 2 and 4 reduced full-length HER2 by 70% and 78%, respectively, compared to non-targeting scrambled shRNA-transduced control cells. Likewise, HER2 knockdown in clones 2 and 4 reduced 611-CTF expression by 46% and 56%, respectively, compared to scrambled shRNA-transduced cells. This HER2 knockdown of full-length HER2 and 611-CTF was able to restore the effect of cetuximab on T24PR3 cells in culture. Cetuximab decreased invasion of the HER2 shRNA-transduced cells by 54.9% ($p=0.047$) and 49.5% ($p=0.034$) after 24 hours.

To determine if the effects of HER2 knockdown were due to knockdown of the full-length HER2 or the 611-CTF fragment, we used HER2-targeting agents to selectively and functionally inhibit HER2 activity. Trastuzumab is a monoclonal antibody targeting exclusively full-length HER2 and should not interact directly with 611-CTF which lacks the extracellular region containing the trastuzumab epitope[225]. Although trastuzumab alone only decreased invasion of T24PR3 cells by 14.5%, the combination of cetuximab plus trastuzumab decreased invasion by 43.8% (Figure 3-5B, $p=0.01$). While there are currently no kinase inhibitors available for use in the clinic that target HER2 selectively, afatinib is an irreversible kinase inhibitor targeting both EGFR and HER2. Afatinib is currently in phase II trials for prostate cancer, glioma, and head and neck cancer as well as phase III clinical trials for breast cancer and non-small cell lung carcinoma[226]. We found that afatinib alone could inhibit the invasion of

T24PR3 cells by 38.1% (Figure 3-5C, p=0.03), and the combination of cetuximab plus afatinib inhibited the invasion of T24PR3 cells by 62.1% (Figure 3-5C, p=0.031).

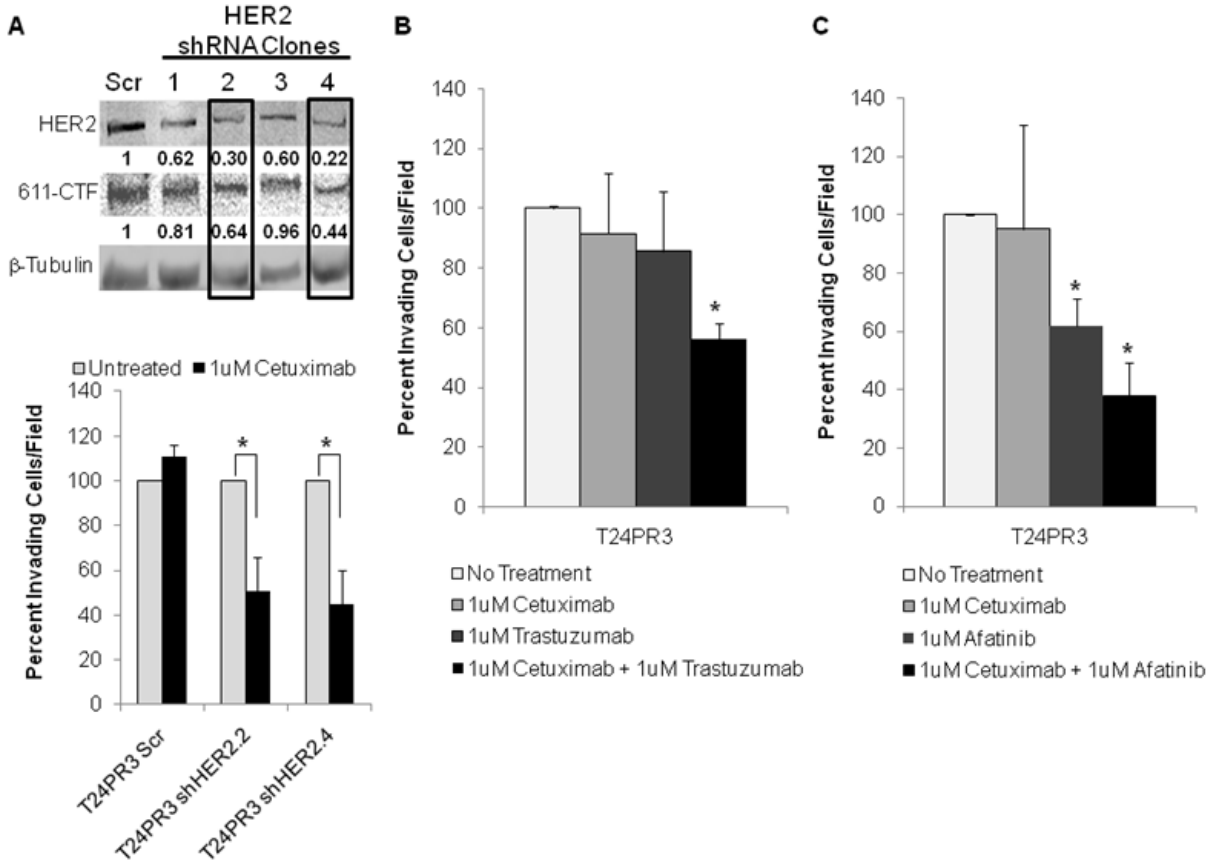

Figure 3-5. Inhibition of HER2 restores cetuximab sensitivity *in vitro*.

(A) T24PR3 cells were transduced with HER2 shRNA-containing lentiviral particles and a representative image of the western blots for full length HER2 and 611-CTF from 4 clones and scramble control lysates are included here. Invasion studies in this figure were performed using 1μM cetuximab or drug free media (*$p<0.05$) and all data are the result of two independent experiments run in duplicate. **(B)** Invasion studies were performed using T24PR3 cells with media containing either vehicle, cetuximab, trastuzumab to inhibit full length HER2, or both cetuximab

and trastuzumab. **(C)** Invasion studies were performed using T24PR3 cells with media containing either vehicle, cetuximab, the EGFR-HER2 kinase inhibitor afatinib, or both cetuximab and afatinib.

While we did not directly examine interactions between cetuximab and selective EGFR kinase inhibitors in an invasion assay, we performed drug response assays with an EGFR kinase inhibitor using cell metabolism as a readout in both cetuximab resistant and cetuximab sensitive cells. The cetuximab resistant and cetuximab sensitive cells demonstrated similar IC_{50}s to the EGFR kinase inhibitor erlotinib, 6.37μM and 9.99μM, respectively (p=n.s.). In contrast, the IC_{50} of cetuximab-resistant cells treated with afatinib was 8.27nM (Figure 3-6). These data suggest that co-targeting EGFR with a dual-specificity tyrosine kinase inhibitor that can also inhibit HER2 and 611-CTF may enhance the effects of EGFR targeting *in vitro* in a cetuximab-resistant cell model.

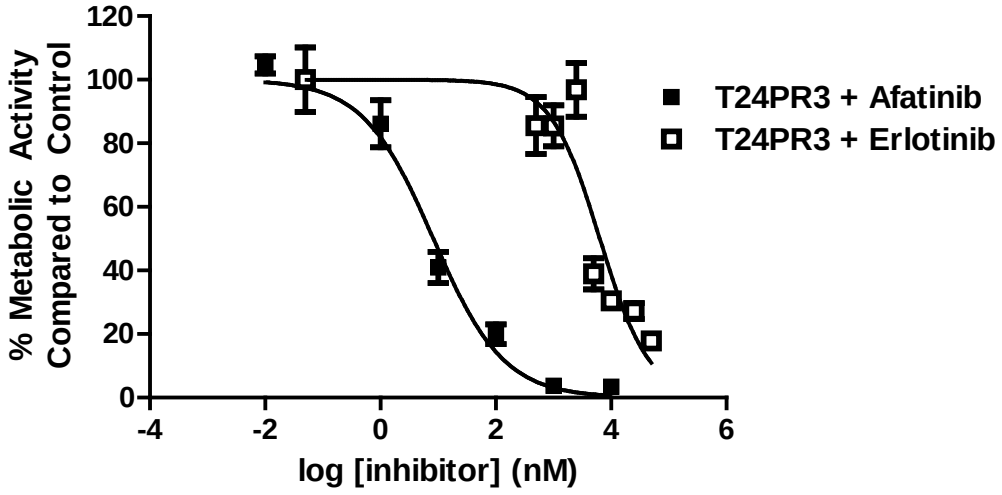

Figure 3-6. Cetuximab resistant cells are more sensitive to afatinib than erlotinib.

Cells were plated to be 50% confluent and treated with varying doses of either afatinib, erlotinib, or DMSO control. After 72 hours, an MTT assay was performed. Data is the result of three independent experiments run in triplicate.

3.3.5 **Dual Kinase Inhibition of EGFR and HER2 Can Enhance the Anti-Tumor Effects of Cetuximab *In Vivo***

In order to test the effects of EGFR and HER2 kinase inhibition on mediating cetuximab sensitivity *in vivo*, we generated xenografts in athymic nude mice by inoculating cetuximab sensitive cells on one flank and cetuximab resistant cells on the other flank of the same mouse (n=40 mice). Following tumor formation, animals were randomized based on tumor volumes and treated with vehicle control, cetuximab alone, afatinib alone, or cetuximab plus afatinib. After 21 days, the treatment regimen of cetuximab plus afatinib yielded a 76.5% reduction in cetuximab-resistant tumor volumes ($p=0.0191$) compared to vehicle control treated tumors (Figure 3-7A).

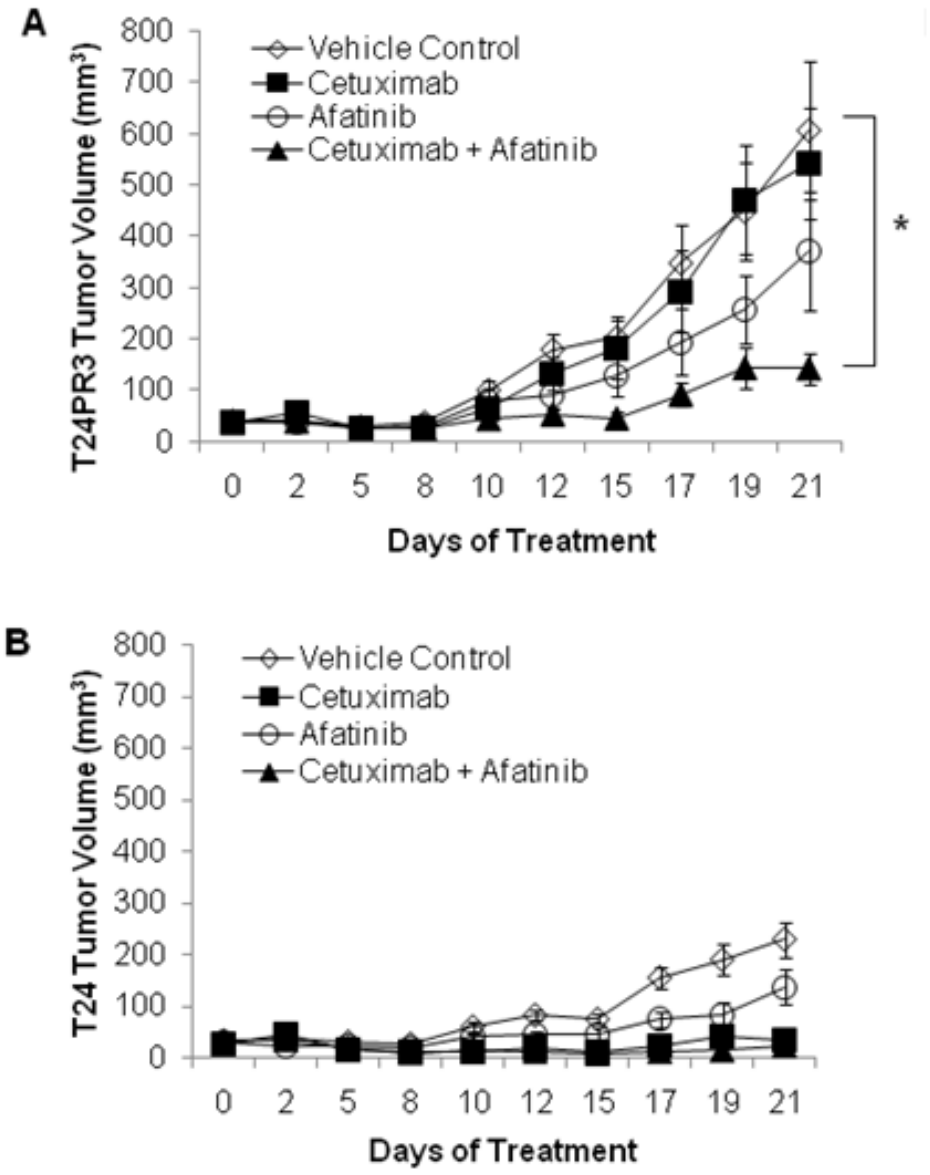

Figure 3-7. Anti-tumor effects of dual kinase inhibition of EGFR and HER2 *in vivo*.

Xenografts were created using cetuximab-resistant T24PR3 cells (A) or cetuximab-sensitive T24 cells (B) in athymic nude mice (n= 40). Mice were randomized based on tumor volumes and treated with vehicle control, afatinib (0.4mg/daily by oral gavage), cetuximab (1.0mg 3x/week by i.p. injection), or both drugs concurrently for 21 days. Tumor volumes were measured 3 times per week for a total of 3 weeks. P-values were generated using a Mann-Whitney Test (*$p<0.05$).

A similar reduction in tumor volumes was seen in cetuximab-sensitive tumors treated with cetuximab and afatinib (89.7%, p=0.0191) (Figure 3-7B), although no additional benefit was observed from adding afatinib to cetuximab therapy in cetuximab-sensitive xenografts because of the already potent anti-tumor effects of cetuximab on these tumors. The difference in tumor volumes between the cetuximab-sensitive and cetuximab-resistant xenografts treated with cetuximab was again significant (p=0.0013) as shown earlier with a higher dose of cetuximab (Figure 2-2A).

Interestingly, 611-CTF expression in the cetuximab-resistant tumors was significantly increased in tumors treated with cetuximab alone but decreased in those treated with the combination of afatinib and cetuximab (Figure 3-8, p=0.015 and p=0.0047, respectively). 611-CTF expression was slightly increased in the afatinib treated tumors, although this difference was not statistically significant (Figure 3-8, p=0.11). Further, the dramatic reduction in cetuximab-resistant tumor volumes that was seen with the combination of cetuximab plus afatinib far surpasses the effect observed when either agent was used as a monotherapy, which suggests that dual kinase inhibition of EGFR and HER2 may be an effective way to enhance the efficacy of cetuximab *in vivo* in the context of acquired resistance.

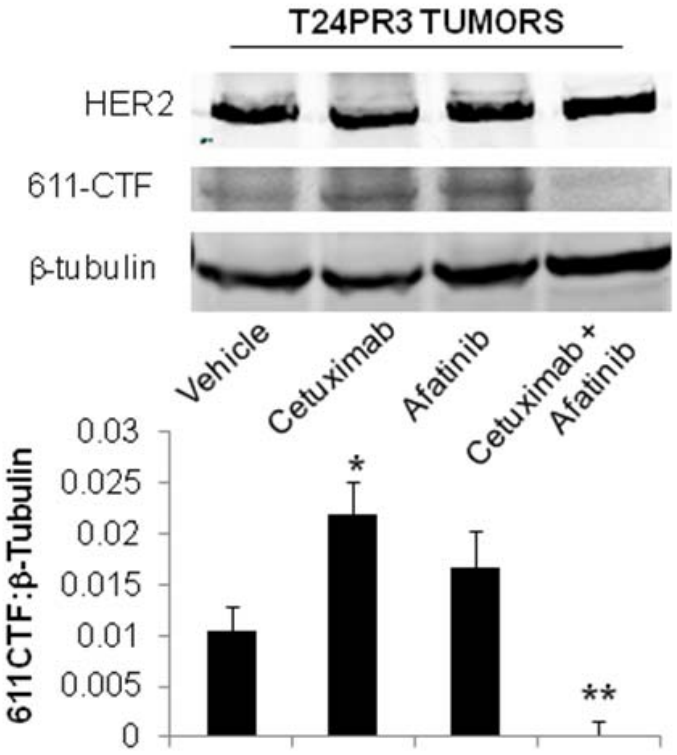

Figure 3-8. 611-CTF is lost in tumors treated with cetuximab and afatinib.

Cell lysates were created from snap-frozen tumor tissue. Whole lysates were analyzed by Western Blot and probed for 611-CTF. Densitometry is the result of four technical replicates from one individual tumor of each treatment group normalized to the β-tubulin loading control for each tumor (*$p<0.05$, **$p<0.005$).

3.4 DISCUSSION

HER kinase receptor switching has been described as a major determinant of acquired resistance to inhibition of these receptors[155]. For this reason, we decided to examine the expression and activation of other ErbB family members in our cetuximab-resistant models. While we observed no marked differences in ErbB family expression or activation across the five cell lines tested *in vivo*, the HER2 fragment 611-CTF was most robustly expressed in the T24 cell line and the SCC1 cell line, which was used to generate the previously published *in vitro* model of cetuximab resistance. Our results associate 611-CTF with cetuximab resistance and suggest that therapeutic targeting of both HER2 and 611-CTF in combination with cetuximab is highly efficacious *in vitro* and *in vivo* (Figure 3-5, Figure 3-7).

The exact mechanism of the increased anti-tumor activity seen with the addition of afatinib to cetuximab and to what extent inhibiting 611-CTF plays a role in this mechanism remains incompletely understood. Interestingly, 611-CTF is thought to be hyperactive because of its ability in models of forced expression to constitutively homodimerize through disulfide bonds as a result of unbalanced extracellular cysteine residues[224]. It is unclear from the literature whether 611-CTF can heterodimerize with full length HER2 or the other ErbB family members. The endogenous presence of non-phosphorylated 611-CTF in several cell lines including A431, SCC1, SCC1c8, and T24 cells (Figure 3-3) suggests that 611-CTF is not always a constitutively active receptor fragment and that it may require heterodimer partners for activation under some conditions. ErbB receptor heterodimerization might also explain, in part, the anti-tumor activity of the trastuzumab/cetuximab combination in the cetuximab and trastuzumab-resistant T24PR3 model. One limitation of the present study is that the precise mechanism of resistance and 611-CTF activation could not be elucidated due to the low levels of endogenous 611-CTF expression

in our cell lines and our attempts at cloning constitutively active and kinase dead forms of 611-CTF for forced expression studies have been unsuccessful to date.

Combinatorial treatment regimens are currently at the forefront of growth factor molecular targeting[155, 227]. Two recent preclinical reports describe the *in vivo* benefit of combining cetuximab with kinase inhibitors specific for EGFR and/or HER2, although in both cases the work was performed in the context of an acquired mutation (T790M) that confers resistance to the EGFR tyrosine kinase inhibitor gefitinib[134, 228]. Both these studies and the current one provide complementary data supporting the use of a treatment regimen that is particularly timely and pertinent with ongoing phase I clinical trials in solid tumors of afatinib plus cetuximab (ClinicalTrials.gov Identifier: NCT01090011) or lapatinib plus cetuximab (ClinicalTrials.gov Identifier: NCT01184482). Surprisingly, there is very little data describing molecular mechanisms in support of this treatment regimen.

One recent report shows that the combination of cetuximab with lapatinib can increase antibody-dependent cell mediated cytotoxicity (ADCC) in ^{51}Cr-release assays by up to 30%[229]. The mechanism by which ADCC is increased with this treatment modality remains unknown, as the authors of the same study do not show a high frequency of lapatinib-mediated accumulation of EGFR at the cell surface as is seen for HER2 with lapatinib and trastuzumab combination treatments[230]. Both studies demonstrate lapatinib-mediated accumulation of inactive HER2 at the cell surface due to loss of ubiquitination and degradation[229, 230], which may explain in part our observation that afatinib does not decrease the expression of 611-CTF in xenografts (Figure 3-8) despite decreasing tumor volume. These data are concordant with published work[230] that shows lapatinib can decrease tumor volumes in animals despite increased accumulation of HER2.

Collectively, these data indicate that kinase inhibition of HER2 and EGFR may enhance sensitivity to cetuximab. To what extent inhibiting 611-CTF may play a role in this enhanced sensitivity remains unknown. Further, the contribution that activated expression of 611-CTF may make to cetuximab resistance is also elusive. The data presented here associate 611-CTF with cetuximab for the first time, and provide a potential mechanism for the enhanced response seen when cetuximab is combined with a kinase inhibitor of EGFR and HER2.

4.0 C-MET AND EGFR KINASE INHIBITORS ARE SYNERGISTIC THROUGH DEACTIVATION OF THE MAPK PATHWAY

4.1 INTRODUCTION

As is the case with cetuximab resistance, no singular mechanism of resistance to EGFR kinase inhibitors has been established apart from c-Met amplification or genetic alterations (Paragraph 1.3.3). Importantly, neither c-Met amplification nor these other well-known genetic alterations (EGFR gatekeeper mutation, K-Ras activating mutations) can account for the entirety of EGFR TKI resistance. The extent to which c-Met may contribute to EGFR kinase inhibitor resistance in HNSCC has not been well described, but is precedent in other cancer types including lung cancer. In contrast to mAb resistance, HER2 and HER3 signaling has been implicated in EGFR inhibitor sensitivity, not resistance. This association has not been examined in HNSCC, making these receptors valid additional targets to examine in the context of EGFR inhibitor sensitivity.

4.1.1 c-Met Signaling in Erlotinib Response

Activation of other receptor tyrosine kinases may confer growth and survival in the presence of EGFR blockade. Signaling through receptor tyrosine kinases is highly redundant: co-activation of multiple receptors has been shown to limit the efficacy of individual targeting[155]. The hepatocyte growth factor receptor, c-Met, is a receptor tyrosine kinase that signals

downstream through many of the same pathways as EGFR. c-Met is correlated with poor prognosis in HNSCC[231], and has been proposed as a molecular co-target with EGFR in HNSCC[158]. c-Met has been shown to play a compensatory role for EGFR kinase activity in breast cancer[232], and is found to be amplified in TKI-resistant lung cancer tumors[157]. We recently reported that HGF and c-Met participate in a paracrine growth pathway in HNSCC[233] and new data demonstrate that combined targeting of EGFR and c-Met leads to synergistic growth inhibition in HNSCC cells[234].

4.1.2 **HER2 and HER3 Signaling in Erlotinib Response**

Although it is counterintuitive, several preclinical models describe increased HER2 and HER3 expression as a mechanism of sensitizing cells to EGFR inhibitors. Inhibition of HER2 by erlotinib has been reported to occur by direct binding of erlotinib to HER2 in the absence of EGFR[235]. EGFR kinase inhibition can also reduce phosphorylation of HER2 or HER2/HER3 heterodimers in cell systems when EGFR levels are low[236]. Increased HER3 RNA levels are associated with EGFR TKI sensitivity in HNSCC cell lines[237] and breast cancer cells overexpressing HER2 have been shown to have heightened sensitivity to EGFR TKI *in vitro* and *in vivo*[238]. Erlotinib-mediated reductions in HER2/HER3 signaling decrease cell survival by blocking AKT association with HER3 that is normally required for AKT phosphorylation[239].

4.2 MATERIALS AND METHODS

4.2.1 **Cells and Reagents**

HN-5, OSC-19, UM-22A, SCC1 and CAL33 are primary HNSCC cell lines and UM-22B, PCI-15B, and 686LN are derived from metastatic cervical lymph nodes from patients with HNSCC[176]. OSC-19 cells were maintained in MEM with 10% FBS and 1% non-essential amino acids. SCC1 was maintained in DMEM with 10% FBS and 0.4ug/mL hydrocortisone. HN-5 and 686LN cells were maintained in DMEM/F-12 + 10% FBS. PCI-15B, UM-22A, UM-22B, and CAL33 cells were maintained in DMEM + 10% FBS.). HeLa cells are a cervical cancer cell line maintained in DMEM + 10% FBS[179]. UM-22A and UM-22B cells were a generous gift from Dr. Tom Carey (University of Michigan), PCI-15B cells were a generous gift from Dr. Theresa Whiteside (University of Pittsburgh) and SCC1 cells were a generous gift from Dr. Paul Harari (University of Wisconsin). All cell lines were validated by genotyping within 6 months of their use using the AmpFISTR Identifiler System (Applied Biosystems). Erlotinib was purchased from Chemietek and resuspended in DMSO for cell studies and SU-11274 was purchased from Calbiochem and also resuspended in DMSO for cell studies.

4.2.2 **Immunoprecipitations**

Immunoprecipitations were performed on whole cell lysates collected 48h after plating using protein G-linked agarose beads with anti-PY99 (Santa Cruz). Immune serum and the remaining supernatant was resolved on SDS-PAGE gels and immunoblotted (Flk-2, Santa Cruz; IGF-1RB, Santa Cruz; c-Met, Santa Cruz).

4.2.3 **Immunoblotting and Statistical Analyses**

Immunoblots shown here were performed on whole cell lysates collected when cells were approximately 70% confluent. Basal conditions were used for all lysates except 686LN and HeLa cells which were serum starved for 2 hours in the presence of 1μM erlotinib or 1μM SU-11274, a c-Met kinase inhibitor. Following 2 hour serum starvation, 686LN and HeLa cells were stimulated with EGF (10ng/mL) or HGF (40ng/mL) for 5 minutes and lysates were collected.

All lysates were resolved on SDS-PAGE gels and immunoblotted with either α-HER2 and α-pHER2 (Y1248, Cell Signaling), α-HER3 (Santa Cruz Biotechnologies), α-AKT and α-pAKT (S473, Cell Signaling), α-p24/44 (MAPK, Cell Signaling) and α-phospho-p42/44 (pMAPK, Cell Signaling), or α-Met (Cell Signaling) and α-pMet (Y1234/5, Cell Signaling) antibodies. Nonparametric Spearman correlations were used to determine the relationship of c-Met protein levels and c-Met phosphorylation levels as well as HER3 protein levels to erlotinib IC_{50}.

4.2.4 **Combination Index Analysis**

30,000 cells were plated in triplicate wells of three 24-well plates. The following day, each plate was treated with erlotinib, SU-11274, or both drugs in combination across a range of doses from 5 to 20 μM along with vehicle controls. After 72 hours, an MTT assay was performed. Combination index (CI) was generated using titrated dosing at a fixed ratio of SU-11274:erlotinib (1:1.69) based on the IC_{50} of each drug separately. CI =(Da + Db) / (Dxa + Dxb) + DaDb / DxaDxb; where Da and Db are the doses of drug A and B that stimulate X% of cell viability as single drugs, and Dxa and Dxb are doses of drug A and B that stimulate X% of cell

viability in a combination regimen. Combination index values were calculated using CalcuSyn Software (BioSoft).

4.2.5 **siRNA Experiments**

30,000 cells were plated in duplicate in a 24-well plate. Cells were transfected with 100nM c-Met pooled siRNA (Dharmacon) or scrambled siRNA (Dharmacon) for 4 hours with Lipofectamine (Invitrogen) in OptiMem media (Gibco). After 24 hours, vehicle control or twice the IC_{50} dose of erlotinib was added to the cells in 24-well plates for another 24 hours at which point cell metabolism assays were performed. Whole cell lysates were harvested simultaneously to confirm c-Met knockdown from cells transfected in parallel.

4.2.6 **c-Met Transfection**

30,000 cells were plated in duplicate in a 24-well plate. Cells were transfected with either 2ug human c-Met cloned into a pcDNA3.1(+) expression vector (courtesy of Dr. Reza Zarnegar at the University of Pittsburgh) or pcDNA3.1(+) empty vector construct for 4 hours with Lipofectamine (Invitrogen) in OptiMem media (Gibco). After 24 hours, vehicle control or twice the IC_{50} dose of erlotinib was added to the cells in 24-well plates for another 24 hours, at which point MTT assays were performed. Whole cell lysates were harvested simultaneously to confirm c-Met expression from cells transfected in parallel.

4.3 RESULTS

4.3.1 **Basal Activation of HER2 and HER3 Signaling Is Not Associated with Erlotinib Response**

In order to test whether HER2 and HER3 signaling may confer sensitivity to kinase inhibition in HNSCC cells, we screened a panel of HNSCC cells with varying response to the EGFR kinase inhibitor erlotinib (Paragraph 2.3.4) for HER2 protein phosphorylation. Whole cell lysates collected under basal conditions did not demonstrate a correlation between erlotinib sensitivity and HER2 protein expression or phosphorylation (Figure 4-1).

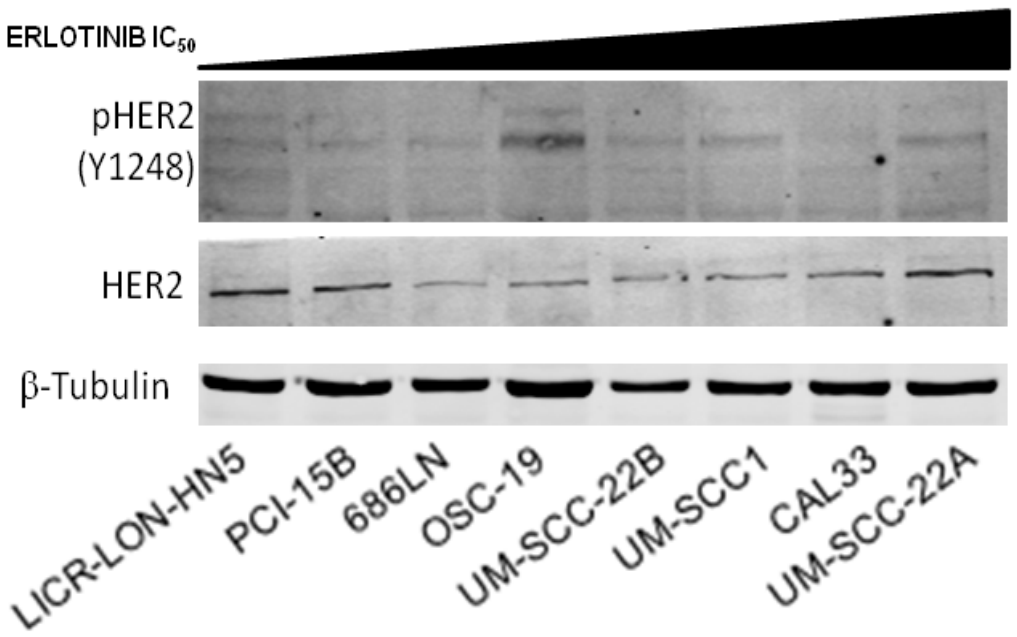

Figure 4-1. HER2 phosphorylation does not correlate with erlotinib sensitivity.

Cell lysates were collected under basal conditions when cells reached 70% confluence. Whole lysates were analyzed by Western Blot and probed for HER2 and pHER2 (Cell Signaling).

In agreement with the lack of correlation between HER2 expression and phosphorylation with erlotinib response, HER3 protein expression did not correlate with response to erlotinib sensitivity (Figure 4-2).

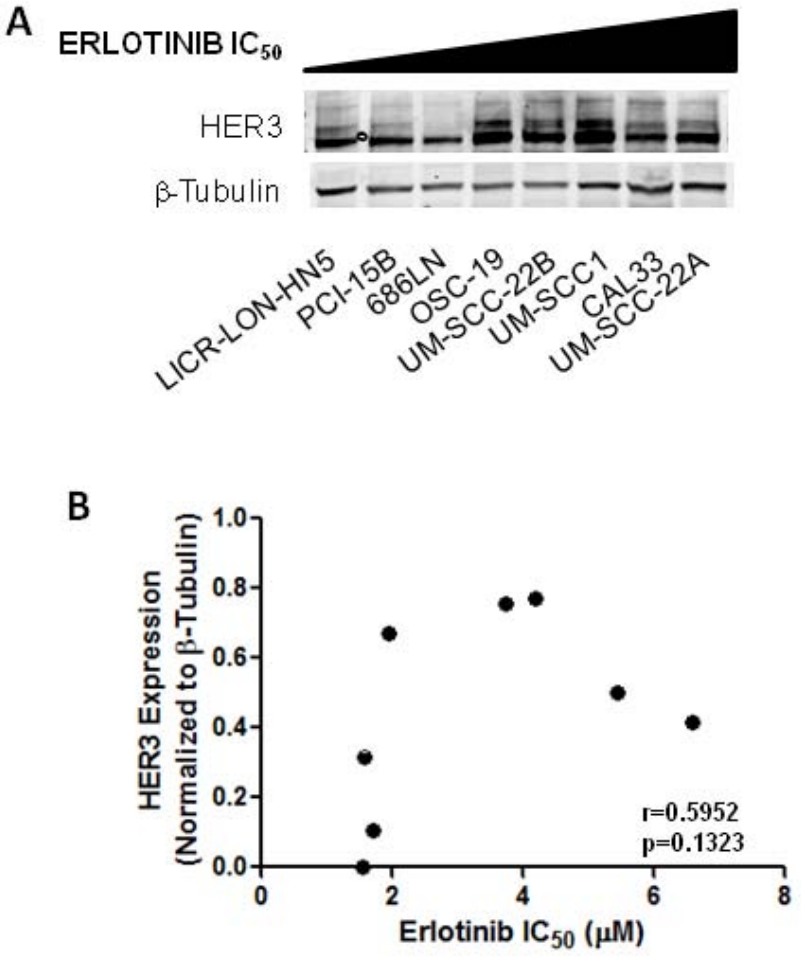

Figure 4-2. HER3 protein expression does not correlate with erlotinib sensitivity.

A. Representative Western Blot where cells were 70% confluent when lysates were collected. Proteins were resolved on an 8% SDS-PAGE Gel and transferred to nitrocellulose membrane that was blotted with α-HER3 (Santa Cruz Biotechnologies). **B.** HER3 expression does not correlate with response to erlotinib (r=0.5952, p=0.1323). Densitometry was calculated using Image J and statistical correlations were calculated using a non-parametric, two-tailed Spearman correlation in GraphPad Software. Data is the result of two independent experiments.

Due to technical issues with the limited phospho-specific HER3 antibodies currently available, we were unable to gain a reproducible immunoblot of HER3 phosphorylation in these lysates. Because HER2-mediated EGFR TKI sensitivity works through HER3 heterodimerization and AKT activation[239], we examined AKT activation in this panel of HNSCC cells to serve as a surrogate marker of HER3 activity. AKT phosphorylation at S473 is a marker of AKT activity because this is one of two residues for which phosphorylation is required to permit activation of the kinase[240]. We did not observe any remarkable changes in AKT expression or phosphorylation across the panel of HNSCC cells (Figure 4-3), suggesting that HER2/HER3-mediated activation of AKT under basal conditions may not play a large role in determining erlotinib response in HNSCC cells.

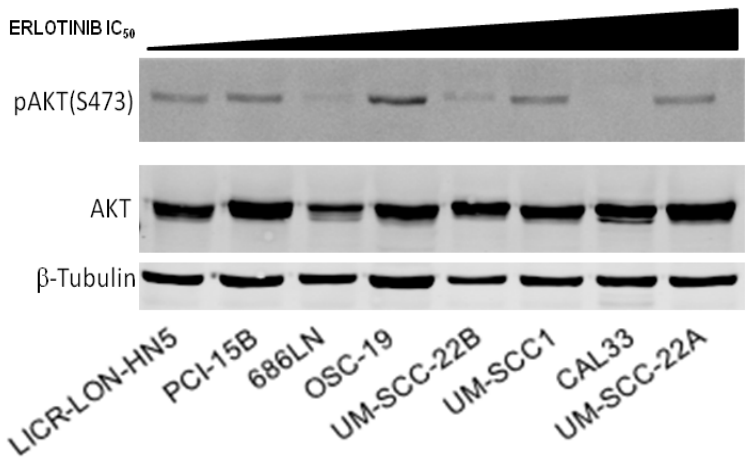

Figure 4-3. AKT phosphorylation does not correlate with erlotinib response.

Cell lysates were collected under basal conditions when cells reached 70% confluence. Whole lysates were analyzed by Western Blot and probed for AKT and pAKT (Cell Signaling).

4.3.2 **c-Met is Hyperphosphorylated in an Erlotinib Resistant Cell Line**

Because EGFR downregulation correlates with decreased sensitivity to EGFR inhibitors (Figure 2-8) but no association was observed between HER2/HER3 signaling and erlotinib sensitivity, we examined other growth factor receptors that may function independently of EGFR to activate the same downstream effectors in the context of erlotinib resistance. IGF-1Rβ has been proposed as a heterodimerization partner with EGFR in HNSCC[241], and drugs targeting VEGFR2 (flk-1) have demonstrated dose-dependent inhibition of EGFR which suggests a role for VEGF in EGFR signaling[242]. Immunoprecipitations with α-phosphotyrosine were performed on TKI-sensitive 686LN cell lysates and Flk-1, IGF-1Rβ, and c-Met were detected by western blot. HeLa cell lysates were used as an erlotinib-resistant control. A dramatic reduction in c-Met phosphorylation was seen in the 686LN cells compared with the TKI-resistant HeLa cells (Figure 4-4) and this was confirmed by immunoblotting on whole cell lysates (data not shown).

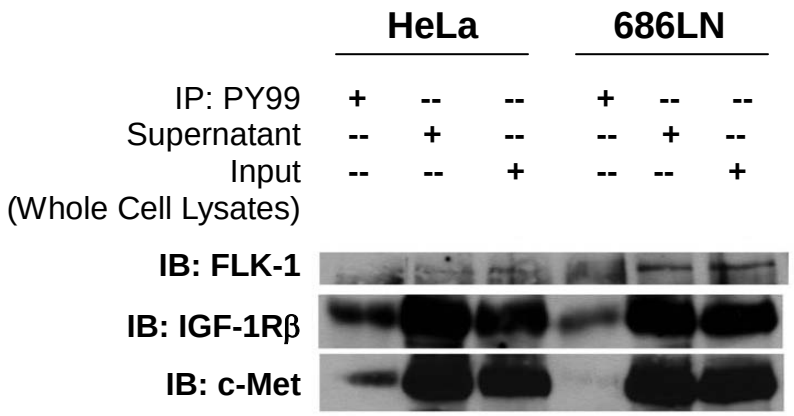

Figure 4-4. c-Met is hyperphosphorylated in an erlotinib resistant cell line.

Immunoprecipitations were performed using α-PY99 (Santa Cruz) and whole cell lysates with protein G-linked agarose beads, resolved on SDS-PAGE gels and immunoblotted (α -Flk-1, α-IGF-1Rβ, α-c-Met, Santa Cruz).

4.3.3 **c-Met Inhibition is Synergistic with EGFR Kinase Inhibition**

To determine the therapeutic significance of decreased c-Met activity in erlotinib sensitive cells, I examined the effects of co-targeting c-Met and EGFR in TKI-resistant cells. Combination studies were performed *in vitro* using erlotinib and SU-11274 (Calbiochem), a c-Met TKI. SU-11274 is known to be synergistic with erlotinib in HNSCC cells[158, 234], and here we report synergistic inhibition of cellular metabolism in the TKI-resistant HeLa cells using SU-11274 and erlotinib. Based on inhibition of cellular metabolism in the presence of erlotinib, SU-11274 or both drugs concurrently, a combination index (CI) value can be determined using the formula of Chou and Talalay[243] (Paragraph 4.2.4). Using this model, a CI>1 is representative of an antagonistic response, a CI=1 is representative of an additive response, and a CI<1 is representative of a synergistic response. The average CI=0.774±0.05 for HeLa cells treated concurrently with erlotinib and SU-11274, indicating a synergistic response when these two drugs are combined *in vitro* (Figure 4-5). The synergistic benefit of co-targeting EGFR and c-Met *in vitro* suggests that further exploring the role of c-Met in TKI resistance may help identify signaling molecules downstream of EGFR and c-Met that could serve as molecular co-targets with EGFR inhibitors.

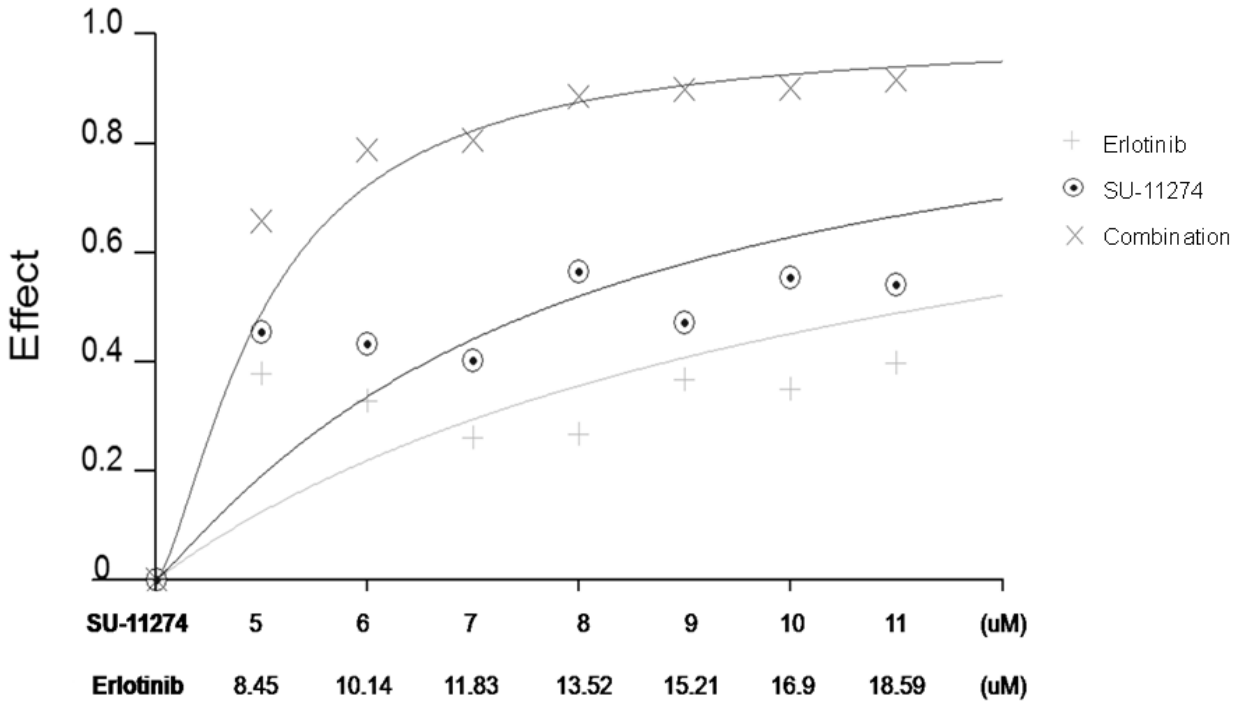

Figure 4-5. c-Met inhibition is synergistic with EGFR inhibition.

Decreases in HeLa cell metabolic activity determined by 72h MTT assay when erlotinib is combined with the c-Met inhibitor SU-11274 at a ratio of 1.69:1, respectively, with [SU-11274] in 1μM intervals from 5-11. The combination index value=0.774±0.05 describes synergy between erlotinib and SU-11274. (>1=antagonistic response, 1=additive response, <1=synergistic response).

Because we did not observe changes in AKT activity in cell lines with varying responses to erlotinib, we hypothesized that the synergistic effects of erlotinib and SU-11274 may stem from deactivation of the MAPK pathway. In accordance with the synergistic effect that is observed in cell metabolism assays when erlotinib is combined with SU-11274, we observed a

marked reduction of MAPK activity when TKI-resistant HeLa cells were treated with erlotinib and SU-11274 prior to stimulation with EGF and HGF (Figure 4-6). We also tested this deactivation of MAPK in TKI-sensitive 686LN cells, and found the same result: inhibition of c-Met and EGFR is required for deactivation of MAPK in the presence of EGFR and c-Met stimulatory ligands (Figure 4-6). This result demonstrates that when EGFR and c-Met signaling is blocked simultaneously, regardless of response to EGFR kinase inhibition, MAPK is deactivated. Further, when either EGFR or c-Met is inhibited singularly, signaling to MAPK through the other receptor can compensate for this blockade.

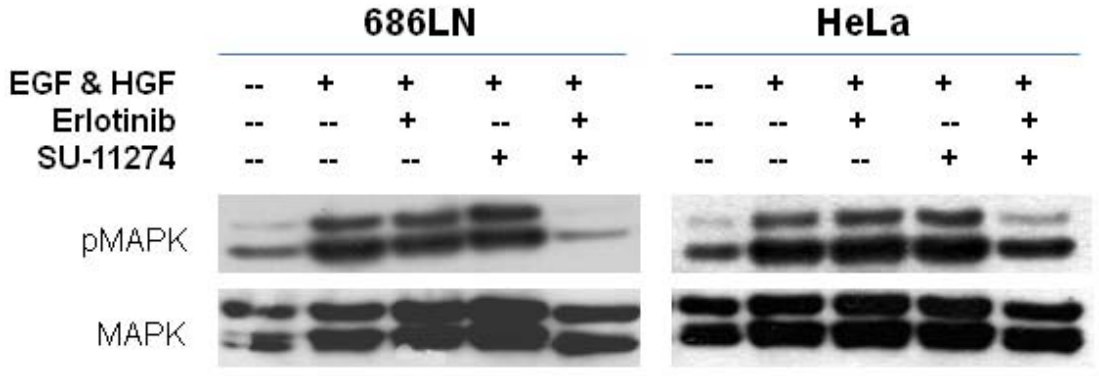

Figure 4-6. Inhibition of c-Met and EGFR is required for decreased MAPK activation.

686LN and HeLa cells were plated at 70% confluency. The following day, cells were serum starved for 2 hours in the presence of either 1μM erlotinib or 1μm SU-11274 as indicated. Cells were then stimulated with either EGF (10ng/mL) or HGF (40ng/mL) for 5 minutes. Cell lysates were harvested on ice and resolved on an SDS-PAGE gel and transferred to a nitrocellulose membrane. Membranes were probed for p24/44 (MAPK, Cell Signaling) or phospho-p42/44 (pMAPK, Cell Signaling).

4.3.4 **c-Met is Not Amplified in an HNSCC Patient Cohort**

c-Met amplification has been reported in lung cancer primarily as a major mechanism of acquired resistance to EGFR kinase inhibition[151], although *de novo* c-Met amplification is observed at a rate of 2-3% in some EGFR kinase inhibitor naïve patients[218]. We hypothesized that c-Met amplification may provide a compensatory mechanism of MAPK activation in the context of erlotinib resistant HNSCC. Only one group has examined c-Met amplification status in HNSCC, reporting 15/23 (65%) tumors with amplified c-Met independent of EGFR TKI treatment as determined by quantitative polymerase chain reaction (qPCR)[158]. To examine a larger cohort of patients, we performed FISH on 77 primary HNSCC tumors and 16 recurrent HNSCC tumors. Our cohort was comprised of 73.1% males and had a median age of 61. Oral cavity and oropharynx tumors comprised 64.5% of our tumor samples and the majority of tumors were stage IV (50.5%). Complete demographics of this cohort can be found in Table 4-2. The FISH analysis conducted by Drs. Simion Chiosea and Sanja Dacic at the University of Pittsburgh Medical Center revealed 0/77 and 0/16 c-Met amplifications in primary and recurrent HNSCC tumors, respectively (Table 4-1). Drs. Chiosea and Dacic also tested 8 of our HNSCC cell lines for c-Met amplification to determine if they were representative of our patient population and we found that c-Met was amplified in 0/8 cell lines, concordant with our patient samples (Table 4-1). All c-Met:CEP7 ratios in both tumors and cell lines were below 2.0, which is the threshold for determining amplification. While our cohort size lacks the statistical power to achieve significance for an amplification that occurs at a rate of 2% in lung cancer, these data suggest that *de novo* c-Met amplification may not occur in HNSCC.

Cell Lines	Total Cells Analyzed	FISH Ratio	Percent High Polysomy	Percent Low Polysomy	Percent Trisomy	Percent Disomy
UM-SCC-22A	60	0.72	1 (1.7%)	4 (6.7%)	32 (53.3%)	23 (38.3%)
UM-SCC-22B	60	0.83	2 (3.3%)	5 (8.3%)	34 (56.7%)	19 (31.7%)
686LN	62	0.71	17 (27.4%)	21 (33.9%)	15 (24.2%)	8 (12.9%)
LICR-LON-HN5	61	0.66	6 (9.8%)	37 (60.7%)	17 (27.9%)	1 (1.6%)
0SC-19	60	0.72	0%	24 (40%)	9 (15%)	27 (45%)
UM-SCC-1	63	0.83	5 (7.9%)	43 (68.3%)	13 (20.6%)	2 (3.1%)
PCI-15B	60	1.14	50 (83.3%)	3 (5%)	7 (11.7%)	0%
CAL33	62	1.02	0%	51 (85.0%)	6 (9.7%)	5 (8.1%)

Tissue	Total Samples Analyzed	Average FISH Ratio	Average Percent High Polysomy	Average Percent Low Polysomy	Average Percent Trisomy	Average Percent Disomy
Primary HNSCC	77	1.05	0.8%	4.2%	15.7%	82.4%
Recurrent HNSCC	16	1.15	0%	5.6%	10.4%	83.7%

Table 4-1. c-MET copy number in HNSCC tumors and cell lines

FISH was performed on 77 primary and 16 recurrent HNSCC tumors as well as 8 HNSCC cell lines. FISH Ratio of CEP7:c-Met staining was analyzed for each specimen. Each cell analyzed was assigned to a category of High Polysomy, Low Polysomy, Trisomy or Disomy based on FISH ratio and averages for each cell line and tumor type are given here. FISH was performed and analyzed by Drs. Simion Chiosea and Sanja Dacic.

	All Cases n=93	
Gender		
Male	68	73.1%
Female	25	26.9%
Age		
Median (Range)	61 (19-85)	
Tumor Type		
Primary	77	82.8%
Recurrence	16	17.2%
Tumor Site		
Oral Cavity	40	43.0%
Oropharynx	20	21.5%
Hypopharynx	1	1.1%
Nasopharynx	1	1.1%
Larynx	23	24.7%
Neck	5	5.4%
Sinus	3	3.2%
Disease Stage		
0-1	17	18.3%
II	5	5.4%
III	14	15.1%
IV	47	50.5%
Recur/Met Unstaged	10	10.8%

Table 4-2. Demographics of c-Met FISH HNSCC patient cohort.

4.3.5 **c-Met Phosphorylation is Not Correlated with Erlotinib Response**

In the absence of any frequent c-Met amplification, we sought to determine if basal c-Met activation may correlate with response to erlotinib in HNSCC cells. One group has reported that c-Met protein expression is not associated with response to erlotinib in HNSCC clinical trials[244], although they did not examine the relationship between c-Met phosphorylation and erlotinib response. We used phosphorylation at Tyr1234/5 as a surrogate marker of c-Met activation since this is the residue at which phosphorylation leads to downstream MAPK activation[245]. All cell lines demonstrated protein expression of the c-Met receptor, and we observed a broad spectrum of basal c-Met phosphorylation across the cell lines (Figure 4-7). Densitometry from three independent western blots was used to determine c-Met expression normalized to β-tubulin and c-Met phosphorylation normalized to total c-Met protein expression. A non-parametric Spearman correlation was used to examine the relationship between erlotinib response and c-Met protein levels and phosphorylation levels. In both cases, c-Met protein expression and c-Met protein phosphorylation, there were no significant associations with erlotinib response ($p=0.9349$ and $p=0.8401$, respectively). The fact that c-Met activity is not inversely correlated with erlotinib sensitivity suggests that while concurrent EGFR and c-Met inhibition is synergistic, c-Met activity may not be required for erlotinib resistance.

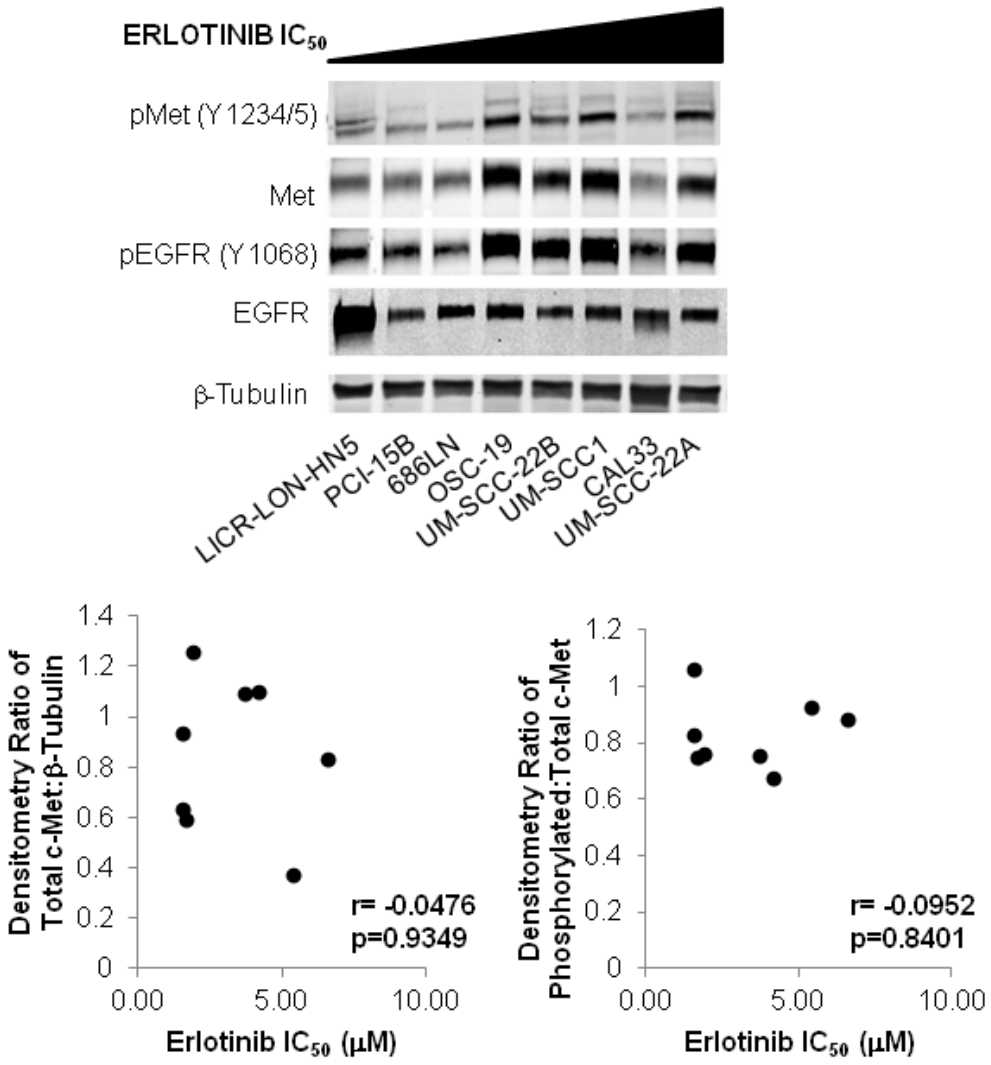

Figure 4-7. Neither c-Met activation nor expression correlates with erlotinib response.

A representative Western Blot is shown where cells were grown to 70% confluency and lysates were collected. Proteins were resolved on an 8% SDS-PAGE Gel and transferred to nitrocellulose membrane that was blotted with α-Met (Cell Signaling) or α-pMet (Cell Signaling). Densitometry was calculated using Image J from three independent experiments and statistical correlations were calculated using GraphPad Software. Met expression and phosphorylation do not correlate with erlotinib response (p=0.9349 and p=0.08401, respectively).

4.3.6 **Altering c-Met Protein Levels Does Not Affect Response to Erlotinib**

To determine whether activation of c-Met confers resistance to erlotinib, we used siRNA to genetically knock down c-Met expression in erlotinib resistant cell lines and examined the response of the cells to erlotinib. c-Met was knocked down in HeLa cells and response to erlotinib was determined by cell metabolism assays 48 hours following erlotinib treatment at a range of doses from 500nM to 50μM. Genetic suppression of c-Met expression did not alter the IC_{50} of HeLa cells treated with erlotinib (Figure 4-8A).

c-Met was also knocked down in UM-22A and CAL33 cell lines and response to erlotinib was determined by cell metabolism assay 24 hours following treatment. Erlotinib decreased cell viability by 33.08±0.26% in vector transfected UM-22A cells and by 31.67±1.22% in UM-22A cells transiently transfected with c-Met siRNA ($p=0.37$, Figure 4-8B). Likewise, erlotinib decreased cell viability by 53.00±3.80% in vector transfected CAL33 cells and by 51.39±23.04% in CAL33 cells transfected with c-Met siRNA ($p=0.95$, Figure 4-8B). These data suggest that transient knockdown of c-Met is not capable of enhancing cellular response to erlotinib.

In line with this, we wanted to determine if c-Met activation is sufficient to confer resistance to erlotinib. We transiently transfected PCI-15B cells with c-Met DNA or vector control DNA and determined response to erlotinib by cell metabolism assays 24 hours after the start of treatment. Erlotinib decreased the cell viability of PCI-15B cells by 31.67±23.16% in vector control transfected cells and by 33.78±25.10% in c-Met transfected cells ($p=0.47$, Figure 4-8C). These data suggest that c-Met is not sufficient for conferring erlotinib resistance in HNSCC cells.

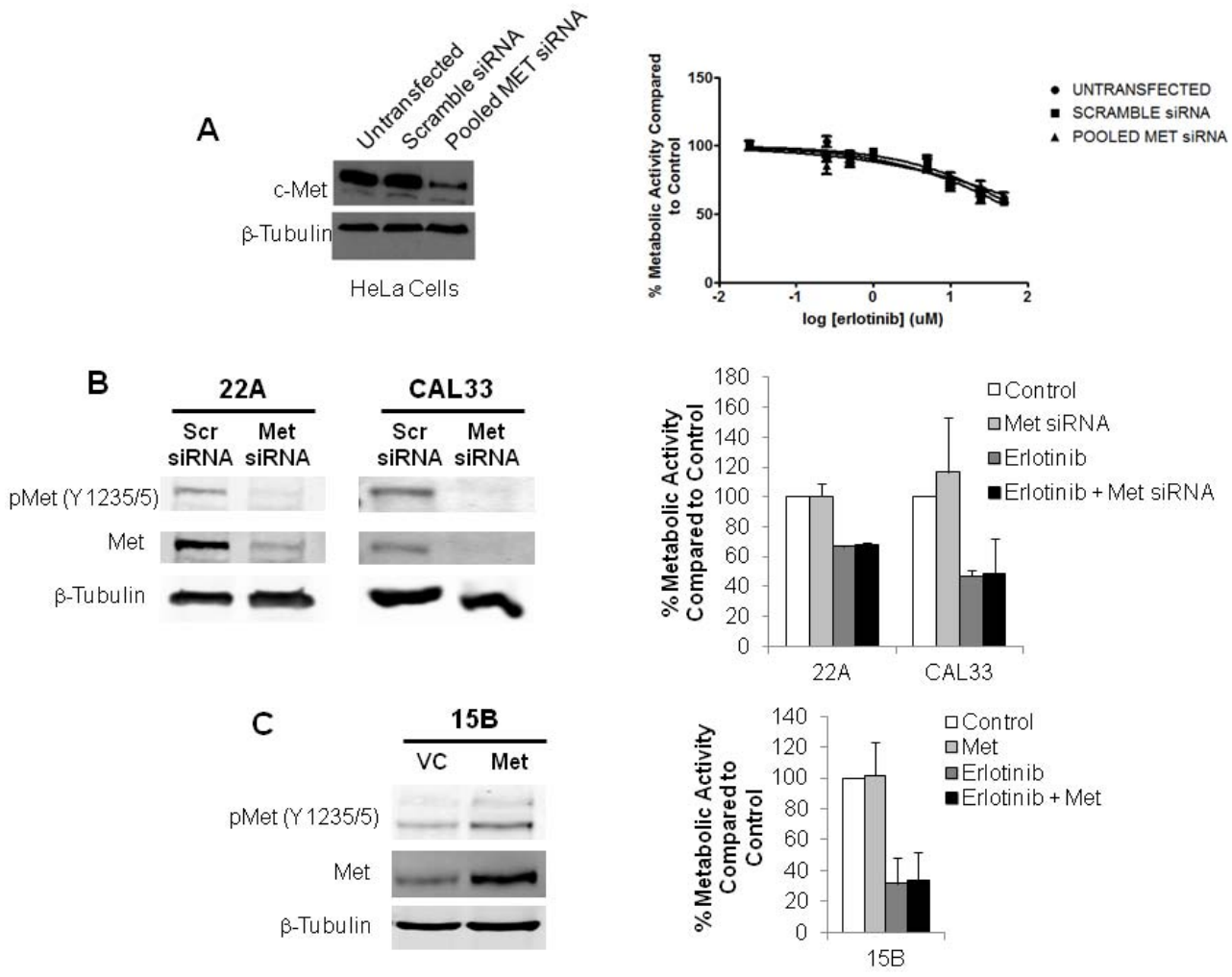

Figure 4-8. Altering c-Met protein level does not affect response to erlotinib.

A. HeLa cells were plated in 96-well plates at a density of 10,000 cells per well. After 24 hours, cells were left untransfected or transfected with 100nM c-Met or scrambled siRNA. The following day, cells were treated with varying concentrations of erlotinib from 500nM to 50μM or DMSO control. Cell metabolism assays (MTT) were performed after 48 hours of drug treatment. Whole cell lysates were harvested on cells transfected in parallel to confirm c-Met knockdown. Data is the result of one experiment. **B.** UM-22A or CAL33 cells were plated in 24-well plates at a density of 30,000 cells per well. After 24 hours, cells were transfected with 100nM c-Met or scrambled siRNA. The following day, DMSO control or twice the IC_{50} dose of erlotinib was added for another 24 hours at which point cell metabolism assays (MTT) were performed. Whole cell lysates were harvested on cells transfected in parallel to confirm c-Met knockdown. Data is the result of two independent experiments run in

duplicate. **C.** PCI-15B cells were plated in 24-well plates at a density of 30,000 cells per well. After 24 hours, cells were transfected with 2ug c-Met or empty vector. The following day, DMSO control or twice the IC_{50} dose of erlotinib was added for another 24 hours at which point cell metabolism assays (MTT) were performed. Whole cell lysates were harvested on cells transfected in parallel to confirm c-Met expression. Data is the result of two independent experiments run in duplicate.

4.4 DISCUSSION

EGFR tyrosine kinase inhibitors have been studied extensively in both lung cancer and HNSCC. Despite the fact that limited response rates are seen with EGFR TKI use, there is no overall survival benefit to erlotinib use in phase III clinical trials in lung cancer[246] and phase III data has not been reported in HNSCC. The greatest benefit in progression-free survival during EGFR TKI use occurs in EGFR mutant lung cancer. The *Journal of Clinical Oncology* recently issued a provisional clinical opinion that EGFR mutation screening should be used as a companion diagnostic to determine erlotinib administration in NSCLC[247]. Unfortunately, EGFR activating mutations are not found in HNSCC which leaves uncertainty regarding the future of erlotinib as a front-line therapy in HNSCC[120]. The studies performed here sought to identify novel molecules that may contribute to erlotinib resistance and, as such, could serve as co-targets to enhance the efficacy of EGFR TKIs in HNSCC.

It is reported in the literature that active HER2 and HER3 signaling can sensitize cells to EGFR inhibitors when EGFR levels are low due to the ability of erlotinib to bind directly to and inhibit HER2[235, 236]. This is in stark contrast to the compensatory signaling from these molecules that is known to contribute to EGFR mAb resistance[98, 216]. Because of the

conflicting nature of these reports, we wanted to examine the status of HER2 and HER3 activity as it relates to EGFR TKI sensitivity.

In the present study, we examined basal levels of HER2 and HER3 expression. We also looked at HER2 phosphorylation and AKT phosphorylation since it is a downstream effector activated by both HER2 and HER3. We did not observe any alterations to basal HER2 and HER3 signaling in association with erlotinib sensitivity. This suggests that unlike in cetuximab resistance, HER2 and HER3 are not differentially contributing to EGFR-independent cell growth in cell lines that are less sensitive to EGFR tyrosine kinase inhibition as compared to cell lines that are more responsive to EGFR TKIs.

HER2 and HER3 signaling is also not preferentially activated in the most erlotinib-sensitive cells. These cells have the highest levels of EGFR (Figure 2-8), so we believe selective EGFR inhibition, not secondary HER2 inhibition, to be the major determinant of EGFR TKI sensitivity in these cells. Either way, our findings do not indicate a role for HER2 or HER3 expression or activity as a predictor of EGFR TKI response.

We also wanted to assess the role of c-Met in EGFR tyrosine kinase inhibitor sensitivity since c-Met has been proposed as a potential therapeutic co-target with EGFR in HNSCC[158]. In our studies, we found that *de novo* c-Met amplification likely does not occur in HNSCC as it does in NSCLC (Table 4-1). Further, we observed a spectrum of c-Met protein expression and phosphorylation that does not correlate with EGFR TKI response (Figure 4-7). We have also shown that increasing or decreasing c-Met protein levels is not sufficient to alter cellular response to erlotinib (Figure 4-8). This data suggests that although EGFR is capable of activating c-Met through a mechanism of lateral receptor crosstalk[234, 248], this may be a

unidirectional mechanism in HNSCC as it does not appear that c-Met is affecting cellular response to EGFR inhibition.

Importantly, despite the lack of cross-talk observed between c-Met and EGFR in these models, we did successfully reproduce the published findings that erlotinib and c-Met TKIs have synergistic anti-metabolic effects in tumor cells[234]. Further, we have corroborated that this mechanism occurs through synergistic reductions in MAPK activity regardless of erlotinib response (Figure 4-6). Our findings suggest that the increased anti-proliferative effects of combination treatment observed with EGFR and c-Met inhibition likely stem from the dual inhibition of growth signals within the cell that has been previously reported by our group and others[158, 234].

Therefore, we propose that the use of c-Met inhibition for the treatment of HNSCC should be considered independently of response to EGFR tyrosine kinase inhibitors. To date, one clinical trial has been published in lung cancer combining a c-Met inhibitor with erlotinib and the authors did not report a statistical benefit over treatment with erlotinib plus placebo, although a benefit was observed in patients harboring KRAS mutations[249]. KRAS mutations are found at a very low frequency in HNSCC, however, suggesting the potentially limited benefit to this co-treatment approach in HNSCC[250].

In summary, we have shown that neither HER2, HER3, nor c-Met signaling correlates with response to EGFR tyrosine kinase inhibition. c-Met alone in not sufficient to alter cellular response to erlotinib, but combined targeting of EGFR and c-Met is effective in reducing MAPK activity and has synergistic anti-metabolic effects on cancer cells. While there may be a role for

co-targeting of EGFR and c-Met in HNSCC, other treatment modalities that work in conjunction with EGFR inhibition to reduce MAPK activity should also be pursued.

5.0 GENERAL DISCUSSION

Squamous cell carcinomas (SCC) are malignant tumors of epithelial origin that comprise over 90% of head and neck cancers. HNSCC accounts for approximately 4% of all malignancies in the United States[57] and it is the sixth most common cancer worldwide, indicating the large public health problem presented by HNSCC[58]. The five year survival rate for oral cancer is approximately 50% and first line treatments have historically included chemotherapy and radiation as well as surgery[59]. In 2006, cetuximab was FDA approved as the first new treatment for head and neck cancer in over 45 years. Cetuximab was approved at that time for the treatment of primary HNSCC in combination with radiation[251] and gained approval in 2011 for concurrent treatment with platinum-based compounds for recurrent or metastatic HNSCC[252]. Despite evidence of limited clinical efficacy with EGFR inhibitors, no one biomarker has been established in HNSCC to predict response to these agents. Elucidation of the mechanism of resistance to EGFR inhibitors has been limited by: 1) the difficulty in obtaining post-treatment tissue from HNSCC patients treated with EGFR inhibitors; and 2) the paucity of preclinical models of EGFR inhibitor resistance.

Two preclinical HNSCC models of resistance to EGFR-targeting agents were recently reported. One model is an HNSCC cell clone selected for gefitinib resistance from Dr. Georgia Chen at Emory University[161], although this model proved to be HNSCC and HeLa cells upon retrospective genotyping. The other model is an HNSCC cell clone selected for cetuximab resistance from Dr. Paul Harari at the University of Wisconsin[162, 163] that has not been

reproducible *in vivo*[164]. Therefore, to determine mechanisms of EGFR inhibitor resistance, additional preclinical models are needed.

5.1.1 **Preclinical Models of Cetuximab Resistance in HNSCC**

In this body of work, I have focused extensively on generating reliable models of cetuximab resistance in HNSCC because of the ramifications that such models could have on our understanding of the molecular basis for resistance to EGFR targeting agents. I initially fashioned my experiments on a report describing the generation of *in vivo* models of resistance to trastuzumab, a monoclonal antibody targeting HER2[180]. This method proved reliable for generation of a bladder cancer model of cetuximab resistance. These bladder cancer models are valid models with which to study mechanisms of cetuximab resistance that may be relevant in HNSCC, however, as both bladder cancer and HNSCC have widespread EGFR expression and lack many of the mutations known to confer resistance to cetuximab in lung and colon cancer.

I also attempted to generate cetuximab resistant models using HNSCC cell line derived xenografts. I was unable to reproduce the cetuximab model generation in xenografts derived from HNSCC cell lines despite manipulating several experimental conditions that are known to affect drug response such as dose and tumor volume. I have had more success in recent collaborations with Dr. Sarah Wheeler (University of Pittsburgh) in which we use a heterotopic tumorgraft model to serve as a basis for selecting cetuximab resistant tumor cells. Previous studies have shown this model to be more representative of clinical response than cell line xenograft studies[187, 188] and we observed cetuximab response rates using these models that are more representative of clinical response rates than the widespread sensitivity to cetuximab that I have observed in HNSCC cell line derived xenografts. The preliminary data I have

presented here suggests that heterotopic tumorgrafts are a reasonable candidate for future studies developing models of cetuximab resistance in HNSCC.

5.1.2 **Co-Targeting HER2 to Enhance Cetuximab Sensitivity**

I used the preclinical model of cetuximab resistance derived from bladder cancer to examine the role of HER2, HER3, and c-Met in cetuximab resistance. With this model, I was able to identify increased phosphorylation of an alternative translation product of HER2 in the cetuximab resistant cells. This protein, 611-CTF, is a carboxyl-terminal fragment of HER2. 611-CTF is targeted with kinase inhibitors and has been implicated in resistance to HER2 antibodies[253]. My studies showed that cortactin, a downstream mediator of 611-CTF signaling[222], is also activated in the context of cetuximab resistance.

Cortactin is potentially an interesting molecular link between EGFR and HER2 that is activated in the context of cetuximab resistance. There are no published reports describing HER2 activation of cortactin apart from what is mediated by 611-CTF. In contrast, evidence of EGF-mediated cortactin expression is widespread and may be mediated by c-Src[254, 255]. Studies examining 611-CTF signaling to c-Src have not been published. It is known, however, that cortactin can increase invasiveness and chemotaxis towards EGF[256-259] and cortactin has been implicated in EGFR endocytosis[260], both of which could be potential mechanisms of EGFR-inhibitor resistance. Further, cortactin has been shown to stabilize the c-Met receptor and confer resistance in HNSCC cells to the EGFR kinase inhibitor gefitinib[237, 261]. Cortactin is an interesting downstream mediator of ErbB receptor signaling, and my studies suggest that its

role in EGFR inhibitor resistance, particularly cetuximab resistance, warrants further investigation.

The studies I have conducted using cetuximab resistant preclinical models demonstrate that kinase inhibition of EGFR and HER2 using afatinib can restore sensitivity to cetuximab *in vitro* and *in vivo* and this occurs *in vivo* alongside loss of 611-CTF expression. A clinical trial is currently underway where cetuximab and afatinib are being combined for the treatment of patients NSCLC. Early results from this trial are encouraging[J Clin Oncol 29: 2011 (suppl; abstr 7525)]; disease control was evident in all patients who received the recommended phase II dosing schedule, and confirmed partial responses were observed in 8/22 (36%) of evaluable patients. Owing to these results, this clinical trial has been expanded and these data suggest that *in vivo* modeling of cetuximab resistance may be a valid way to determine novel co-targets for the treatment of cancer.

5.1.3 **Preclinical Models of Erlotinib Resistance in HNSCC**

Clinical trials are underway in HNSCC using erlotinib, although it has not gained FDA approval for use in the treatment of HNSCC and phase II results do not describe any benefit beyond a modest increase in progression-free survival[113]. In the present work, I chose to focus on assessing primary as opposed to acquired responses to erlotinib in order to identify a biomarker that may serve as a predictor of erlotinib response. These types of biomarkers for primary resistance can facilitate the selection of patients most likely to respond to erlotinib treatment during clinical trials as well as provide a rationale for molecular co-targeting with erlotinib.

Here, I determined the response of several HNSCC cell lines to erlotinib and found that, as with cetuximab, EGFR response correlates with EGFR protein expression. The studies I have presented here do not make over-reaching claims of cell line sensitivity versus resistance to erlotinib based on *in vitro* data, but rather include a thorough analysis of erlotinib response across multiple HNSCC cell lines, which has not been previously reported. These data demonstrate a range of erlotinib responses in HNSCC cell lines that can be used for correlative studies analyzing biomarkers in the preclinical setting.

5.1.4 **Co-Targeting of c-Met with Erlotinib**

c-Met has been proposed as a co-target with EGFR kinase inhibition in HNSCC[158, 234] so I used a panel of HNSCC cell lines with differential responses to erlotinib to examine the role of c-Met in erlotinib resistance. While I was able to reproduce the synergistic effects of EGFR and c-Met kinase inhibition regardless of erlotinib response, I did not observe association of c-Met activity with erlotinib response. These results, unfortunately, do not help identify a subset of patients in which this co-targeting may be particularly beneficial. A recent trial combining a c-Met kinase inhibitor with erlotinib in NSCLC does not show a benefit above that of erlotinib plus placebo[249], and no trials have been published to date combining c-Met inhibitors with erlotinib in HNSCC.

It may be clinically useful to recapitulate the downstream signaling effect of combined EGFR and c-Met kinase inhibition on MAPK activity that I and others have observed[234] directly by combining erlotinib with a MEK inhibitor. This approach has not been tested

clinically to date, but preclinical data bolsters the rationale for this treatment regimen. A recent study in lung cancer cells shows MEK inhibitors can mediate decreases in cell proliferation, invasion, migration, and anchorage-independent growth *in vitro* as well as decreased tumor growth *in vivo* in the context of EGFR TKI resistance[262]. Examining other downstream signaling molecules that are synergistically inhibited with erlotinib and c-Met TKIs may also elucidate other potential co-targets for erlotinib treatment.

5.2 CONCLUDING REMARKS

This dissertation has focused on the generation of preclinical models of resistance to EGFR targeting agents with the ultimate goal of identifying biomarkers that may predict response to these agents and/or serve as molecular co-targets with EGFR inhibitors. I have investigated the generation of cetuximab-resistant HNSCC models using both HNSCC cell line derived xenografts and heterotopic tumorgrafts, with the latter being potentially more representative of clinical response to cetuximab.

I have generated a peer-reviewed model of cetuximab resistance *in vivo* using bladder cancer cell line derived xenografts and showed that, in line with my original hypothesis, HER2 signaling, as identified by 611-CTF and cortactin phosphorylation, may contribute in part to the cetuximab resistant phenotype.

In contrast, I have not identified any positive correlations between HER2, HER3, and c-Met activity with regard to erlotinib response in HNSCC cells. However, the requirement for both EGFR and c-Met TKIs to decrease activity of MAPK in the presence of EGF and HGF

suggests a potential role for pursuing inhibition of MAPK either through these receptors or their downstream signaling molecules.

As a whole, this body of work demonstrates the limitations of using cell lines and cell line derived xenografts as models to reflect the heterogeneous responses to EGFR targeting agents in the clinic. However, these studies also suggest that validated preclinical models may be useful tools with which to examine biomarkers of EGFR inhibitor response and to identify potential novel co-targets.

BIBLIOGRAPHY

1. Savage, C.R., Jr., T. Inagami, and S. Cohen, *The primary structure of epidermal growth factor.* J Biol Chem, 1972. **247**(23): p. 7612-21.
2. Cohen, S., *Isolation of a mouse submaxillary gland protein accelerating incisor eruption and eyelid opening in the new-born animal.* J Biol Chem, 1962. **237**: p. 1555-62.
3. Cohen, S., G. Carpenter, and L. King, Jr., *Epidermal growth factor-receptor-protein kinase interactions. Co-purification of receptor and epidermal growth factor-enhanced phosphorylation activity.* J Biol Chem, 1980. **255**(10): p. 4834-42.
4. Ullrich, A., et al., *Human epidermal growth factor receptor cDNA sequence and aberrant expression of the amplified gene in A431 epidermoid carcinoma cells.* Nature, 1984. **309**(5967): p. 418-25.
5. Donaldson, R.W. and S. Cohen, *Epidermal growth factor stimulates tyrosine phosphorylation in the neonatal mouse: association of a M(r) 55,000 substrate with the receptor.* Proc Natl Acad Sci U S A, 1992. **89**(18): p. 8477-81.
6. Higashiyama, S., et al., *A heparin-binding growth factor secreted by macrophage-like cells that is related to EGF.* Science, 1991. **251**(4996): p. 936-9.
7. Komurasaki, T., et al., *Epiregulin binds to epidermal growth factor receptor and ErbB-4 and induces tyrosine phosphorylation of epidermal growth factor receptor, ErbB-2, ErbB-3 and ErbB-4.* Oncogene, 1997. **15**(23): p. 2841-8.
8. Kimura, H., W.H. Fischer, and D. Schubert, *Structure, expression and function of a schwannoma-derived growth factor.* Nature, 1990. **348**(6298): p. 257-60.
9. Marquardt, H., et al., *Rat transforming growth factor type 1: structure and relation to epidermal growth factor.* Science, 1984. **223**(4640): p. 1079-82.
10. Shing, Y., et al., *Betacellulin: a mitogen from pancreatic beta cell tumors.* Science, 1993. **259**(5101): p. 1604-7.
11. Shoyab, M., et al., *Structure and function of human amphiregulin: a member of the epidermal growth factor family.* Science, 1989. **243**(4894 Pt 1): p. 1074-6.
12. Yarden, Y. and M.X. Sliwkowski, *Untangling the ErbB signalling network.* Nat Rev Mol Cell Biol, 2001. **2**(2): p. 127-37.
13. Garrett, T.P., et al., *Crystal structure of a truncated epidermal growth factor receptor extracellular domain bound to transforming growth factor alpha.* Cell, 2002. **110**(6): p. 763-73.
14. Mohammadi, M., et al., *Aggregation-induced activation of the epidermal growth factor receptor protein tyrosine kinase.* Biochemistry, 1993. **32**(34): p. 8742-8.
15. Quian, X.L., S.J. Decker, and M.I. Greene, *p185c-neu and epidermal growth factor receptor associate into a structure composed of activated kinases.* Proc Natl Acad Sci U S A, 1992. **89**(4): p. 1330-4.
16. Hsieh, M.Y., et al., *Stochastic simulations of ErbB homo and heterodimerisation: potential impacts of receptor conformational state and spatial segregation.* IET Syst Biol, 2008. **2**(5): p. 256-72.

17. Hsu, C.Y., et al., *Autophosphorylation of the intracellular domain of the epidermal growth factor receptor results in different effects on its tyrosine kinase activity with various peptide substrates. Phosphorylation of peptides representing Tyr(P) sites of phospholipase C-gamma.* J Biol Chem, 1991. **266**(1): p. 603-8.
18. Frederick, L., et al., *Diversity and frequency of epidermal growth factor receptor mutations in human glioblastomas.* Cancer Res, 2000. **60**(5): p. 1383-7.
19. Liu, D., et al., *EGFR is a transducer of the urokinase receptor initiated signal that is required for in vivo growth of a human carcinoma.* Cancer Cell, 2002. **1**(5): p. 445-57.
20. Hernandez-Sotomayor, S.M., et al., *Epidermal growth factor stimulates substrate-selective protein-tyrosine- phosphatase activity.* Proc Natl Acad Sci U S A, 1993. **90**(16): p. 7691-5.
21. Bhola, N.E. and J.R. Grandis, *Crosstalk between G-protein-coupled receptors and epidermal growth factor receptor in cancer.* Front Biosci, 2008. **13**: p. 1857-65.
22. Guy, P.M., et al., *Insect cell-expressed p180erbB3 possesses an impaired tyrosine kinase activity.* Proc Natl Acad Sci U S A, 1994. **91**(17): p. 8132-6.
23. Klapper, L.N., et al., *The ErbB-2/HER2 oncoprotein of human carcinomas may function solely as a shared coreceptor for multiple stroma-derived growth factors.* Proc Natl Acad Sci U S A, 1999. **96**(9): p. 4995-5000.
24. Cohen, B.D., et al., *The relationship between human epidermal growth-like factor receptor expression and cellular transformation in NIH3T3 cells.* J Biol Chem, 1996. **271**(48): p. 30897-903.
25. Alvarado, D., D.E. Klein, and M.A. Lemmon, *ErbB2 resembles an autoinhibited invertebrate epidermal growth factor receptor.* Nature, 2009. **461**(7261): p. 287-91.
26. Alvarado, D., D.E. Klein, and M.A. Lemmon, *Structural basis for negative cooperativity in growth factor binding to an EGF receptor.* Cell, 2010. **142**(4): p. 568-79.
27. Borg, J.P., et al., *ERBIN: a basolateral PDZ protein that interacts with the mammalian ERBB2/HER2 receptor.* Nat Cell Biol, 2000. **2**(7): p. 407-14.
28. Brachmann, R., et al., *Transmembrane TGF-alpha precursors activate EGF/TGF-alpha receptors.* Cell, 1989. **56**(4): p. 691-700.
29. Wong, S.T., et al., *The TGF-alpha precursor expressed on the cell surface binds to the EGF receptor on adjacent cells, leading to signal transduction.* Cell, 1989. **56**(3): p. 495-506.
30. Vieira, A.V., C. Lamaze, and S.L. Schmid, *Control of EGF receptor signaling by clathrin-mediated endocytosis.* Science, 1996. **274**(5295): p. 2086-9.
31. Masui, H., L. Castro, and J. Mendelsohn, *Consumption of EGF by A431 cells: evidence for receptor recycling.* J Cell Biol, 1993. **120**(1): p. 85-93.
32. Kurten, R.C., D.L. Cadena, and G.N. Gill, *Enhanced degradation of EGF receptors by a sorting nexin, SNX1.* Science, 1996. **272**(5264): p. 1008-10.
33. Grovdal, L.M., et al., *Direct interaction of Cbl with pTyr 1045 of the EGF receptor (EGFR) is required to sort the EGFR to lysosomes for degradation.* Exp Cell Res, 2004. **300**(2): p. 388-95.
34. Baulida, J., et al., *All ErbB receptors other than the epidermal growth factor receptor are endocytosis impaired.* J Biol Chem, 1996. **271**(9): p. 5251-7.
35. Lin, S.Y., et al., *Nuclear localization of EGF receptor and its potential new role as a transcription factor.* Nat Cell Biol, 2001. **3**(9): p. 802-8.

36. Libermann, T.A., et al., *Amplification, enhanced expression and possible rearrangement of EGF receptor gene in primary human brain tumours of glial origin.* Nature, 1985. **313**(5998): p. 144-7.
37. Cohen, D.W., et al., *Expression of transforming growth factor-alpha and the epidermal growth factor receptor in human prostate tissues.* J Urol, 1994. **152**(6 Pt 1): p. 2120-4.
38. Rubin Grandis, J., et al., *Quantitative immunohistochemical analysis of transforming growth factor- alpha and epidermal growth factor receptor in patients with squamous cell carcinoma of the head and neck.* Cancer, 1996. **78**(6): p. 1284-92.
39. Grandis, J.R. and D.J. Tweardy, *Elevated levels of transforming growth factor alpha and epidermal growth factor receptor messenger RNA are early markers of carcinogenesis in head and neck cancer.* Cancer Res, 1993. **53**(15): p. 3579-84.
40. Grandis, J.R., et al., *Levels of TGF-alpha and EGFR protein in head and neck squamous cell carcinoma and patient survival.* J Natl Cancer Inst, 1998. **90**(11): p. 824-32.
41. Tsiambas, E., et al., *HER2/neu expression and gene alterations in pancreatic ductal adenocarcinoma: a comparative immunohistochemistry and chromogenic in situ hybridization study based on tissue microarrays and computerized image analysis.* JOP, 2006. **7**(3): p. 283-94.
42. Andersson, U., et al., *Epidermal growth factor receptor family (EGFR, ErbB2-4) in gliomas and meningiomas.* Acta Neuropathol, 2004. **108**(2): p. 135-42.
43. Di Lorenzo, G., et al., *Expression of epidermal growth factor receptor correlates with disease relapse and progression to androgen-independence in human prostate cancer.* Clin Cancer Res, 2002. **8**(11): p. 3438-44.
44. Mayer, A., et al., *The prognostic significance of proliferating cell nuclear antigen, epidermal growth factor receptor, and mdr gene expression in colorectal cancer.* Cancer, 1993. **71**(8): p. 2454-60.
45. Brunt, E.M. and P.E. Swanson, *Immunoreactivity for c-erbB-2 oncopeptide in benign and malignant diseases of the liver.* Am J Clin Pathol, 1992. **97**(5 Suppl 1): p. S53-61.
46. Berchuck, A., et al., *Epidermal growth factor receptor expression in normal ovarian epithelium and ovarian cancer. I. Correlation of receptor expression with prognostic factors in patients with ovarian cancer.* Am J Obstet Gynecol, 1991. **164**(2): p. 669-74.
47. Kameda, T., et al., *Expression of ERBB2 in human gastric carcinomas: relationship between p185ERBB2 expression and the gene amplification.* Cancer Res, 1990. **50**(24): p. 8002-9.
48. Slamon, D.J., et al., *Studies of the HER-2/neu proto-oncogene in human breast and ovarian cancer.* Science, 1989. **244**(4905): p. 707-12.
49. Cohen, J.A., et al., *Expression pattern of the neu (NGL) gene-encoded growth factor receptor protein (p185neu) in normal and transformed epithelial tissues of the digestive tract.* Oncogene, 1989. **4**(1): p. 81-8.
50. Bennett, C., et al., *Expression of growth factor and epidermal growth factor receptor encoded transcripts in human gastric tissues.* Cancer Res, 1989. **49**(8): p. 2104-11.
51. Sobol, R.E., et al., *Epidermal growth factor receptor expression in human lung carcinomas defined by a monoclonal antibody.* J Natl Cancer Inst, 1987. **79**(3): p. 403-7.
52. Sainsbury, J.R., et al., *Epidermal-growth-factor receptor status as predictor of early recurrence of and death from breast cancer.* Lancet, 1987. **1**(8547): p. 1398-402.
53. Yokota, J., et al., *Amplification of c-erbB-2 oncogene in human adenocarcinomas in vivo.* Lancet, 1986. **1**(8484): p. 765-7.

54. Grandis, J.R. and D.J. Tweardy, *TGF-alpha and EGFR in head and neck cancer.* J Cell Biochem Suppl, 1993: p. 188-91.
55. Xia, W., et al., *Combination of EGFR, HER-2/neu, and HER-3 is a stronger predictor for the outcome of oral squamous cell carcinoma than any individual family members.* Clin Cancer Res, 1999. **5**(12): p. 4164-74.
56. O-charoenrat, P., et al., *C-erbB receptors in squamous cell carcinomas of the head and neck: clinical significance and correlation with matrix metalloproteinases and vascular endothelial growth factors.* Oral Oncol, 2002. **38**(1): p. 73-80.
57. Jemal, A., et al., *Cancer statistics, 2008.* CA Cancer J Clin, 2008. **58**(2): p. 71-96.
58. Hunter, K.D., E.K. Parkinson, and P.R. Harrison, *Profiling early head and neck cancer.* Nat Rev Cancer, 2005. **5**(2): p. 127-35.
59. Marur, S. and A.A. Forastiere, *Head and neck cancer: changing epidemiology, diagnosis, and treatment.* Mayo Clin Proc, 2008. **83**(4): p. 489-501.
60. Brachman, D.G., et al., *Occurrence of p53 gene deletions and human papilloma virus infection in human head and neck cancer.* Cancer Res, 1992. **52**(17): p. 4832-6.
61. Stransky, N., et al., *The mutational landscape of head and neck squamous cell carcinoma.* Science, 2011. **333**(6046): p. 1157-60.
62. Perrone, F., et al., *Molecular and cytogenetic subgroups of oropharyngeal squamous cell carcinoma.* Clin Cancer Res, 2006. **12**(22): p. 6643-51.
63. Scheffner, M., et al., *The E6 oncoprotein encoded by human papillomavirus types 16 and 18 promotes the degradation of p53.* Cell, 1990. **63**(6): p. 1129-36.
64. Mrhalova, M., et al., *Epidermal growth factor receptor--its expression and copy numbers of EGFR gene in patients with head and neck squamous cell carcinomas.* Neoplasma, 2005. **52**(4): p. 338-43.
65. Grandis, J.R., Q. Zeng, and D.J. Tweardy, *Retinoic acid normalizes the increased gene transcription rate of TGF- alpha and EGFR in head and neck cancer cell lines.* Nat Med, 1996. **2**(2): p. 237-40.
66. Rubin Grandis, J., et al., *Levels of TGF-alpha and EGFR protein in head and neck squamous cell carcinoma and patient survival.* J Natl Cancer Inst, 1998. **90**(11): p. 824-32.
67. Beckhardt, R.N., et al., *HER-2/neu oncogene characterization in head and neck squamous cell carcinoma.* Arch Otolaryngol Head Neck Surg, 1995. **121**(11): p. 1265-70.
68. Rautava, J., et al., *ERBB receptors in developing, dysplastic and malignant oral epithelia.* Oral Oncol, 2008. **44**(3): p. 227-35.
69. Ekberg, T., et al., *Expression of EGFR, HER2, HER3, and HER4 in metastatic squamous cell carcinomas of the oral cavity and base of tongue.* Int J Oncol, 2005. **26**(5): p. 1177-85.
70. Agulnik, M., et al., *Predictive and pharmacodynamic biomarker studies in tumor and skin tissue samples of patients with recurrent or metastatic squamous cell carcinoma of the head and neck treated with erlotinib.* J Clin Oncol, 2007. **25**(16): p. 2184-90.
71. Temam, S., et al., *Epidermal growth factor receptor copy number alterations correlate with poor clinical outcome in patients with head and neck squamous cancer.* J Clin Oncol, 2007. **25**(16): p. 2164-70.
72. Young, R.J., et al., *Relationship between epidermal growth factor receptor status, p16(INK4A), and outcome in head and neck squamous cell carcinoma.* Cancer Epidemiol Biomarkers Prev, 2011. **20**(6): p. 1230-7.

73. Chung, C.H., et al., *Increased epidermal growth factor receptor gene copy number is associated with poor prognosis in head and neck squamous cell carcinomas.* J Clin Oncol, 2006. **24**(25): p. 4170-6.
74. Ang, K.K., et al., *Impact of epidermal growth factor receptor expression on survival and pattern of relapse in patients with advanced head and neck carcinoma.* Cancer Res, 2002. **62**(24): p. 7350-6.
75. Grandis, J.R., et al., *Quantitative immunohistochemical analysis of transforming growth factor- alpha and epidermal growth factor receptor in patients with squamous cell carcinoma of the head and neck.* Cancer, 1996. **78**(6): p. 1284-92.
76. Rubin Grandis, J., et al., *Downmodulation of TGF-alpha protein expression with antisense oligonucleotides inhibits proliferation of head and neck squamous carcinoma but not normal mucosal epithelial cells.* J Cell Biochem, 1998. **69**(1): p. 55-62.
77. Sok, J.C., et al., *Mutant epidermal growth factor receptor (EGFRvIII) contributes to head and neck cancer growth and resistance to EGFR targeting.* Clin Cancer Res, 2006. **12**(17): p. 5064-73.
78. Batra, S.K., et al., *Epidermal growth factor ligand-independent, unregulated, cell-transforming potential of a naturally occurring human mutant EGFRvIII gene.* Cell Growth Differ, 1995. **6**(10): p. 1251-9.
79. Nagane, M., et al., *Drug resistance of human glioblastoma cells conferred by a tumor-specific mutant epidermal growth factor receptor through modulation of Bcl-XL and caspase-3-like proteases.* Proc Natl Acad Sci U S A, 1998. **95**(10): p. 5724-9.
80. Mamot, C., et al., *Epidermal growth factor receptor-targeted immunoliposomes significantly enhance the efficacy of multiple anticancer drugs in vivo.* Cancer Res, 2005. **65**(24): p. 11631-8.
81. Bigner, S.H., et al., *Characterization of the epidermal growth factor receptor in human glioma cell lines and xenografts.* Cancer Res, 1990. **50**(24): p. 8017-22.
82. Grandis, J.R. and J.C. Sok, *Signaling through the epidermal growth factor receptor during the development of malignancy.* Pharmacol Ther, 2004. **102**(1): p. 37-46.
83. Luttrell, D.K., et al., *Involvement of pp60c-src with two major signaling pathways in human breast cancer.* Proc Natl Acad Sci U S A, 1994. **91**(1): p. 83-7.
84. Olayioye, M.A., et al., *ErbB receptor-induced activation of stat transcription factors is mediated by Src tyrosine kinases.* J Biol Chem, 1999. **274**(24): p. 17209-18.
85. Wasilenko, W.J., et al., *Phosphorylation and activation of epidermal growth factor receptors in cells transformed by the src oncogene.* Mol Cell Biol, 1991. **11**(1): p. 309-21.
86. Boerner, J.L., et al., *Transactivating agonists of the EGF receptor require Tyr 845 phosphorylation for induction of DNA synthesis.* Mol Carcinog, 2005. **44**(4): p. 262-73.
87. Thomas, S.M., et al., *Ras is essential for nerve growth factor- and phorbol ester-induced tyrosine phosphorylation of MAP kinases.* Cell, 1992. **68**(6): p. 1031-40.
88. Park, S., et al., *Activated Src tyrosine kinase phosphorylates Tyr-457 of bovine GTPase-activating protein (GAP) in vitro and the corresponding residue of rat GAP in vivo.* J Biol Chem, 1992. **267**(24): p. 17194-200.
89. Silva, C.M., *Role of STATs as downstream signal transducers in Src family kinase-mediated tumorigenesis.* Oncogene, 2004. **23**(48): p. 8017-23.
90. Leeman, R.J., V.W. Lui, and J.R. Grandis, *STAT3 as a therapeutic target in head and neck cancer.* Expert Opin Biol Ther, 2006. **6**(3): p. 231-41.

91. Sartor, C.I., et al., *Role of epidermal growth factor receptor and STAT-3 activation in autonomous proliferation of SUM-102PT human breast cancer cells.* Cancer Res, 1997. **57**(5): p. 978-87.
92. Garcia, R., et al., *Constitutive activation of Stat3 by the Src and JAK tyrosine kinases participates in growth regulation of human breast carcinoma cells.* Oncogene, 2001. **20**(20): p. 2499-513.
93. Shi, C.S. and J.H. Kehrl, *Pyk2 amplifies epidermal growth factor and c-Src-induced Stat3 activation.* J Biol Chem, 2004. **279**(17): p. 17224-31.
94. Quadros, M.R., et al., *Complex regulation of signal transducers and activators of transcription 3 activation in normal and malignant keratinocytes.* Cancer Res, 2004. **64**(11): p. 3934-9.
95. Lowenstein, E.J., et al., *The SH2 and SH3 domain-containing protein GRB2 links receptor tyrosine kinases to ras signaling.* Cell, 1992. **70**(3): p. 431-42.
96. Chang, F., et al., *Signal transduction mediated by the Ras/Raf/MEK/ERK pathway from cytokine receptors to transcription factors: potential targeting for therapeutic intervention.* Leukemia, 2003. **17**(7): p. 1263-93.
97. Zhang, T., J. Ma, and X. Cao, *Grb2 regulates Stat3 activation negatively in epidermal growth factor signalling.* Biochem J, 2003. **376**(Pt 2): p. 457-64.
98. Xia, L., et al., *Identification of both positive and negative domains within the epidermal growth factor receptor COOH-terminal region for signal transducer and activator of transcription (STAT) activation.* J Biol Chem, 2002. **277**(34): p. 30716-23.
99. Grandis, J.R., et al., *Requirement of Stat3 but not Stat1 activation for epidermal growth factor receptor- mediated cell growth in vitro.* J Clin Invest, 1998. **102**(7): p. 1385-92.
100. Kijima, T., et al., *STAT3 activation abrogates growth factor dependence and contributes to head and neck squamous cell carcinoma tumor growth in vivo.* Cell Growth Differ, 2002. **13**(8): p. 355-62.
101. Xi, S., et al., *Src kinases mediate STAT growth pathways in squamous cell carcinoma of the head and neck.* J Biol Chem, 2003. **278**(34): p. 31574-83.
102. Carnero, A., et al., *The PTEN/PI3K/AKT signalling pathway in cancer, therapeutic implications.* Curr Cancer Drug Targets, 2008. **8**(3): p. 187-98.
103. Laffargue, M., et al., *An epidermal growth factor receptor/Gab1 signaling pathway is required for activation of phosphoinositide 3-kinase by lysophosphatidic acid.* J Biol Chem, 1999. **274**(46): p. 32835-41.
104. Scaltriti, M. and J. Baselga, *The epidermal growth factor receptor pathway: a model for targeted therapy.* Clin Cancer Res, 2006. **12**(18): p. 5268-72.
105. Lai, S.Y., et al., *Intratumoral epidermal growth factor receptor antisense DNA therapy in head and neck cancer: first human application and potential antitumor mechanisms.* J Clin Oncol, 2009. **27**(8): p. 1235-42.
106. Huang, Z., et al., *A pan-HER approach for cancer therapy: background, current status and future development.* Expert Opin Biol Ther, 2009. **9**(1): p. 97-110.
107. Ward, W.H., et al., *Epidermal growth factor receptor tyrosine kinase. Investigation of catalytic mechanism, structure-based searching and discovery of a potent inhibitor.* Biochem Pharmacol, 1994. **48**(4): p. 659-66.
108. Lynch, T.J., et al., *Activating mutations in the epidermal growth factor receptor underlying responsiveness of non-small-cell lung cancer to gefitinib.* N Engl J Med, 2004. **350**(21): p. 2129-39.

109. Shepherd, F.A., et al., *Erlotinib in previously treated non-small-cell lung cancer.* N Engl J Med, 2005. **353**(2): p. 123-32.
110. Miller, V.A., et al., *Molecular characteristics of bronchioloalveolar carcinoma and adenocarcinoma, bronchioloalveolar carcinoma subtype, predict response to erlotinib.* J Clin Oncol, 2008. **26**(9): p. 1472-8.
111. Mitsudomi, T., et al., *Gefitinib versus cisplatin plus docetaxel in patients with non-small-cell lung cancer harbouring mutations of the epidermal growth factor receptor (WJTOG3405): an open label, randomised phase 3 trial.* Lancet Oncol, 2010. **11**(2): p. 121-8.
112. Pao, W. and J. Chmielecki, *Rational, biologically based treatment of EGFR-mutant non-small-cell lung cancer.* Nat Rev Cancer, 2010. **10**(11): p. 760-74.
113. Soulieres, D., et al., *Multicenter phase II study of erlotinib, an oral epidermal growth factor receptor tyrosine kinase inhibitor, in patients with recurrent or metastatic squamous cell cancer of the head and neck.* J Clin Oncol, 2004. **22**(1): p. 77-85.
114. Thomas, F., et al., *Pilot study of neoadjuvant treatment with erlotinib in nonmetastatic head and neck squamous cell carcinoma.* Clin Cancer Res, 2007. **13**(23): p. 7086-92.
115. Siu, L.L., et al., *Phase I/II trial of erlotinib and cisplatin in patients with recurrent or metastatic squamous cell carcinoma of the head and neck: a Princess Margaret Hospital phase II consortium and National Cancer Institute of Canada Clinical Trials Group Study.* J Clin Oncol, 2007. **25**(16): p. 2178-83.
116. Paez, J.G., et al., *EGFR mutations in lung cancer: correlation with clinical response to gefitinib therapy.* Science, 2004. **304**(5676): p. 1497-500.
117. Pao, W., et al., *EGF receptor gene mutations are common in lung cancers from "never smokers" and are associated with sensitivity of tumors to gefitinib and erlotinib.* Proc Natl Acad Sci U S A, 2004. **101**(36): p. 13306-11.
118. Yun, C.H., et al., *The T790M mutation in EGFR kinase causes drug resistance by increasing the affinity for ATP.* Proc Natl Acad Sci U S A, 2008. **105**(6): p. 2070-5.
119. Mulloy, R., et al., *Epidermal growth factor receptor mutants from human lung cancers exhibit enhanced catalytic activity and increased sensitivity to gefitinib.* Cancer Res, 2007. **67**(5): p. 2325-30.
120. Murray, S., et al., *Screening for EGFR Mutations in Patients with Head and Neck Cancer Treated with Gefitinib on a Compassionate-Use Program: A Hellenic Cooperative Oncology Group Study.* J Oncol, 2010. **2010**: p. 709678.
121. Li, S., et al., *Structural basis for inhibition of the epidermal growth factor receptor by cetuximab.* Cancer Cell, 2005. **7**(4): p. 301-11.
122. Sato, J.D., et al., *Biological effects in vitro of monoclonal antibodies to human epidermal growth factor receptors.* Mol Biol Med, 1983. **1**(5): p. 511-29.
123. Kawaguchi, Y., et al., *Cetuximab induce antibody-dependent cellular cytotoxicity against EGFR-expressing esophageal squamous cell carcinoma.* Int J Cancer, 2007. **120**(4): p. 781-7.
124. Dechant, M., et al., *Complement-dependent tumor cell lysis triggered by combinations of epidermal growth factor receptor antibodies.* Cancer Res, 2008. **68**(13): p. 4998-5003.
125. Bonner, J.A., et al., *Radiotherapy plus cetuximab for squamous-cell carcinoma of the head and neck.* N Engl J Med, 2006. **354**(6): p. 567-78.
126. Vermorken, J.B., et al., *Platinum-based chemotherapy plus cetuximab in head and neck cancer.* N Engl J Med, 2008. **359**(11): p. 1116-27.

127. Vermorken, J.B., et al., *Open-label, uncontrolled, multicenter phase II study to evaluate the efficacy and toxicity of cetuximab as a single agent in patients with recurrent and/or metastatic squamous cell carcinoma of the head and neck who failed to respond to platinum-based therapy.* J Clin Oncol, 2007. **25**(16): p. 2171-7.
128. Jonker, D.J., et al., *Cetuximab for the treatment of colorectal cancer.* N Engl J Med, 2007. **357**(20): p. 2040-8.
129. Lopez-Albaitero, A. and R.L. Ferris, *Immune activation by epidermal growth factor receptor specific monoclonal antibody therapy for head and neck cancer.* Arch Otolaryngol Head Neck Surg, 2007. **133**(12): p. 1277-81.
130. Van Cutsem, E., et al., *Open-label phase III trial of panitumumab plus best supportive care compared with best supportive care alone in patients with chemotherapy-refractory metastatic colorectal cancer.* J Clin Oncol, 2007. **25**(13): p. 1658-64.
131. Mukohara, T., et al., *Differential effects of gefitinib and cetuximab on non-small-cell lung cancers bearing epidermal growth factor receptor mutations.* J Natl Cancer Inst, 2005. **97**(16): p. 1185-94.
132. Khambata-Ford, S., et al., *Analysis of potential predictive markers of cetuximab benefit in BMS099, a phase III study of cetuximab and first-line taxane/carboplatin in advanced non-small-cell lung cancer.* J Clin Oncol, 2010. **28**(6): p. 918-27.
133. Ji, H., et al., *The impact of human EGFR kinase domain mutations on lung tumorigenesis and in vivo sensitivity to EGFR-targeted therapies.* Cancer Cell, 2006. **9**(6): p. 485-95.
134. Regales, L., et al., *Dual targeting of EGFR can overcome a major drug resistance mutation in mouse models of EGFR mutant lung cancer.* J Clin Invest, 2009. **119**(10): p. 3000-10.
135. Burtness, B., et al., *Phase III randomized trial of cisplatin plus placebo compared with cisplatin plus cetuximab in metastatic/recurrent head and neck cancer: an Eastern Cooperative Oncology Group study.* J Clin Oncol, 2005. **23**(34): p. 8646-54.
136. Lemos-Gonzalez, Y., et al., *Absence of activating mutations in the EGFR kinase domain in Spanish head and neck cancer patients.* Tumour Biol, 2007. **28**(5): p. 273-9.
137. Maemondo, M., et al., *Gefitinib or chemotherapy for non-small-cell lung cancer with mutated EGFR.* N Engl J Med, 2010. **362**(25): p. 2380-8.
138. Mok, T.S., et al., *Gefitinib or carboplatin-paclitaxel in pulmonary adenocarcinoma.* N Engl J Med, 2009. **361**(10): p. 947-57.
139. Cunningham, D., et al., *Cetuximab monotherapy and cetuximab plus irinotecan in irinotecan-refractory metastatic colorectal cancer.* N Engl J Med, 2004. **351**(4): p. 337-45.
140. Kobayashi, S., et al., *EGFR mutation and resistance of non-small-cell lung cancer to gefitinib.* N Engl J Med, 2005. **352**(8): p. 786-92.
141. Jackman, D., et al., *Clinical definition of acquired resistance to epidermal growth factor receptor tyrosine kinase inhibitors in non-small-cell lung cancer.* J Clin Oncol, 2010. **28**(2): p. 357-60.
142. Van Cutsem, E., et al., *Cetuximab and chemotherapy as initial treatment for metastatic colorectal cancer.* N Engl J Med, 2009. **360**(14): p. 1408-17.
143. Pao, W., et al., *Acquired resistance of lung adenocarcinomas to gefitinib or erlotinib is associated with a second mutation in the EGFR kinase domain.* PLoS Med, 2005. **2**(3): p. e73.

144. Bell, D.W., et al., *Inherited susceptibility to lung cancer may be associated with the T790M drug resistance mutation in EGFR.* Nat Genet, 2005. **37**(12): p. 1315-6.
145. Girard, N., et al., *Analysis of genetic variants in never-smokers with lung cancer facilitated by an Internet-based blood collection protocol: a preliminary report.* Clin Cancer Res, 2010. **16**(2): p. 755-63.
146. Vikis, H., et al., *EGFR-T790M is a rare lung cancer susceptibility allele with enhanced kinase activity.* Cancer Res, 2007. **67**(10): p. 4665-70.
147. Pao, W., et al., *KRAS mutations and primary resistance of lung adenocarcinomas to gefitinib or erlotinib.* PLoS Med, 2005. **2**(1): p. e17.
148. Karapetis, C.S., et al., *K-ras mutations and benefit from cetuximab in advanced colorectal cancer.* N Engl J Med, 2008. **359**(17): p. 1757-65.
149. Amado, R.G., et al., *Wild-type KRAS is required for panitumumab efficacy in patients with metastatic colorectal cancer.* J Clin Oncol, 2008. **26**(10): p. 1626-34.
150. Hoa, M., et al., *Amplification of wild-type K-ras promotes growth of head and neck squamous cell carcinoma.* Cancer Res, 2002. **62**(24): p. 7154-6.
151. Engelman, J.A., et al., *MET amplification leads to gefitinib resistance in lung cancer by activating ERBB3 signaling.* Science, 2007. **316**(5827): p. 1039-43.
152. Onitsuka, T., et al., *Comprehensive molecular analyses of lung adenocarcinoma with regard to the epidermal growth factor receptor, K-ras, MET, and hepatocyte growth factor status.* J Thorac Oncol, 2010. **5**(5): p. 591-6.
153. Quesnelle, K.M., A.L. Boehm, and J.R. Grandis, *STAT-mediated EGFR signaling in cancer.* J Cell Biochem, 2007. **102**(2): p. 311-9.
154. Erjala, K., et al., *Signaling via ErbB2 and ErbB3 associates with resistance and epidermal growth factor receptor (EGFR) amplification with sensitivity to EGFR inhibitor gefitinib in head and neck squamous cell carcinoma cells.* Clin Cancer Res, 2006. **12**(13): p. 4103-11.
155. Stommel, J.M., et al., *Coactivation of receptor tyrosine kinases affects the response of tumor cells to targeted therapies.* Science, 2007. **318**(5848): p. 287-90.
156. Frederick, B.A., et al., *Epithelial to mesenchymal transition predicts gefitinib resistance in cell lines of head and neck squamous cell carcinoma and non-small cell lung carcinoma.* Mol Cancer Ther, 2007. **6**(6): p. 1683-91.
157. Bean, J., et al., *MET amplification occurs with or without T790M mutations in EGFR mutant lung tumors with acquired resistance to gefitinib or erlotinib.* Proc Natl Acad Sci U S A, 2007. **104**(52): p. 20932-7.
158. Seiwert, T.Y., et al., *The MET receptor tyrosine kinase is a potential novel therapeutic target for head and neck squamous cell carcinoma.* Cancer Res, 2009. **69**(7): p. 3021-31.
159. Turke, A.B., et al., *Preexistence and clonal selection of MET amplification in EGFR mutant NSCLC.* Cancer Cell, 2010. **17**(1): p. 77-88.
160. Yano, S., et al., *Hepatocyte growth factor induces gefitinib resistance of lung adenocarcinoma with epidermal growth factor receptor-activating mutations.* Cancer Res, 2008. **68**(22): p. 9479-87.
161. Muller, S., et al., *Distinctive E-cadherin and epidermal growth factor receptor expression in metastatic and nonmetastatic head and neck squamous cell carcinoma: predictive and prognostic correlation.* Cancer, 2008. **113**(1): p. 97-107.

162. Benavente, S., et al., *Establishment and Characterization of a Model of Acquired Resistance to Epidermal Growth Factor Receptor Targeting Agents in Human Cancer Cells.* Clin Cancer Res, 2009.
163. Wheeler DL, H.S., Kruser TJ, Nechrebecki MM, Armstrong EA, Benavente S, Gondi V, Hsu KT, Harari PM., *Mechanisms of acquired resistance to cetuximab: role of HER (ErbB) family members.* Oncogene, 2008.
164. Quesnelle, K.M. and J.R. Grandis, *Dual kinase inhibition of EGFR and HER2 overcomes resistance to cetuximab in a novel in vivo model of acquired cetuximab resistance.* Clin Cancer Res, 2011. **17**(18): p. 5935-44.
165. Yamasaki, F., et al., *Sensitivity of breast cancer cells to erlotinib depends on cyclin-dependent kinase 2 activity.* Mol Cancer Ther, 2007. **6**(8): p. 2168-77.
166. Yao, Z., et al., *TGF-beta IL-6 axis mediates selective and adaptive mechanisms of resistance to molecular targeted therapy in lung cancer.* Proc Natl Acad Sci U S A, 2010. **107**(35): p. 15535-40.
167. Haddad, Y., W. Choi, and D.J. McConkey, *Delta-crystallin enhancer binding factor 1 controls the epithelial to mesenchymal transition phenotype and resistance to the epidermal growth factor receptor inhibitor erlotinib in human head and neck squamous cell carcinoma lines.* Clin Cancer Res, 2009. **15**(2): p. 532-42.
168. Krumbach, R., et al., *Primary resistance to cetuximab in a panel of patient-derived tumour xenograft models: activation of MET as one mechanism for drug resistance.* Eur J Cancer, 2011. **47**(8): p. 1231-43.
169. Perrotte, P., et al., *Anti-epidermal growth factor receptor antibody C225 inhibits angiogenesis in human transitional cell carcinoma growing orthotopically in nude mice.* Clin Cancer Res, 1999. **5**(2): p. 257-65.
170. Prewett, M., et al., *Mouse-human chimeric anti-epidermal growth factor receptor antibody C225 inhibits the growth of human renal cell carcinoma xenografts in nude mice.* Clin Cancer Res, 1998. **4**(12): p. 2957-66.
171. Viloria-Petit, A., et al., *Acquired resistance to the antitumor effect of epidermal growth factor receptor-blocking antibodies in vivo: a role for altered tumor angiogenesis.* Cancer Res, 2001. **61**(13): p. 5090-101.
172. Niu, G., et al., *Cetuximab-based immunotherapy and radioimmunotherapy of head and neck squamous cell carcinoma.* Clin Cancer Res, 2010. **16**(7): p. 2095-105.
173. Huang, S.M., J. Li, and P.M. Harari, *Molecular inhibition of angiogenesis and metastatic potential in human squamous cell carcinomas after epidermal growth factor receptor blockade.* Mol Cancer Ther, 2002. **1**(7): p. 507-14.
174. Ciardiello, F., et al., *Antitumor activity of ZD6474, a vascular endothelial growth factor receptor tyrosine kinase inhibitor, in human cancer cells with acquired resistance to antiepidermal growth factor receptor therapy.* Clin Cancer Res, 2004. **10**(2): p. 784-93.
175. Paranavitana, C.M., *Non-radioactive detection of K-ras mutations by nested allele specific PCR and oligonucleotide hybridization.* Mol Cell Probes, 1998. **12**(5): p. 309-15.
176. Lin, C.J., et al., *Head and neck squamous cell carcinoma cell lines: established models and rationale for selection.* Head Neck, 2007. **29**(2): p. 163-88.
177. Bubenik, J., et al., *Established cell line of urinary bladder carcinoma (T24) containing tumour-specific antigen.* Int J Cancer, 1973. **11**(3): p. 765-73.
178. Linsley, P.S. and C.F. Fox, *Direct linkage of EGF to its receptor: characterization and biological relevance.* J Supramol Struct, 1980. **14**(4): p. 441-59.

179. Scherer, W.F., J.T. Syverton, and G.O. Gey, *Studies on the propagation in vitro of poliomyelitis viruses. IV. Viral multiplication in a stable strain of human malignant epithelial cells (strain HeLa) derived from an epidermoid carcinoma of the cervix.* J Exp Med, 1953. **97**(5): p. 695-710.
180. Ritter, C.A., et al., *Human breast cancer cells selected for resistance to trastuzumab in vivo overexpress epidermal growth factor receptor and ErbB ligands and remain dependent on the ErbB receptor network.* Clin Cancer Res, 2007. **13**(16): p. 4909-19.
181. Goldstein, N.I., et al., *Biological efficacy of a chimeric antibody to the epidermal growth factor receptor in a human tumor xenograft model.* Clin Cancer Res, 1995. **1**(11): p. 1311-8.
182. Leeman-Neill, R.J., et al., *Guggulsterone enhances head and neck cancer therapies via inhibition of signal transducer and activator of transcription-3.* Carcinogenesis, 2009. **30**(11): p. 1848-56.
183. Molli, P.R., L. Adam, and R. Kumar, *Therapeutic IMC-C225 antibody inhibits breast cancer cell invasiveness via Vav2-dependent activation of RhoA GTPase.* Clin Cancer Res, 2008. **14**(19): p. 6161-70.
184. Capon, D.J., et al., *Complete nucleotide sequences of the T24 human bladder carcinoma oncogene and its normal homologue.* Nature, 1983. **302**(5903): p. 33-7.
185. Luwor, R.B., et al., *Constitutively active Harvey Ras confers resistance to epidermal growth factor receptor-targeted therapy with cetuximab and gefitinib.* Cancer Lett, 2011. **306**(1): p. 85-91.
186. Garber, K., *From human to mouse and back: 'tumorgraft' models surge in popularity.* J Natl Cancer Inst, 2009. **101**(1): p. 6-8.
187. Hidalgo, M., et al., *A pilot clinical study of treatment guided by personalized tumorgrafts in patients with advanced cancer.* Mol Cancer Ther, 2011. **10**(8): p. 1311-6.
188. Morelli, M.P., et al., *Prioritizing Phase I Treatment Options Through Preclinical Testing on Personalized Tumorgraft.* J Clin Oncol, 2011.
189. Hirsch, F.R., et al., *Increased epidermal growth factor receptor gene copy number detected by fluorescence in situ hybridization associates with increased sensitivity to gefitinib in patients with bronchioloalveolar carcinoma subtypes: a Southwest Oncology Group Study.* J Clin Oncol, 2005. **23**(28): p. 6838-45.
190. Cappuzzo, F., et al., *Epidermal growth factor receptor gene and protein and gefitinib sensitivity in non-small-cell lung cancer.* J Natl Cancer Inst, 2005. **97**(9): p. 643-55.
191. Cappuzzo, F., et al., *Prospective study of gefitinib in epidermal growth factor receptor fluorescence in situ hybridization-positive/phospho-Akt-positive or never smoker patients with advanced non-small-cell lung cancer: the ONCOBELL trial.* J Clin Oncol, 2007. **25**(16): p. 2248-55.
192. Sequist, L.V., et al., *Molecular predictors of response to epidermal growth factor receptor antagonists in non-small-cell lung cancer.* J Clin Oncol, 2007. **25**(5): p. 587-95.
193. Pirker, R., et al., *EGFR expression as a predictor of survival for first-line chemotherapy plus cetuximab in patients with advanced non-small-cell lung cancer: analysis of data from the phase 3 FLEX study.* Lancet Oncol, 2012. **13**(1): p. 33-42.
194. Licitra, L., et al., *Evaluation of EGFR gene copy number as a predictive biomarker for the efficacy of cetuximab in combination with chemotherapy in the first-line treatment of recurrent and/or metastatic squamous cell carcinoma of the head and neck: EXTREME study.* Ann Oncol, 2011. **22**(5): p. 1078-87.

195. Lopez-Albaitero, A., et al., *Role of polymorphic Fc gamma receptor IIIa and EGFR expression level in cetuximab mediated, NK cell dependent in vitro cytotoxicity of head and neck squamous cell carcinoma cells.* Cancer Immunol Immunother, 2009.
196. Milas, L., et al., *In vivo enhancement of tumor radioresponse by C225 antiepidermal growth factor receptor antibody.* Clin Cancer Res, 2000. **6**(2): p. 701-8.
197. Luo, F.R., et al., *Correlation of pharmacokinetics with the antitumor activity of Cetuximab in nude mice bearing the GEO human colon carcinoma xenograft.* Cancer Chemother Pharmacol, 2005. **56**(5): p. 455-64.
198. Kute, T.E., et al., *Breast tumor cells isolated from in vitro resistance to trastuzumab remain sensitive to trastuzumab anti-tumor effects in vivo and to ADCC killing.* Cancer Immunol Immunother, 2009. **58**(11): p. 1887-96.
199. Clynes, R.A., et al., *Inhibitory Fc receptors modulate in vivo cytoxicity against tumor targets.* Nat Med, 2000. **6**(4): p. 443-6.
200. Thomas, J.M., *A lung colony clonogenic cell assay for human malignant melanoma in immune-suppressed mice and its use to determine chemosensitivity, radiosensitivity and the relationship between tumour size and response to therapy.* Br J Surg, 1979. **66**(10): p. 696-700.
201. Zhu, S., A. Belkhiri, and W. El-Rifai, *DARPP-32 increases interactions between epidermal growth factor receptor and ERBB3 to promote tumor resistance to gefitinib.* Gastroenterology, 2011. **141**(5): p. 1738-48 e1-2.
202. Studer, G., et al., *Volumetric staging (VS) is superior to TNM and AJCC staging in predicting outcome of head and neck cancer treated with IMRT.* Acta Oncol, 2007. **46**(3): p. 386-94.
203. Fridman, R., et al., *Enhanced tumor growth of both primary and established human and murine tumor cells in athymic mice after coinjection with Matrigel.* J Natl Cancer Inst, 1991. **83**(11): p. 769-74.
204. Kleinman, H.K., et al., *Basement membrane complexes with biological activity.* Biochemistry, 1986. **25**(2): p. 312-8.
205. Liotta, L.A., C.N. Rao, and U.M. Wewer, *Biochemical interactions of tumor cells with the basement membrane.* Annu Rev Biochem, 1986. **55**: p. 1037-57.
206. Terranova, V.P., et al., *Modulation of the metastatic activity of melanoma cells by laminin and fibronectin.* Science, 1984. **226**(4677): p. 982-5.
207. Turpeenniemi-Hujanen, T., et al., *Laminin increases the release of type IV collagenase from malignant cells.* J Biol Chem, 1986. **261**(4): p. 1883-9.
208. Fridman, R., et al., *Reconstituted basement membrane (matrigel) and laminin can enhance the tumorigenicity and the drug resistance of small cell lung cancer cell lines.* Proc Natl Acad Sci U S A, 1990. **87**(17): p. 6698-702.
209. Hamilton, M., et al., *Effects of smoking on the pharmacokinetics of erlotinib.* Clin Cancer Res, 2006. **12**(7 Pt 1): p. 2166-71.
210. Memon, A.A., et al., *Positron emission tomography (PET) imaging with [11C]-labeled erlotinib: a micro-PET study on mice with lung tumor xenografts.* Cancer Res, 2009. **69**(3): p. 873-8.
211. Petty, W.J., et al., *Epidermal growth factor receptor tyrosine kinase inhibition represses cyclin D1 in aerodigestive tract cancers.* Clin Cancer Res, 2004. **10**(22): p. 7547-54.

212. Huang, W.C., et al., *Nuclear translocation of epidermal growth factor receptor by Akt-dependent phosphorylation enhances breast cancer-resistant protein expression in gefitinib-resistant cells.* J Biol Chem, 2011. **286**(23): p. 20558-68.
213. Li, C., et al., *Nuclear EGFR contributes to acquired resistance to cetuximab.* Oncogene, 2009. **28**(43): p. 3801-13.
214. Narayan, M., et al., *Trastuzumab-induced HER reprogramming in "resistant" breast carcinoma cells.* Cancer Res, 2009. **69**(6): p. 2191-4.
215. Hynes, N.E. and H.A. Lane, *ERBB receptors and cancer: the complexity of targeted inhibitors.* Nat Rev Cancer, 2005. **5**(5): p. 341-54.
216. Sergina, N.V., et al., *Escape from HER-family tyrosine kinase inhibitor therapy by the kinase-inactive HER3.* Nature, 2007. **445**(7126): p. 437-41.
217. Zhao, M., et al., *Assembly and initial characterization of a panel of 85 genomically validated cell lines from diverse head and neck tumor sites.* Clin Cancer Res, 2011. **17**(23): p. 7248-64.
218. Ou, S.H., et al., *Activity of crizotinib (PF02341066), a dual mesenchymal-epithelial transition (MET) and anaplastic lymphoma kinase (ALK) inhibitor, in a non-small cell lung cancer patient with de novo MET amplification.* J Thorac Oncol, 2011. **6**(5): p. 942-6.
219. Kernan, W.N., et al., *Stratified randomization for clinical trials.* J Clin Epidemiol, 1999. **52**(1): p. 19-26.
220. Tengs, T., et al., *A transforming MET mutation discovered in non-small cell lung cancer using microarray-based resequencing.* Cancer Lett, 2006. **239**(2): p. 227-33.
221. Tyner, J.W., et al., *MET receptor sequence variants R970C and T992I lack transforming capacity.* Cancer Res, 2010. **70**(15): p. 6233-7.
222. Garcia-Castillo, J., et al., *HER2 carboxyl-terminal fragments regulate cell migration and cortactin phosphorylation.* J Biol Chem, 2009. **284**(37): p. 25302-13.
223. Anido, J., et al., *Biosynthesis of tumorigenic HER2 C-terminal fragments by alternative initiation of translation.* Embo J, 2006. **25**(13): p. 3234-44.
224. Pedersen, K., et al., *A naturally occurring HER2 carboxy-terminal fragment promotes mammary tumor growth and metastasis.* Mol Cell Biol, 2009. **29**(12): p. 3319-31.
225. Scaltriti, M., et al., *Clinical benefit of lapatinib-based therapy in patients with human epidermal growth factor receptor 2-positive breast tumors coexpressing the truncated p95HER2 receptor.* Clin Cancer Res. **16**(9): p. 2688-95.
226. Yap, T.A., et al., *Phase I trial of the irreversible EGFR and HER2 kinase inhibitor BIBW 2992 in patients with advanced solid tumors.* J Clin Oncol. **28**(25): p. 3965-72.
227. Ocana, A. and A. Pandiella, *Personalized therapies in the cancer "omics" era.* Mol Cancer, 2010. **9**: p. 202.
228. Kim, H.P., et al., *Combined lapatinib and cetuximab enhance cytotoxicity against gefitinib-resistant lung cancer cells.* Mol Cancer Ther, 2008. **7**(3): p. 607-15.
229. Mimura, K., et al., *Lapatinib inhibits receptor phosphorylation and cell growth and enhances antibody dependent cellular cytoxicity (ADCC) of EGFR and HER2 over-expressing esophageal cancer cell lines.* Int J Cancer, 2011. **129**(10): p. 2408-16.
230. Scaltriti, M., et al., *Lapatinib, a HER2 tyrosine kinase inhibitor, induces stabilization and accumulation of HER2 and potentiates trastuzumab-dependent cell cytotoxicity.* Oncogene, 2009. **28**(6): p. 803-14.

231. Lo Muzio, L., et al., *Effect of c-Met expression on survival in head and neck squamous cell carcinoma.* Tumour Biol, 2006. **27**(3): p. 115-21.
232. Mueller, K.L., et al., *Met and c-Src cooperate to compensate for loss of epidermal growth factor receptor kinase activity in breast cancer cells.* Cancer Res, 2008. **68**(9): p. 3314-22.
233. Knowles, L.M., et al., *HGF and c-Met participate in paracrine tumorigenic pathways in head and neck squamous cell cancer.* Clin Cancer Res, 2009. **15**(11): p. 3740-50.
234. Xu, H., et al., *Dual blockade of EGFR and c-Met abrogates redundant signaling and proliferation in head and neck carcinoma cells.* Clin Cancer Res, 2011. **17**(13): p. 4425-38.
235. Schaefer, G., et al., *Erlotinib directly inhibits HER2 kinase activation and downstream signaling events in intact cells lacking epidermal growth factor receptor expression.* Cancer Res, 2007. **67**(3): p. 1228-38.
236. Hirata, A., et al., *HER2 overexpression increases sensitivity to gefitinib, an epidermal growth factor receptor tyrosine kinase inhibitor, through inhibition of HER2/HER3 heterodimer formation in lung cancer cells.* Cancer Res, 2005. **65**(10): p. 4253-60.
237. Hickinson, D.M., et al., *Identification of biomarkers in human head and neck tumor cell lines that predict for in vitro sensitivity to gefitinib.* Clin Transl Sci, 2009. **2**(3): p. 183-92.
238. Piechocki, M.P., et al., *Breast cancer expressing the activated HER2/neu is sensitive to gefitinib in vitro and in vivo and acquires resistance through a novel point mutation in the HER2/neu.* Cancer Res, 2007. **67**(14): p. 6825-43.
239. Piechocki, M.P., et al., *Gefitinib prevents cancer progression in mice expressing the activated rat HER2/neu.* Int J Cancer, 2008. **122**(8): p. 1722-9.
240. Meier, R., et al., *Mitogenic activation, phosphorylation, and nuclear translocation of protein kinase Bbeta.* J Biol Chem, 1997. **272**(48): p. 30491-7.
241. Barnes, C.J., et al., *Insulin-like growth factor receptor as a therapeutic target in head and neck cancer.* Clin Cancer Res, 2007. **13**(14): p. 4291-9.
242. Ciardiello, F., et al., *Antitumor effects of ZD6474, a small molecule vascular endothelial growth factor receptor tyrosine kinase inhibitor, with additional activity against epidermal growth factor receptor tyrosine kinase.* Clin Cancer Res, 2003. **9**(4): p. 1546-56.
243. Chou, T.C. and P. Talalay, *Quantitative analysis of dose-effect relationships: the combined effects of multiple drugs or enzyme inhibitors.* Adv Enzyme Regul, 1984. **22**: p. 27-55.
244. Chau, N.G., et al., *The association between EGFR variant III, HPV, p16, c-MET, EGFR gene copy number and response to EGFR inhibitors in patients with recurrent or metastatic squamous cell carcinoma of the head and neck.* Head Neck Oncol, 2011. **3**: p. 11.
245. Bardelli, A., et al., *A peptide representing the carboxyl-terminal tail of the met receptor inhibits kinase activity and invasive growth.* J Biol Chem, 1999. **274**(41): p. 29274-81.
246. Zhou, C., et al., *Erlotinib versus chemotherapy as first-line treatment for patients with advanced EGFR mutation-positive non-small-cell lung cancer (OPTIMAL, CTONG-0802): a multicentre, open-label, randomised, phase 3 study.* Lancet Oncol, 2011. **12**(8): p. 735-42.

247. Keedy, V.L., et al., *American Society of Clinical Oncology provisional clinical opinion: epidermal growth factor receptor (EGFR) Mutation testing for patients with advanced non-small-cell lung cancer considering first-line EGFR tyrosine kinase inhibitor therapy.* J Clin Oncol, 2011. **29**(15): p. 2121-7.
248. Dulak, A.M., et al., *HGF-independent potentiation of EGFR action by c-Met.* Oncogene, 2011. **30**(33): p. 3625-35.
249. Sequist, L.V., et al., *Randomized phase II study of erlotinib plus tivantinib versus erlotinib plus placebo in previously treated non-small-cell lung cancer.* J Clin Oncol, 2011. **29**(24): p. 3307-15.
250. Weber, A., et al., *Mutations of the BRAF gene in squamous cell carcinoma of the head and neck.* Oncogene, 2003. **22**(30): p. 4757-9.
251. Bonner, J.A., et al. *Cetuximab prolongs survival in patients with locoregionally advanced squamous cell carcinoma of head and neck: A phase III study of high dose radiation therapy with or without cetuximab.* in *American Society of Clinical Oncology, Abstract No. 5507*. 2004.
252. Merlano, M., et al., *Cisplatin-based chemoradiation plus cetuximab in locally advanced head and neck cancer: a phase II clinical study.* Ann Oncol, 2011. **22**(3): p. 712-7.
253. Scaltriti, M., et al., *Expression of p95HER2, a truncated form of the HER2 receptor, and response to anti-HER2 therapies in breast cancer.* J Natl Cancer Inst, 2007. **99**(8): p. 628-38.
254. Goi, T., et al., *An EGF receptor/Ral-GTPase signaling cascade regulates c-Src activity and substrate specificity.* Embo J, 2000. **19**(4): p. 623-30.
255. Mader, C.C., et al., *An EGFR-Src-Arg-cortactin pathway mediates functional maturation of invadopodia and breast cancer cell invasion.* Cancer Res, 2011. **71**(5): p. 1730-41.
256. Desmarais, V., et al., *N-WASP and cortactin are involved in invadopodium-dependent chemotaxis to EGF in breast tumor cells.* Cell Motil Cytoskeleton, 2009. **66**(6): p. 303-16.
257. Fantozzi, I., et al., *Overexpression of cortactin in head and neck squamous cell carcinomas can be uncoupled from augmented EGF receptor expression.* Acta Oncol, 2008. **47**(8): p. 1502-12.
258. Kimura, F., et al., *Epidermal growth factor-dependent enhancement of invasiveness of squamous cell carcinoma of the breast.* Cancer Sci, 2010. **101**(5): p. 1133-40.
259. Yamada, S., et al., *Overexpression of cortactin increases invasion potential in oral squamous cell carcinoma.* Pathol Oncol Res, 2010. **16**(4): p. 523-31.
260. Lynch, D.K., et al., *A Cortactin-CD2-associated protein (CD2AP) complex provides a novel link between epidermal growth factor receptor endocytosis and the actin cytoskeleton.* J Biol Chem, 2003. **278**(24): p. 21805-13.
261. Timpson, P., et al., *Aberrant expression of cortactin in head and neck squamous cell carcinoma cells is associated with enhanced cell proliferation and resistance to the epidermal growth factor receptor inhibitor gefitinib.* Cancer Res, 2007. **67**(19): p. 9304-14.
262. Morgillo, F., et al., *Antitumour efficacy of MEK inhibitors in human lung cancer cells and their derivatives with acquired resistance to different tyrosine kinase inhibitors.* Br J Cancer, 2011. **105**(3): p. 382-92.